The PHILOSOPHICAL MAGAZINE

FIRST PUBLISHED IN 1798

. 45 SEVENTH SERIES No. 369 October 1954

DEC 17 '54
LIBRARY

A Journal of Theoretical Experimental and Applied Physics

EDITOR
PROFESSOR N F. MOTT, M.A., D.Sc., F.R.S.

EDITORIAL BOARD
SIR LAWRENCE BRAGG, O.B.E., M.C., M.A., D.Sc., F.R.S.
SIR GEORGE THOMSON, M.A., D.Sc., F.R.S.
PROFESSOR A. M TYNDALL, C.B.E., D.Sc., F.R.S.

PRICE 15s. 0d.
Annual Subscription £8 0s. 0d. payable in advance

AND PUBLISHED BY TAYLOR & FRANCIS LTD., RED LION COURT, FLEET ST., LONDON, E.C.4.

ATOMIC ENERGY

A SURVEY

by

PROFESSOR J. ROTBLAT

Published April 1954

Given as a course of lectures at the University of London under the auspices of the Atomic Scientists' Association *and the Department of Extra-Mural Studies*

CONTENTS

Atomic Research at Harwell

Speaker: Sir JOHN D. COCKCROFT, K.C.B., SC.D., LL.D., F.R.S.

Chairman: Sir RODERIC HILL, K.C.B., M.C., A.F.C., M.A.

Atomic Weapons

Speaker: Professor O. R. FRISCH, O.B.E., D.SC., F.R.S.

Chairman: Professor P. M. S. BLACKETT, M.A., D.SC., F.R.S.

Power from Atomic Energy

Speaker: Professor F. E. SIMON, C.B.E., PH.D., F.R.S.

Chairman: Sir CHRISTOPHER HINTON, M.I.C.E., M.I.MECH.E.

Radiation Hazards of Atomic Energy

Speaker: Dr. J. F. LOUTIT, M.D., M.R.C.P.

Chairman: Sir ERNEST ROCK CARLING, F.R.C.S., F.R.C.P.

Medical Uses of Atomic Energy

Speaker: Dr. E. E. POCHIN, M.D., F.R.C.P.

Chairman: Sir HENRY DALE, O.M., G.B.E., F.R.C.P., F.R.S.

Atomic Energy and Moral Issues

Speakers: Professor KATHLEEN LONSDALE, D.SC., F.R.S.
Sir GEORGE P. THOMSON, D.SC., LL.D., F.R.S.

Chairman: Professor A. V. HILL, C.H., O.B.E., SC.D., F.R.S.

Paper bound: 4/9 (70 cents) Cloth bound: 6/9 ($1)
(including postage)

Printed and Published by
TAYLOR & FRANCIS, LTD.,
RED LION COURT, FLEET STREET, LONDON, E.C.4

PERGAMON PRESS

242 MARYLEBONE ROAD · N.W.1

Atlas of Typical Expansion Chamber Photographs

By W. GENTNER, H. MAIER-LEIBNITZ and W. BOTHE *5 gns. net*

194 large photographs dealing with the applications of the cloud chamber to radioactivity and nuclear physics and including historical as well as new material. With diagrams (Compton effect, pair production, beta radiation, etc.) and detailed descriptions in English, French and German. *Demy 4to. 200 pp.*

Atlas of Cloud Chamber Photographs of the Cosmic Radiation *70s. net*

By G. D. ROCHESTER and J. G. WILSON

"... (gives) a refreshing sense of reality to the existence and wonderful behaviour of elementary particles possessed with fantastic energy; and persons in many walks of life may be led to feel a vivid appreciation of the extraordinary phenomena portrayed." Kenneth Greisen in *Science*

Atlas of Emulsion Method Photographs

By C. F. POWELL, F.R.S.

This volume is in preparation and will be published in 1955.

Theory of Cohesion

By M. A. JASWON *37s. 6d. net*

A discussion of the cohesive properties of electrons in atoms, molecules and solids on the basis of wave mechanics; useful to the chemist, metallurgist, solid state and theoretical physicist and mathematician. *Demy 8vo. 253 pages. 42 illustrations.*

Rocket Exploration of the Upper Atmosphere

Edited by R. L. F. BOYD, M. J. SEATON and H. S. W. MASSEY, F.R.S. *75s. net*

The proceedings of the Oxford Conference on Rocket Research (August, 1953). *Crown 4to. 384 pages. 232 illustrations.*

Journal of Nuclear Energy

Editors: J. V. DUNWORTH, J. GUÉRON and G. RANDERS

Since it has become evident that the development of economical civilian power from nuclear energy is likely to succeed, it has been decided to form this journal to provide an outlet for research work dealing with the scientific, engineering, biological and economic aspects of nuclear energy and its by-products. Published quarterly, with 300 pages per volume.

For details of the subscription rates please apply to the publishers.

CX. *An Experimental Investigation of the Interaction of a Shock Wave with a Subsonic Stream Bounded by a Wall*

By D. W. Holder, A. Chinneck and G. E. Gadd
Aerodynamics Division, National Physical Laboratory*

[Received May 24, 1954]

Summary

An experimental study has been made of a model of a boundary layer consisting of a subsonic stream bounded on one side by a wall and on the other by a supersonic main stream. The subsonic stream was approximately uniform at the point where it first met the main stream, but it became progressively less uniform downstream of this point because of mixing with the main stream and the growth of the boundary layer at the wall.

Particular attention is given to the pressure rise which takes place at the wall when a wedge is attached to it. It is found that the pressure begins to rise ahead of the apex of the wedge, and that the magnitude of this upstream effect increases as the Mach number of the secondary stream is reduced. A comparison between the measured values of the upstream effect, and the values predicted by a theory which has been advanced by Lighthill, shows reasonable agreement.

§ 1. Introduction

In the absence of boundary-layer effects, the static pressure at a wall past which air is flowing at a supersonic speed rises abruptly where a shock wave strikes the wall. Two examples are sketched in figs. 1 (*a*) and (*b*) ; in the first the shock wave is generated in the supersonic stream, and in the second by a sudden change in the slope of the wall. When a boundary layer is present on the wall, the static pressure begins to rise some distance upstream of the shock wave, and this upstream effect has been the subject of many investigations.

At an early stage, attempts were made to explain the upstream effect in terms of the propagation of disturbances through the subsonic part of the boundary layer. A mathematical discussion of this problem was given by Tsien and Finston (1949) who considered a simple model of the boundary layer consisting of a uniform subsonic stream flowing parallel to the wall. The present experiment was originally planned to check the predictions of Tsien and Finston's theory, and the apparatus was accordingly arranged as sketched in fig. 2 ; this diagram also shows the notation† used in the following paragraphs. A secondary subsonic airstream was produced running parallel to the supersonic main stream, and bounded on one side by the main stream and on the other by a wall. The arrangement was such that the width *b* of the secondary stream, and its Mach number M_3 could be adjusted. It was decided to investigate the flow up a wedge attached to the wall because, for several reasons, it was simpler to deal with this case experimentally than with the case of a shock wave generated by a wedge in the main stream.

---

* Communicated by the Authors.

† A list of the symbols used is also given on page 1008.

Fig. 1

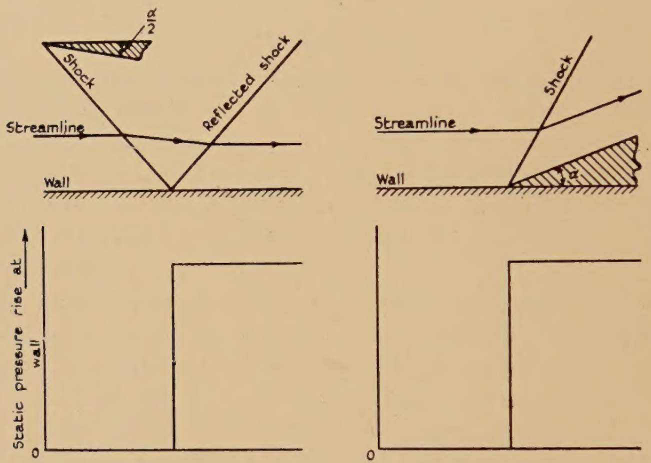

(*a*) (*b*)

Sketches of the flow patterns and pressure distributions in the absence of the boundary layer.

Fig. 2

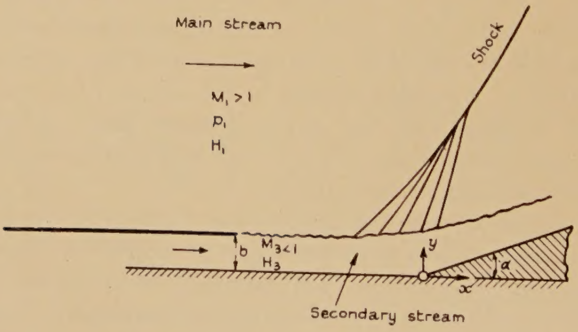

Sketch of the arrangement used in the experiment.

A long delay occurred before the apparatus was completed and the experiment made, and in this period the state of knowledge advanced considerably. It was found that the upstream effect predicted by Tsien and Finston's model was much smaller than that found experimentally for a boundary layer. Moreover, the large difference which was observed between the upstream effects for laminar and turbulent boundary layers could not be explained (Liepmann, Roshko and Dhawan 1952) in terms of the relative thicknesses of the subsonic parts of the layer.

It is now well known (see, for example, Gadd, Holder and Regan 1954) that large upstream effects are associated with separation of the boundary layer, and that the differences between these effects for laminar and turbulent layers arise mainly from the difference between the pressure rise that they withstand before separating. The relatively small* upstream effect which is present for shock waves which are so weak† that separation does not occur (or for expansion waves of any strength) is nevertheless of interest. This has been the subject of a recent theoretical treatment by Lighthill (1952, 1953) who predicts values of the upstream effect for both laminar and turbulent boundary layers which are of the same order as those observed. The results of the present experiment provide further comparisons with Lighthill's theory and, since the problem which formed the original object has already been settled, it is in this connection that it has the greatest value.

§ 2. DESCRIPTION OF THE APPARATUS

The general arrangement of the apparatus is shown diagrammatically in fig. 3. The supersonic main stream was produced by the nozzle blocks AB and CD which were designed to give uniform flow at a Mach number of 1·6 downstream of the Mach lines OB and OD. The mean Mach number M_1 actually produced by the nozzle was found to be 1·59. The dimensions of the tunnel at the exit from the nozzle were 5·9 in. by 3 in.; the side walls were made of glass to permit photography of the flow.

The secondary stream entered, in a direction parallel to the main stream, from the orifice formed between the lip D and the flat plate EF; the width of the orifice could be adjusted between 0·1 in. and 0·4 in. by moving the plate by means of the screws S. The wedges over which the flow was to be examined could be attached to the flat plate at either of two positions, one such that the distance from the apex of the wedge to the secondary-stream orifice was 3·1 in. and the other such that this distance was 6·1 in. Holes for measuring the static pressure were provided in the flat plate and wedges along the centre line.

Since the static pressure in the secondary stream is closely equal to p_1, the static pressure of the supersonic main stream, the Mach number M_3

---

* Of the order of one boundary-layer thickness for turbulent layers, and ten boundary-layer thicknesses for laminar layers.

† Very roughly, it is found (Gadd, Holder and Regan 1954) that a laminar boundary layer separates when the angle α (fig. 2) exceeds 4 deg., and a turbulent layer separates when this angle exceeds 12 deg.

in the secondary stream is related to its total head H_3 by the equation

$$\frac{p_1}{H_3}=\left(\frac{2}{2+(\gamma-1)M_3^2}\right)^{\frac{\gamma}{\gamma-1}} \quad . \quad . \quad . \quad . \quad . \quad . \quad . \quad . \quad (1)$$

The secondary-stream Mach number could thus be adjusted by varying the total head H_3, and this was done by means of a control valve at the entry to the secondary-stream settling chamber.

Fig. 3

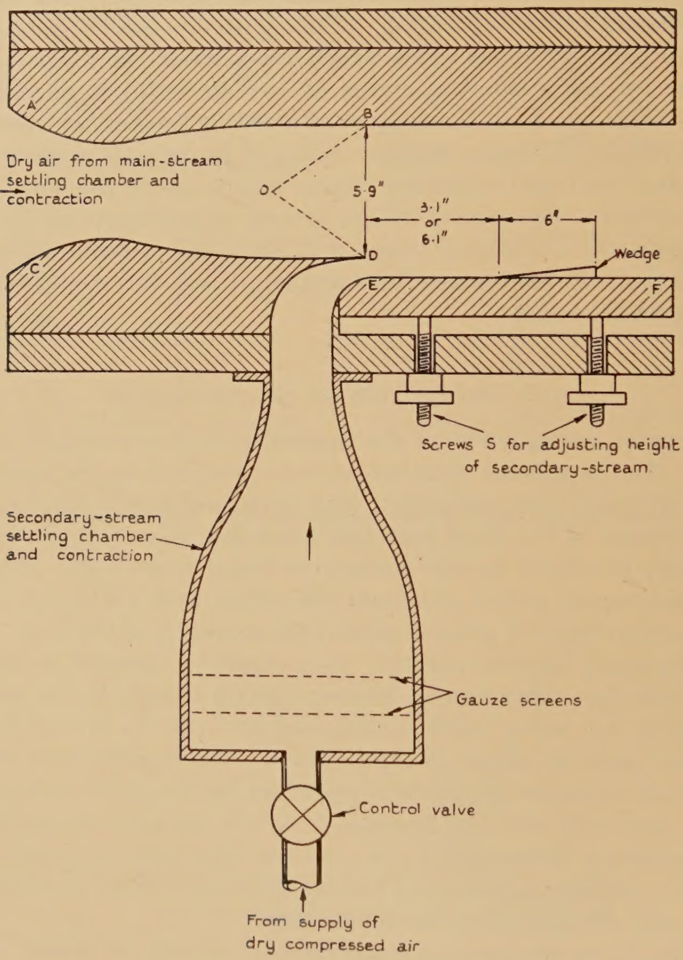
A
B
Dry air from main-stream settling chamber and contraction
O
5·9"
3·1" or 6·1"
6"
Wedge
C
D
E
F
Screws S for adjusting height of secondary-stream
Secondary-stream settling chamber and contraction
Gauze screens
Control valve
From supply of dry compressed air

General arrangement of the apparatus (diagrammatic).

In fact, the secondary stream is of course not uniform. The flow near the outer edge is complicated by the presence of the boundary layers shed from the lip D and by mixing with the main stream, and the flow near the flat plate by the presence of the boundary layer on the plate. The method described above was, therefore, used to adjust the average Mach number, and for each value of this quantity detailed measurements of the total-head profile across the stream were made at several stations. Typical results are reproduced in fig. 4 for an orifice width b of 0·3 inch ; the total head H at distance y from the flat plate is plotted against y for several positions along the secondary stream, and for four values of the nominal Mach number M_3. The latter was determined, by the use of eqn. (1), from the reading of a total-head tube placed in the secondary-stream contraction. Except very close to the lip of the secondary-stream orifice where a small region of low total head (associated with the wake shed from the lip) is visible, the total head falls smoothly through the mixing region from a value equal to the main stream total head on one side, to an approximately constant value corresponding to that in the core of the secondary stream on the other. Close to the wall the total head falls again because of the presence of the secondary-stream boundary layer. The apparatus did not permit accurate measurements very close to the wall, and for the reason described in § 4, the curves have been drawn as if slip occurred at the wall, the local Mach number there being 0·6 times that in the core of the stream. As pointed out later, the error introduced by using this crude approximation to the true form of the turbulent boundary-layer profile at the wall is negligible for the present purposes.

The total head corresponding to the nominal Mach number M_3 of the secondary stream is shown for each profile by a broken line. It is seen that close to the orifice this corresponds to the total head measured in the core of the stream, but that further downstream the core gradually disappears because of the spread of the mixing region and the growth of the boundary layer on the wall.

Although it is of no direct value in the present application, it is of interest to consider briefly the rate at which the mixing region spreads. The boundaries of this region have been estimated from the profiles shown in fig. 4 and, except near the orifice, are found to be approximately straight. Their slopes are set out in table 1 which also includes values calculated for

Table 1. Comparison between the Slopes of the Observed Boundaries of the Mixing Region and those calculated for Incompressible Mixing of Two Streams of Equal Density

M_3	Boundary with secondary stream		Boundary with main stream	
	Observed	Calculated	Observed	Calculated
0·50	−0·046	−0·116	0·005	0·073
0·75	−0·034	−0·094	0·005	0·068
0·91	−0·024	−0·081	0·005	0·064
0·98	−0·018	−0·076	0·005	0·060

Fig. 4

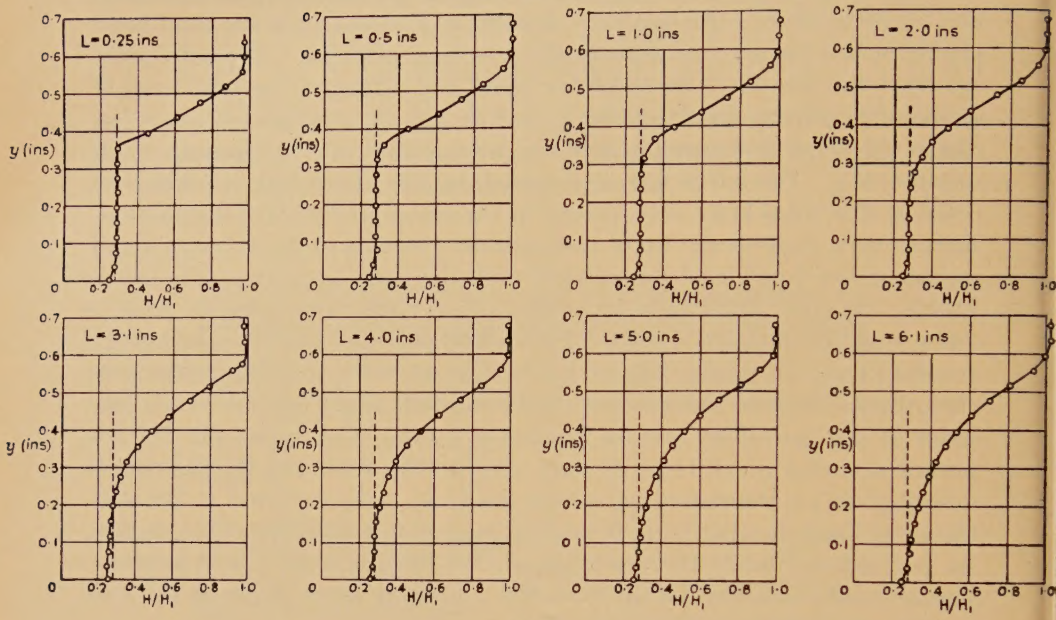

(*a*)

Total head profiles at various distances downstream from the secondary-stream orifice $M_3 = 0{\cdot}50$.

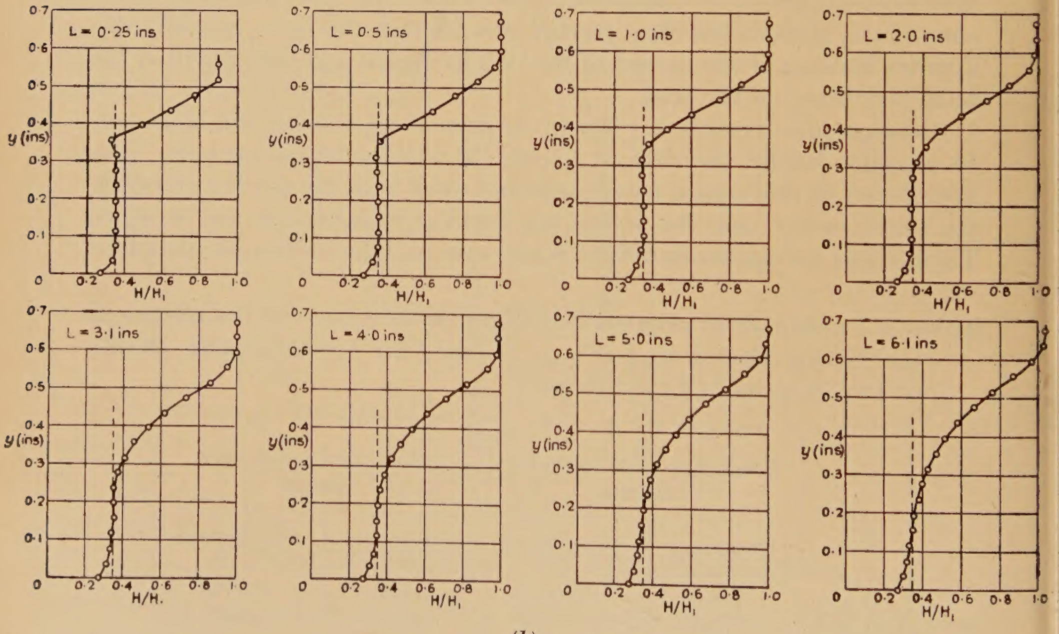

(*b*)

Total head profiles at various distances downstream from the secondary-stream orifice $M_3 = 0{\cdot}75$.

L = distance downstream from orifice.

Fig. 4

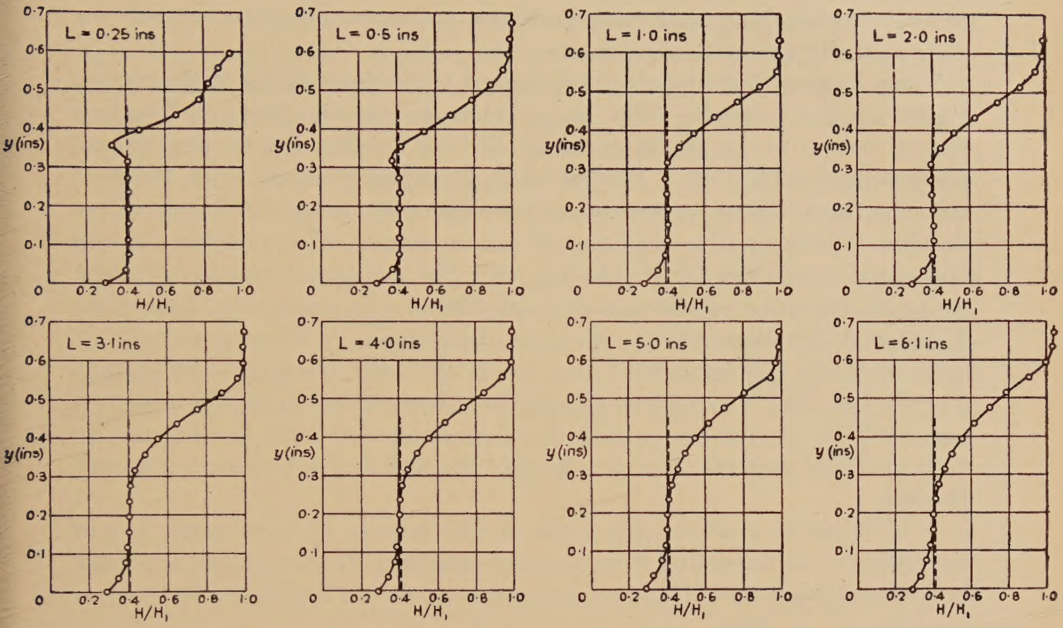

(*c*)

Total head profiles at various distances downstream from the secondary-stream orifice M_3=0·91.

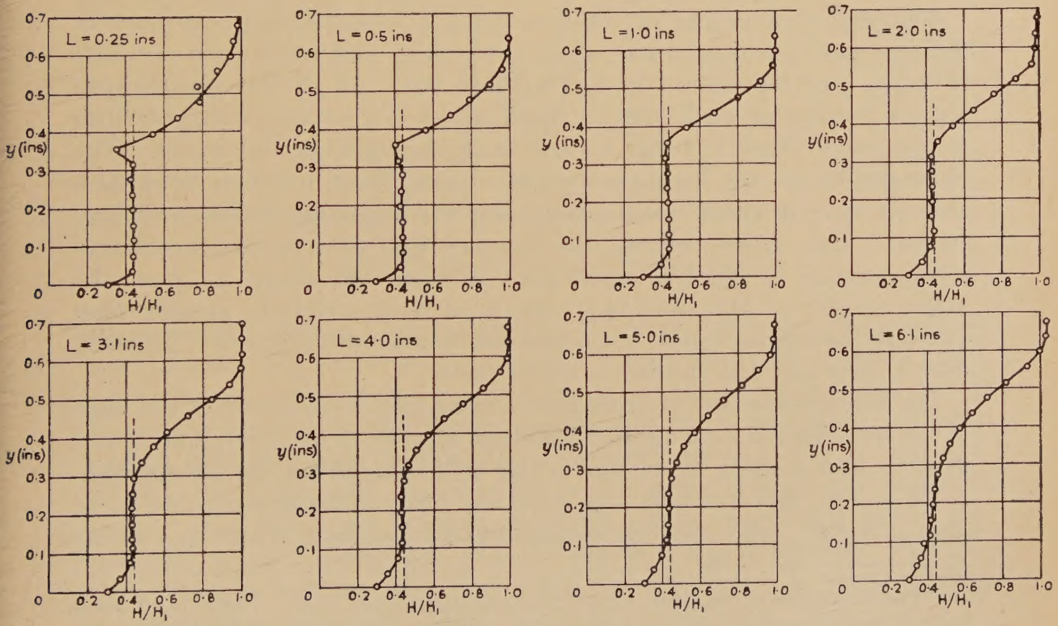

(*d*)

Total head profiles at various distances downstream from the secondary-stream orifice M_3=0·98.

L=distance downstream from orifice.

incompressible flow from Kuethe's formulae (Kuethe 1935) for the mixing of two streams of equal density and with the same values of the velocity ratio as in the present experiment.

Table 1 shows that the observed slopes* of the boundaries of the mixing region are much smaller than those calculated on the basis of Kuethe's theory using the empirical constant for the mixing length determined for incompressible flow. Part of this discrepancy arises from the fact that the theory takes no account of the effects of compressibility or of the difference between the densities of the streams. The presence of the boundary layers shed from the lip, and the constraint imposed by the wall may, however, also have important effects. Experiments (Gooderum, Wood and Brevoort 1950) with a jet discharging freely into still air at approximately the same Mach number as the main stream of the present experiment show a considerably smaller difference between the observed slopes of the mixing region and the slopes calculated for incompressible flow, and this suggests that the effect of the wall in the present work may be large.

It is hoped to start further work on the mixing of high-speed jets in the near future (including further observations with an apparatus similar to that described above), and to issue a more detailed report at a later date.

§ 3. PRESSURE DISTRIBUTIONS AND FLOW PATTERNS NEAR A WEDGE ATTACHED TO THE WALL

Schlieren photographs of the flow when a 5 deg. wedge is present in the upstream position (3·1 in. from the orifice) and for an orifice width of 0·3 in. are reproduced in fig. 5 (Plate 30). All of the photographs show a number of weak oblique shock waves originating at irregularities in the nozzle block CD (fig. 3), and from the lip D of the orifice. The photographs for the higher secondary-stream Mach numbers show also a shock wave or shock-wave system near the beginning of the secondary stream. This arises because the channel upstream of the secondary-stream orifice is slightly convergent-divergent in shape so that the Mach number of the secondary stream at exit is slightly greater than unity at the higher values of the secondary-stream total head; subsonic flow is then restored through a shock wave.

The compression waves arising from the concave curvature of the edge of the secondary stream are just visible at $M_3=0{\cdot}75$ (fig. 5 (*a*)), but do not develop into a shock wave within the field covered by the photograph. At $M_3=0{\cdot}91$ and $M_3=0{\cdot}98$ (figs. 5 (*b*) and (*c*)), the disturbances are more clearly visible; they are formed considerably upstream of the apex of the wedge, and a shock wave develops a few inches from the surface. In fig. 5 (*d*) the secondary-stream Mach number has been raised to a value approximately equal* to that of the main stream, and the upstream effect of the wedge is almost zero ; a shock wave which is approximately straight (apart from refraction within the mixing region) is then formed at the apex of the wedge.

---

* These are measured from a direction parallel to the wall. The rate of mass flow in the secondary stream and mixing region was evaluated by integration and it was found that for $M_3=0{\cdot}75$, 0·91 and 0·98 the free-stream was approximately parallel to the wall. At $M_3=0{\cdot}50$, however, the free-stream appeared to be inclined slightly (by about 0·6 deg.) towards the wall.

Typical pressure distributions at the wall are reproduced in figs. 6 and 7. The curves of fig. 6 show the effect of increasing the nominal Mach number M_3 of the secondary stream for a constant value of the width b of the orifice. The increase in the upstream effect of the wedge which occurs as the secondary-stream Mach number is reduced is clearly visible in this diagram. The effect of changing the width of the secondary-stream orifice for a constant value ($M_3=0{\cdot}98$) of the nominal Mach number of the secondary stream is shown in fig. 7 for two values of the distance of the wedge from the orifice. If, when the width of the orifice was changed, the profiles in the secondary stream were scaled up and down in proportion, the curves in this diagram would coincide. This is, of course, not the case in the present experiment and the changes in profile lead to the differences between the individual curves. The discrepancy between the curves falls as the width of the orifice is increased, and it is thought that this arises because, for large widths, the major part of the upstream effect is associated with the region of approximately constant Mach number in the core ; the width of this region is very roughly proportional to the orifice width when the latter is large.

Fig. 6

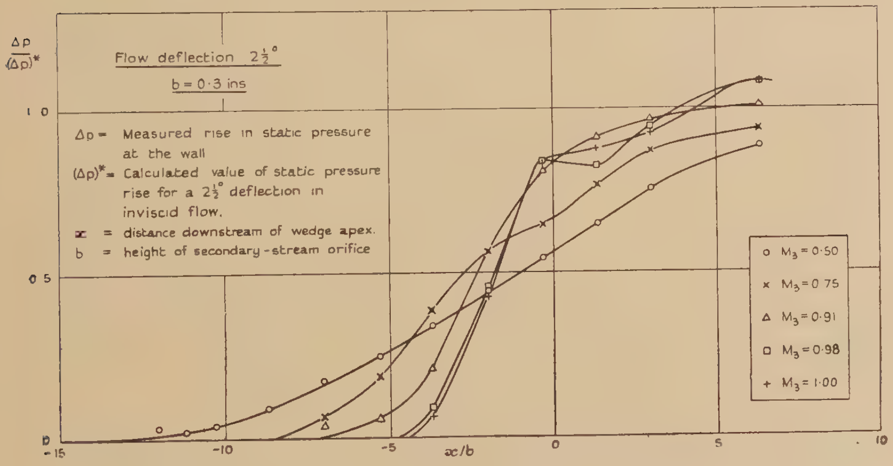

The pressure rise at the wall for constant b.

---

* Under these conditions the flow at exit from the orifice is, of course, no longer parallel to the undisturbed main stream.

§ 4. COMPARISON BETWEEN THE OBSERVED UPSTREAM EFFECT AND THAT PREDICTED BY LIGHTHILL'S THEORY

The upstream effect of a shock wave arising from the interaction with a boundary layer in the absence of boundary-layer separation has recently been examined theoretically by Lighthill (1952, 1953). The static pressure at the wall upstream of the wedge varies as $e^{-\kappa x}$ where κ is given by

$$\frac{1}{\kappa}=\frac{M_1^{\,2}}{\sqrt{(M_1^{\,2}-1)}}\left[\int_{\epsilon}^{\delta}\left(\frac{1}{M^2}-1\right)dy+\frac{M_1^{\,2}-1}{M_1^{\,4}}\int_{\epsilon}^{\delta}M^2\,dy\right]. \qquad . \quad (2)$$

Here the x axis is parallel to the undisturbed flow, y is the distance from the wall and δ is the thickness of the boundary layer. The Mach number of the main stream is denoted by M_1, and the local Mach number at distance y from the wall by M. The length ϵ is the (small) value of y at which M is equal (using Lighthill's notation) to M_2, a Mach number which Lighthill determines by considering the flow in the part of the boundary layer adjoining the wall (' the inner viscous sub-layer ').

Fig. 7

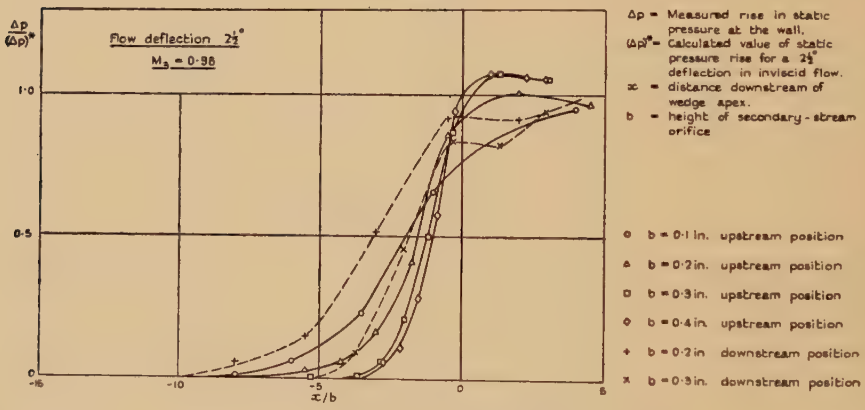

The pressure rise a the wall for constant M_3.

For the purposes of comparison with the measurements of the present experiment, where the Mach number profile in the secondary stream consists of a region of approximately constant Mach number M_3 with only a moderately thin turbulent boundary layer at the wall, it is convenient to write eqn. (2) in the form

$$\frac{1}{\kappa}=\frac{M_1^{\,2}}{\sqrt{(M_1^{\,2}-1)}}\left[\int_{\epsilon}^{\bar{y}}\left(\frac{1}{M^2}-1\right)dy\right.$$
$$\left.+\int_{\bar{y}}^{\delta}\left(\frac{1}{M^2}-1\right)dy+\frac{M_1^{\,2}-1}{M_1^{\,4}}\int_{\bar{y}}^{\delta}M^2dy\right], \quad . \quad . \quad . \quad . \quad . \quad (3)$$

where $\bar{y}$ is small* but, of course, greater than ϵ. If $\bar{y}$ is taken as the value of y for which $M=0{\cdot}6\ M_3$ it is found that, for the present secondary-

---

[*] So that in eqn. (3) the term $\int_{\epsilon}^{\bar{y}}M^2\,dy$ need not be considered.

stream profiles, the first term in eqn. (3) is negligible compared with the other two, and detailed integration near the wall is thus avoided. The expression to be evaluated thus becomes

$$\frac{1}{\kappa}=\frac{M_1^2}{\sqrt{(M_1^2-1)}}\left[\int_{\bar{y}}^{\delta}\left(\frac{1}{M^2}-1\right)dy+\frac{M_1^2-1}{M_1^4}\int_{\bar{y}}^{\delta}M^2\,dy\right], \quad . \quad (3\,a)$$

and this was done by a graphical method for the secondary-stream profiles measured in the undisturbed stream at the point occupied by the apex of the wedge when it was inserted. The integrations were made for all values of M_3 and of the secondary-stream orifice width b for which observations were made. Lighthill's theory is strictly valid only at some distance ahead of the apex of the wedge, but if it is assumed that the exponential variation of pressure holds up to the apex and that the full pressure rise is reached there, it is possible to compare the upstream effects with those observed. To facilitate this comparison it was necessary to select some measure of the upstream effect which could be determined accurately in the experiment. Accordingly the values of κ found by using eqn. (3 a) were used to calculate the distance x upstream of the apex of the wedge at which the static pressure rise at the wall fell to 0·1 of the maximum static pressure rise.

Fig. 8

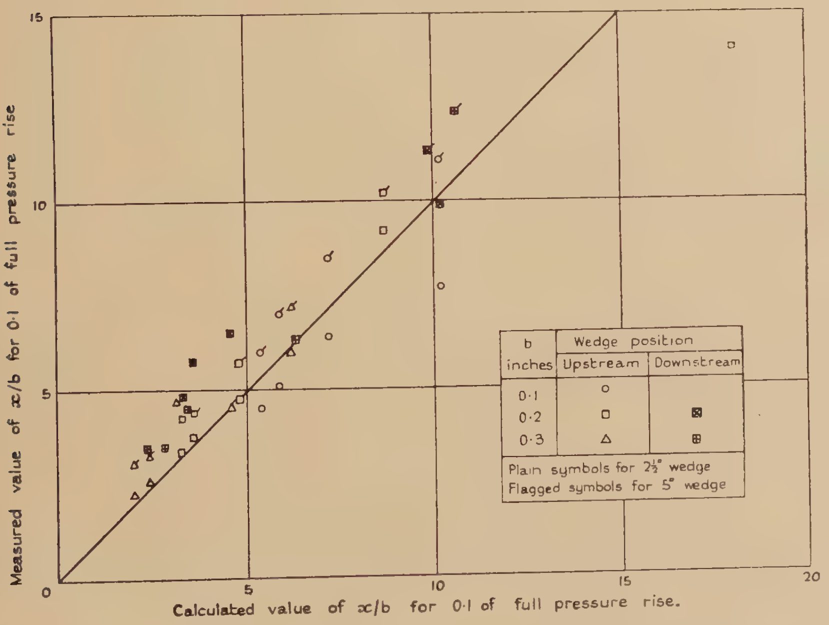

Comparison between the measured and calculated values of the upstream effect.

The measured values of the distance x for 0·1 of the maximum pressure rise* are plotted against the calculated values in fig. 8. Separate symbols are used for each value of the secondary-stream height b, wedge angle, and wedge position. In view of the possible sources of error in the experiment, and the approximations of the theory, the agreement is considered to be satisfactory.

§ 5. CONCLUSIONS

The upstream effect of the wedge on the static pressure at the wall is appreciable for a distance of the order of ten secondary-stream thicknesses when the secondary-stream Mach number is 0·5, and, as expected, falls as the secondary-stream Mach number is raised. The observed upstream effects are in reasonable agreement with the values calculated for the measured secondary-stream profiles by Lighthill's theory.

ACKNOWLEDGMENT

The work described above was carried out in the Aerodynamics Division of the National Physical Laboratory, and it is published on the recommendation of the Aeronautical Research Council and by permission of the Director of the Laboratory.

Mrs. N. A. North assisted with the experimental work and the reduction of the observations.

List of Symbols

p_1	static pressure of the undisturbed stream.
Δp	static pressure rise at the wall.
$(\Delta p)^*$	full static pressure rise for the flow at a Mach number M_1 up a wedge of angle α.
H_1	total head of the main stream.
H_3	total head of the secondary stream at the orifice.
H	local total head in the secondary stream.
M_1	Mach number of the main stream.
M_2	Mach number in Lighthill's theory at $y=\epsilon$ (see p. 1006).
M_3	nominal Mach number of the secondary stream.
M	local Mach number in the secondary stream.
x	distance upstream of the apex of the wedge.
y	distance from the wall.
$\bar{y}$	value of y for $M=0{\cdot}6\ M_3$ (see p. 1006).
δ	thickness of the secondary stream.
b	width of the secondary-stream orifice.
L	distance downstream of the secondary-stream orifice.
α	apex angle of the wedge.

---

* Calculated for inviscid supersonic flow (with free-stream Mach number M_1) up the wedge.

References

Gadd, G. E., Holder, D. W., and Regan, J. D., 1954, An Experimental Investigation of the Interaction Between Shock Waves and Boundary Layers. *A.R.C.*, 16,680—F.M. 2054. To be published in *Proc. Roy. Soc.* A.

Gooderum, P. B., Wood, G. P., and Brevoort, M. J., 1950, Investigation with an Interferometer of the Turbulent Mixing of a Free Supersonic Jet. *N.A.C.A. Report*, 963.

Kuethe, A. M., 1935, Investigations of the Turbulent Mixing Regions formed by Jets. *A.S.M.E., J. App. Mech.*, **57,** A–87.

Liepmann, H. W., Roshko, A., and Dhawan, S., 1952, On the Reflection of Shock Waves from a Boundary Layer. *N.A.C.A. Report*, 1100.

Lighthill, M. J., 1952, On Boundary Layers and Upstream Influence.—II Supersonic flows without separation. *A.R.C.*, 15,298—F.M. 1805 a ; 1953, *Proc. Roy. Soc.* A, **217,** 478.

Tsien, H. S., and Finston, M., 1949, Interaction between Parallel Streams of Subsonic and Supersonic Velocities. *J. Ae. Sc.*, **16,** 515.

CXI. *Astrophysical Considerations Regarding Freundlich's Red-Shift*

By W. H. McCrea
Royal Holloway College*

[Received April 7, 1954]

Abstract

Were the red-shift of lines in the spectra of astronomical light sources, given by a formula proposed by Freundlich, a consequence of photon–photon interaction as Freundlich presumes it to be, it is shown that in the case of eclipsing binary stars there would result certain large effects that are certainly not observed. Also, were the energy lost in the reddening to reappear as radio-emission, this emission in the case of the Galaxy would conflict with observation as regards both quantity and distribution. However, since only parameters of the radiation-field appear in the formula, if the effect is not produced by photon–photon interaction it is doubtful whether it exists at all. It is shown, in fact, that it does not agree with the variation of the measured shift across the solar disk, and that the agreement with observation claimed in the cases of certain other stars is uncertain. It is then pointed out that the existence of the gravitational red-shift and the existence of the cosmic recessional red-shift are demanded by very general physical principles and that, consequently, the interpretation of the relevant observations does not require the existence in addition of the universal red-shift postulated by Freundlich. Born's interpretation of the postulate suggests an interesting association of the effect with radio-emission; but it is pointed out that the possibly significant feature in Born's suggestion could be independent of Freundlich's postulate.

In spite of these criticisms of general aspects of Freundlich's discussion, the actual phenomena to which he directs attention call for much further investigation, both observational and theoretical.

§ 1. Introduction

Finlay-Freundlich (1953, 1954 a, b) believes there to be evidence that the spectral lines of all astronomical light-sources exhibit a red-shift resulting from a hitherto-unrecognized universal physical process; this he presumes to be a photon–photon interaction. If light of frequency ν traverses distance l through a radiation-field of temperature T then, according to Freundlich's investigation, its frequency is changed to $\nu+\Delta\nu$, where

$$\Delta\nu/\nu = -AlT^4 \quad A=2\times10^{-29}\,\mathrm{cm}^{-1}\,\mathrm{deg.}^{-4} \quad . \quad . \quad . \quad . \quad (1)$$

or

$$\Delta\nu/\nu = -Blu \quad (aB=A,\ a=7{\cdot}66\times10^{-15}\ \mathrm{erg\ cm}^{-3}\ \mathrm{deg.}^{-4}) \quad . \quad . \quad (2)$$

---

* Communicated by the Author.

where u is the energy–density of the radiation-field, a is the Stefan–Boltzmann constant, and A is a new universal constant. In applying (1) to stellar absorption lines, Freundlich takes T to be the effective temperature T_e and l the depth of the stellar atmosphere.

Three questions arise which it is convenient to take in the following order :—

(*a*) If the effect described by (1) exists, can it be interpreted as a photon–photon interaction?

(*b*) If the answer to (*a*) is negative, is there nevertheless some universal process that produces such an effect?

(*c*) If the answers to (*a*) and (*b*) are negative, are there some red-shifts that are not explicable by known physical processes?

§ 2. PHOTON–PHOTON INTERACTION

The radiation-density at a point outside a stellar atmosphere distant r from O, the centre of the star, is not less* than

$$u=\tfrac{1}{4}aT_e^4(R/r)^2, \quad . \quad . \quad . \quad . \quad . \quad . \quad . \quad . \quad . \quad (3)$$

where R is the stellar radius. Accordingly, from (2), light from an external source traversing this radiation-field along a line whose shortest distance from O is r_0 ($>R$) should suffer a frequency-change exceeding

$$\Delta\nu/\nu=-\int_{-\infty}^{\infty}\tfrac{1}{4}AT_e^4R^2(r_0^2+l^2)^{-1}dl=-\tfrac{1}{4}\pi AT_e^4R^2/r_0. \quad . \quad . \quad (4)$$

If $\Delta_l\nu$ is the frequency-change calculated by Freundlich for the same light traversing distance l within the stellar atmosphere, then (4) gives

$$\Delta\nu/\Delta_l\nu=\tfrac{1}{4}\pi R^2/(lr_0). \quad . \quad . \quad . \quad . \quad . \quad . \quad . \quad . \quad . \quad (5)$$

In the case of a B-star, for instance, Freundlich has $\Delta_l\nu=+10$ km/sec (expressed as an apparent doppler shift) and $l=10^7$ cm ; for such a star R is about 4×10^{11} cm. *If such a star belongs to an eclipsing binary, then, taking* $r_0=R$ *in* (5), *near the time of eclipse of the companion, the light from the latter should exhibit a shift about* $\Delta\nu=+3\times10^5$ km/sec. It need scarcely be said that no such effect is seen.

Freundlich ignores the effect of the radiation-field outside the stellar atmosphere. On the basis of a calculation similar to the foregoing, but applied to the light from the star itself, ter Haar (1954) has already pointed out that this part of the field would be expected to have a much greater effect than the part within the atmosphere. Nevertheless, it *might* be possible (i) to propose a type of photon–photon interaction that would have a much diminished effect as between photons belonging to the same radiation stream, so that ter Haar's argument would not apply with full effect to light coming from the star itself, or (ii) to reinterpret Freundlich's formula (1) in the case of light from a single star so as to take account of the whole extent of the radiation-field traversed. This is why I applied the argument to photons from another source and, in particular, to the case of an eclipsing binary. If (i) were possible, it would not affect my conclusion in this case. Even if (ii) were possible, the light from a companion near the time of eclipse should show an additional shift comparable with that of the eclipsing star, and this also is not observed.

---

* This is the asymptotic formula for large r ; as r approaches R the coefficient increases from $\frac{1}{4}$ to $\frac{1}{2}$.

In order to achieve (ii), however, ter Haar's and my calculations show that it would be necessary to replace l by a distance proportional to R with an appropriate adjustment of the constant A. But this would be equivalent to making the effect depend upon a power of T_c different from that used by Freundlich and so would vitiate the observational support which he claims for his formula.

Provisionally ignoring these arguments, we can proceed to enquire as to the fate of the energy lost in consequence of the red-shift if a shift given as (1) is produced by photon–photon interaction. For a general red-shift of amount $\Delta\nu/\nu$ entails the removal of a fraction $\Delta\nu/\nu$ of the energy of the radiation emitted by the photosphere of the star concerned.

In order to produce the postulated effect, this energy must be lost in 'quanta' small compared with the energy-quanta of the primary radiation. Born (1953, 1954) suggests that some of these quanta are those of radio-emission. But Born's analysis shows that the total energy-loss resulting from Freundlich's hypothesis in the case of the Sun is about 10^8 times the Sun's normal radio-emission (see Born 1953, equation (3.10) where $\gamma \doteqdot 10^{-8}$ if $T' \doteqdot 10^6$ deg. as would be appropriate in this case). For various reasons, Born is prepared to accept this enormous reduction. A simpler view is, however, that the analysis very strongly indicates that Freundlich's hypothesis would result in far too much radio-emission and that it thereby supplies a further reason for rejecting the hypothesis.

This conclusion is reinforced by the result of applying Freundlich's hypothesis to the general radiation-field of the Galaxy. The density of stellar radiation in the neighbourhood of the Sun is estimated to correspond to a temperature of 3·18 deg. (Eddington 1926). Since the Galaxy has the form of a thin disk of radius about 10^4 parsecs, the density of starlight cannot be much less anywhere within a sphere of the same radius concentric with the galaxy. Light escaping from the Galaxy traverses a mean distance through this radiation-field also of the order of 10^4 parsecs. According to (1) it would therefore suffer a reddening given approximately by

$$\Delta\nu/\nu = 2\times 10^{-29}(3{\cdot}2)^4\ 3{\cdot}1\times 10^{22} \doteqdot 6{\cdot}5\times 10^{-5}.$$

Taking the luminosity of the Galaxy to be 4×10^{42} ergs/sec, were all this reddening to go into the production of radio-emission the latter would be about $2{\cdot}6\times 10^{38}$ ergs/sec. This is of the order of 100 times the total radio-emission of a normal Galaxy. It would be additional to the emission from individual stars or their immediate surroundings and would not in fact, show much concentration towards the Galactic plane.* Its existence would therefore completely conflict with observation. Of course, a reduction by a factor of the order 10^8 as in Born's case would make the effect negligible. But the reason for considering this particular case is that the radio-emission should here take place in regions where no losses of radio-radiation are to be expected.

Thus there are convincing astrophysical reasons against Freundlich's shift, if it exists, being produced by photon–photon interaction. But if it is not produced in this way, it is unlikely that it exists. For, as is seen from the form (2), it depends upon nothing but properties (the density and extent) of the radiation-field.

§ 3. EVIDENCE FOR FREUNDLICH'S RED-SHIFT

3.1. *Solar and Stellar Spectral Lines*

In the case of the Sun, Freundlich shows that (1) would account for somewhat less than one-half the measured shift for light from the centre of the disk. The rest he is prepared to attribute to a gravitational shift of about one-fifth of Einstein's value. In fact, he is prepared to accept the use of (1) in this way as supplying evidence in favour of such a reduced value of the gravitational shift; consequently, he is not claiming the *amount* of the measured shift as confirmation of (1).

Freundlich does, however, regard the *variation* across the disk of the measured shift as affording confirmation. In this application of (1) he takes $T=T_e$ for all θ and $l=l_0 \sec \theta$, the geometrical depth along the sight-line of a solar atmosphere having fixed radial depth l_0, where θ is the angle between the sight-line and the solar radius to the point on the solar surface from which the light is received. But these assumptions require some examination.

According to Freundlich's hypothesis, light of all frequencies† is reddened by passing through the radiation-field in the solar atmosphere, but this reddening has nothing directly to do with the material contents of the atmosphere. In particular, it has nothing directly to do with the processes concerned in the formation of a spectral line; the relevance of a spectral line is that it permits the reddening to be detected. Although the processes producing the line and the postulated processes producing the reddening operate independently, both sets would have to be taken into account in the transfer-problem of calculating the line-profile that would be observed. This problem would then have a novel and complicated form. However, from general considerations it can be concluded that the line-shift would always be approximately the same as the shift for photons belonging to the neighbouring part of the continuous spectrum. Evidently this is also Freundlich's conclusion since his formula is independent of the line-strength.

---

*This would be true of the contribution to radio-emission as here estimated. The statement would be modified were account taken of the probable enhancement of the optical radiation-field around the galactic 'nucleus', but the present criticism as a whole would thereby be only strengthened.

† In passing, it may be noted that, for a given value of θ, all photons of a given initial frequency are not equally affected. Freundlich's figures give for $\theta=0$ an average loss of energy per photon equal to a fraction about $2{\cdot}6\times10^{-7}$ of the initial energy. Born's interpretation gives an average loss per photon–photon encounter equal to two secondary photons of wavelength about 15 cm; in the case of a primary photon of wavelength 6000 Å, this is a fraction 8×10^{-6} of the initial energy. Thus only a small fraction (about 1/30) of the emergent photons would suffer an effective encounter. The circumstance that Freundlich's shift might be produced in this way does not, of course, affect his discussion, but it would need to be taken into account were the relevant problems of radiative-transfer to be solved in detail.

Thus Freundlich's distance l must be a measure of the depth to which we see into the solar atmosphere along the sight-line, when we observe in light in a given part of the continuous spectrum. For varying θ, this depth must correspond to a nearly constant optical depth along the sight-line. This means that we see down to a diminishing radial geometrical depth as we move our sight-line from the centre of the disk to the limb. This gives less variation of l from centre to limb than that assumed by Freundlich. Moreover, it means that we see down to layers of diminishing temperature as we move from centre to limb. As is well known, this is the explanation of the observed phenomenon of 'limb-darkening'.

The approximate formula derived by Eddington (1926) for the effective temperature $T_e(\theta)$ of the radiation coming from angular distance θ from the centre of the disk in terms of the effective temperature T_e of the Sun as a whole is

$$T_e^4(\theta)=\tfrac{1}{4}(2+3\cos\theta)T_e^4. \quad (6)$$

This is in good agreement with the observed limb-darkening (Woolley and Stibbs 1953). If the appropriate value of T in the application of (1) to the Sun as a whole is T_e, as is implied by Freundlich's applications to other stars, then $T_e(\theta)$ ought to be the appropriate value for the present application. By virtue of the agreement of (6) with observation, if we use (6) to take account of the fact that for increasing θ we see into layers of diminishing mean temperature (and so of diminishing radiation-density) we are not using any more theory of the solar atmosphere than is required for the immediate interpretation of the observed limb-darkening.

From what was said above, Freundlich's assumption that $l=l_0\sec\theta$ gives an upper bound to l. So we conclude from this and (6) that Freundlich's shift as a function of θ must vary less rapidly than

$$\Delta\nu/\nu=-Al_0T_e^4(\tfrac{1}{2}\sec\theta+\tfrac{3}{4}), \quad (7)$$

instead of varying as

$$\Delta\nu/\nu=-Al_0T_e^4\sec\theta \quad (8)$$

as Freundlich asserts. The range of $\sec\theta$ over which he claims that (8) gives agreement with the measurements is about 1 to 5·5. According to

(7) the numerical value of $\Delta\nu/\nu$ should increase in this range by less than the factor 2·8 instead of 5·5 as given by (8). Thus the agreement is destroyed and the measurements appear actually to provide evidence against the existence of the shift.

The most striking evidence quoted by Freundlich in support of his formula is that from two cases of binaries containing Wolf-Rayet components, which have been studied by O. C. Wilson (1940 a, 1949). However, in order to get agreement with (1), Freundlich has to assume for these components an effective temperature of about 40 000 deg. In the case of HD 190918 (for which Freundlich reproduces the radial velocity curve and where the curve for the Wolf-Rayet component is got from measurements of only a single emission line λ 4686) Wilson gives no estimate of the temperature; in discussing HD 193576, Wilson tentatively uses an effective temperature of 80 000 deg.; in his general discussion of such stars (Wilson 1940 b) he quotes the range 50 000 to 100 000 deg. Thus the temperature is likely to be much higher than Freundlich assumes. Since it enters to the fourth power in (1), it is doubtful whether these stars afford confirmation of the formula or just the reverse.

Freundlich's effect gives a shift of +10 km/sec for stars of type B2 and approaching twice this for O-stars. According to his hypothesis, such shifts would *invariably* have to be present. But the writer is informed that recent work on very luminous stars associated with hydrogen emission regions does not reveal a general preponderance of apparent recessional motion such as would be expected in accordance with the hypothesis.

Freundlich's discussion made it appear that wherever his effect could be expected to be observable, over the whole range of stellar surface-temperatures, it is in fact observable. But we now see that fairly direct astrophysical evidence throws considerable doubt upon this claim.

3.2. *Gravitational Red-Shift*

We now turn to less direct evidence. Here we note that, believing there to be the universal effect expressed by (1), Freundlich's object is to evaluate it in order then to re-examine the observational evidence for a gravitational red-shift.

Now it is the case that the existence of the gravitational shift predicted by Einstein has not yet been established by observation. This is not surprising, since the only cases* offering any hope of detecting it at present are those of the Sun and one or two white dwarf stars having normal companion-stars. But, in the case of the Sun it is doubtful whether all the necessary corrections are yet known with sufficient accuracy to say whether the minute expected effect is present or not. One pressure-shift, the Lindholm effect, of the same order as the Einstein effect has been recognized (Adam 1948), but it is by no means certain that other pressure-shifts are negligible to this order; also there may be effects of radial motions in the solar atmosphere. It is, in fact, almost certainly significant that the full Einstein shift is actually observed in light coming from close to the solar limb. For radial motion, if present, has no effect there, and pressure effects are smallest there since that is where we see to the smallest depth in the atmosphere.

---

* Apart from statistical investigations.

In the case of the atmospheres of white dwarfs the conditions are so remote from those of normal stellar atmospheres that almost nothing can yet be said about their possible formation of the spectral lines that are required to reveal the gravitational shift. Indeed, it may well be found that, whenever a star has a value of surface gravity large enough to produce a measurable gravitational shift, this circumstance itself necessarily precludes the formation of spectral lines of such a kind as would enable the effect to be detected. Moreover, even were its detection possible in principle, it could not be isolated from the effect of radial motion unless the star concerned had a companion that did not show the gravitational effect. But this means a more luminous companion and then it is apparently impossible to know whether the spectrum obtained is that of the fainter star or that of scattered light from this companion. For such reasons, Freundlich's suggestion, taking account of his postulated new effect, that there is now observational evidence that the gravitational shift is about one-fifth the amount predicted by Einstein has to be regarded with considerable reserve.

Turning to general physical considerations, it has to be noted that the Einstein effect is inferred from physical principles that can be regarded as experimentally established to the degree of exactness required to make the inference. These are the conservation of energy, the equivalence of mass and energy, and the proportionality of inertial and gravitational mass. For the gravitational red-shift of the amount predicted by Einstein is precisely the change, between the source and the observer, of potential energy of the mass-equivalent of the radiation. Were the shift to be less than the predicted amount, then the circumstance could in principle be employed to create an indefinite amount of energy. For, if a body at a distance from, say, the Sun were allowed to absorb solar radiation, thereby producing a change in the physical or chemical state of the body, its mass would be increased by the mass-equivalent of the energy absorbed; if the body were then allowed to fall on to the Sun, the potential energy released on reaching the Sun would exceed the potential energy lost by the radiation in escaping from the Sun.*

This is not to deny the interest of examining the observational evidence for the gravitational red-shift. But if it were established as not being present in some particular case, the natural inference would be that some detail in the behaviour of the atomic systems in the light-source happens to counteract the effect of the gravitational field. Now Freundlich's hypothesis contains within itself no implication of any process that would operate in this way. In fact, it simply postulates a red-shift additional to and independent of whatever gravitational shift is present. Since the difficulty in the case of the Sun, for instance, is to explain why the full Einstein shift is not observed over the whole disk, an effect that only increases the difficulty must be met with scepticism.

---

* I believe that I owe this line of thought to a conversation, some years ago, with Mr. T. Gold.

3.3. *Cosmical Red-Shift*

The situation in regard to the cosmical red-shift (' expansion of the universe ') is generally similar to that in regard to the gravitational red-shift. Here again we are concerned with an effect that can be inferred from general physical principles without appeal to any particular system of cosmology (see, for instance, Bondi 1952, Couderc 1952). For all treatments of gravitation, with or without ' cosmical repulsion ', show that the universe must be expanding or contracting, since they agree in showing that a stable static state is impossible. And the only known escape from Olbers's difficulty about the background light of the sky is afforded by the expansion of the universe. These arguments suffice to show almost conclusively that there must be some recession of the galaxies producing some cosmical red-shift, although admittedly they do not serve to predict its amount. They make it almost impossible to accept Freundlich's suggestion that the whole of the shift is produced in quite a different way. And here again, as in the case of the gravitational shift, there is certainly no need for any additional agency giving an effect of a similar character. Still less is it worth considering the possibility of a contracting universe with a cosmical blue-shift over-compensated by Freundlich's red-shift (even if in that case the reverse of Freundlich's process could still be neglected).

It may be remarked that here an observational discrimination between the two types of red-shift is possible in principle, though scarcely yet in practice. For in Freundlich's case a red-shift $\Delta\nu/\nu$ (a negative quantity) gives a reduction in the apparent total luminosity of a galaxy by a factor $(1+\Delta\nu/\nu)$ while a red-shift of the same amount produced by recession gives a reduction by a factor $(1+\Delta\nu/\nu)^2$.

§ 4. UNEXPLAINED RED-SHIFTS

In spite of the foregoing reasons against accepting the interpretations that Freundlich places upon the observations, it must readily be allowed that he has recalled attention to problems that demand urgent consideration. Some of these problems arise out of observational material that is now quite old. It is much to be hoped that Freundlich's work will show the need for a repetition of the measurements with the use of modern techniques.

It is scarcely likely, however, that a revision of the observations will show Freundlich to be mistaken in his view that there are line-shifts in stellar spectra that are not accounted for by existing *astrophysical* theory and that tend to be greater the higher the effective temperature of the stars concerned. There is, nevertheless, no indication at present that the explanation of any of these effects is outside the scope of existing *physical* theory.

§ 5. SIGNIFICANCE OF BORN'S DISCUSSION

It might be thought that Born's identification of the secondary photons in a photon–photon interaction with radio-emission is too remarkable for the possibility of such interaction to be dismissed by the foregoing arguments. However, we note that this identification rests essentially upon the fact that the ratio of the radio wavelengths to the optical wavelengths concerned is about equal to the ratio of the optical wavelengths to the Compton wavelength (Born 1953, equation (2.13)). This fact may be found to have significance. It does not, however, appear to have any essential connection with Freundlich's hypothesis. For, in order to express this hypothesis in non-dimensional form, Born has to select an elementary length λ_0, which he takes to be the Compton wavelength, and also an elementary density u_0. As Born remarks, the choice of λ_0 is very restricted. Thus, had Freundlich's hypothesis been something different, the difference would almost certainly have been borne by a different choice of u_0, so that Born's identification of the radio-emission would not have been affected.

Finally, Born expresses the view that, if an elementary length λ_0 is involved in the description of light-propagation, then ordinary relativity theory would not be adequate to deal with it. This conclusion must be correct as regards certain aspects of the propagation. It might even necessitate the abandonment of the conservation of energy on the atomic scale. But it would not be expected to violate the conservation on the macroscopic scale in the manner shown in § 3.2 above to result from a reduction of the value of the gravitational red-shift.

In preparing this paper, I have had the benefit of discussions with several colleagues. There are other considerations regarding line-shifts in astronomical spectra that could also be brought forward in the present connection and these are likely to be dealt with elsewhere by other writers.

REFERENCES

ADAM, M. G., 1948, *Mon. Not. Roy. Astro. Soc.*, **108**, 446.
BONDI, H., 1952, *Cosmology* (Cambridge : University Press).
BORN, M., 1943, *Göttinger Nachrichten*, 102 ; 1954, *Proc. Phys. Soc.* A, **67**, 193.
COUDERC, P., 1952, *The Expansion of the Universe* (London : Faber and Faber).
EDDINGTON, A. S., 1926, *Internal Constitution of the Stars* (Cambridge : University Press), p. 324.
FINLAY-FREUNDLICH, E., 1953, *Göttinger Nachrichten*, 95 ; 1954 a, *Proc. Phys. Soc.* A, **67**, 192 ; 1954 b, *Phil. Mag.* (7), **45**, 303.
TER HAAR, D., 1954, *Phil. Mag.* (7), **45**, 320.
WILSON, O. C., 1940 a, *Astrophys. J.*, **91**, 379 ; 1940 b, *Ibid.*, **91**, 394 ; 1949, *Ibid.*, **109**, 76.
WOOLLEY, R. v. d. R., and STIBBS, D. W. N., 1953, *The Outer Layers of a Star* (Oxford : Clarendon Press), p. 6.

CXII. *On the Observational Data Relating to Freundlich's Proposed Red-shift Law*[*]

By E. Margaret Burbidge
Cambridge

and G. R. Burbidge
Cavendish Laboratory, Cambridge[†]

[Received May 4, 1954]

Abstract

The observational data used by Freundlich in deriving the numerical constant in his proposed red-shift law are critically discussed in the light of the most recent information available. Some of the astronomical data used by Freundlich to adduce support for his proposed law are also critically discussed. Apart from the term due to the gravitational red-shift, it is shown that all the spectral line-shifts considered by Freundlich can be accounted for by relative motions of stars or by motions within stellar atmospheres.

Recently E. Finlay-Freundlich (1953, 1954 a, b) has proposed a new law of the form $\Delta\lambda/\lambda = AT^4 l$, where T is the temperature of the radiation field and l is the path length, in order to explain certain observed shifts of lines in astronomical spectra. W. H. McCrea (1954) has given a critical discussion of the astrophysical implications of such a law, and has concluded that there is no indication at present that the explanation of the observed line-shifts is outside the scope of existing physical theory.

Some remarks may also be made concerning the observational values used in the derivation of the constant A. Further, McCrea's discussion of the use of certain astronomical data to support the hypothesis may be extended to rest of the data cited by Freundlich.

(1) *The* O *and* B *stars*. Freundlich (1954 b) takes a value of +10 km/sec as the red-shift in the spectra of the B type stars in the Orion Nebula group relative to the nebula itself, and bases the numerical value of the constant in the proposed law on this value for stars of effective temperature 20000°. If such an effect were present and were of the size suggested, then it would be demonstrated in statistical studies of the radial velocities of high-temperature stars (O and B types) relative to the radial velocities of cooler stars. Freundlich has in his introduction mentioned the existence of such an effect, the well-known K-term, which is a systematic apparent recessional velocity of the O and B stars.

---

[*] A communication on the same lines has also been received from Anne B. Underhill (Dominion Astronomical Observatory) entitled "The Interpretation of Red-shifts in Stellar Spectra".—(*Editor*.)

[†] Communicated by Professor W. H. McCrea, F.R.S.

For the *nearby* O and B stars the value of the K-term is generally accepted to lie between 4 and 5 km/sec, i.e., half of the figure used by Freundlich as the standard shift for B-type stars (Smart and Green 1936, Trumpler and Weaver 1953). Also, the K-term varies with distance and is approximately zero for the more distant stars (Plaskett 1930, Popper 1950).

The usual method of setting up equations for the derivation of the K-term implicitly assumes :

(*a*) that the stars are situated in the plane of the galaxy, but are randomly distributed in it, and

(*b*) that the individual motions of the stars, when the effects of galactic rotation and the K-term are removed, are random. Recent investigations show that both these are invalid assumptions. Morgan, Whitford and Code (1953) and Weaver (1953) have shown that the O and B stars lie in sharply defined spiral arms in the Galaxy. The diagrams of the arms shown by them immediately dispose of the idea that these stars are randomly distributed. Further, these stars have a well-known tendency to occur in aggregates, each of which may possess a group space motion. The inclusion of members of various aggregates with group motion in the determination of the K-term will clearly introduce fictitious effects. The predominant effect of the stars in the Scorpio–Centaurus Stream was long ago suggested by Plaskett and Pearce (1929) as the origin of the K-term.

Weaver (1954) has recently examined the problem in the light of the non-random distribution of these stars and the occurrence of aggregates with group motion. He has shown that the K-term is thus diminished to about +2·5 km/sec, which may be attributed mainly to the gravitational red-shift.

(2) *The* O *and* B *stars in the Orion Nebula Group.* Freundlich has assumed that the observed difference in line-of-sight velocity between these stars and the nebula itself must have some explanation other than that of relative motion. However, it might be explained as a real velocity difference. The Orion Nebula group belongs to the large Orion aggregate of high temperature stars. Blaauw (1952) and Delhaye and Blaauw (1953) have demonstrated the existence of considerable expansion in an aggregate of stars (the Zeta Persei aggregate) which is of the same nature as, though smaller than, the Orion aggregate. Similar expansions may exist in other aggregates. For example, Blaauw and Morgan (1953) have discussed the motion of the O-type star HD 34078, and its possible physical connection with the Orion aggregate. This star has the large space velocity of 128 km/sec. They have pointed out that the line of motion if extended backwards passes near the centre of the Orion aggregate, indicating that the star may have originated there.

Recent unpublished work by Oort and Spitzer (Blaauw and Morgan 1953) has shown that gaseous clouds may acquire high velocities as a result of acceleration caused by one-sided ionization by O-type stars nearby. If effects such as this can occur, then a relative motion of

10 km/sec between the Orion Nebula group and the nebula itself might easily be present, and the stars may at the present time be passing through the nebula.

(3) *The Wolf–Rayet stars.* McCrea has pointed out that the temperature taken by Freundlich for these stars is too low. In addition, the apparent shifts of the order of 100 km/sec quoted by Freundlich for the Wolf–Rayet components of the binary stars HD 190918 and HD 193576 can almost certainly be attributed to the peculiar nature of the atmospheres of these stars. The radial velocity curve of HD 190918, shown by Freundlich (1954 b), is derived from measures of one spectrum line only, i.e., the broad *emission* line of He II 4686. There are still unsolved problems in the interpretation of Wolf–Rayet spectra (Plaskett 1947), but from the extensive work of Beals it is generally accepted that material is being ejected from these stars, and this is shown in some of the spectra by violet-shifted absorption lines lying alongside the broad emission lines. In those spectra where such absorption lines are not visible, there are probably self-absorption effects which may cause spurious shifts in the measured positions of the emission lines.

(4) *Supergiant* M *stars and* A *stars.* For the A stars in general shifts of between 0·1 and 0·9 km/sec are quoted by Freundlich (1954 b). However. these are of the same order as the observational and selectional errors. A more recent determination of the K-term for A stars made by Smart and Green (1936) gives 0·0 km/sec.

The suggestion of motions varying with height in the atmospheres of M-type supergiants should not be dismissed, since the evidence at present available supports this idea. For example, certain lines in the spectra of these stars show doubling, indicating motions which increase with height in the atmosphere (Adams 1941). The line Hα in the spectrum of the A-type supergiant α Cygni, and in other supergiants, is in emission, with an absorption component displaced to the violet of the emission. This indicates outward motion of the atmosphere.

Conclusion

From the observational evidence available today, it would seem reasonable to suppose that apart from the component due to the gravitational red-shift, all the cases of spectral line shifts discussed by Freundlich can be accounted for by Doppler shifts due to relative motions in the stellar atmospheres or of the stars themselves.

We are indebted to Professor W. H. McCrea for correspondence on this topic, and also for sending us a draft of his paper.

References

Adams, W. S., 1941, *Ap. J.*, **93**, 11.
Blaauw, A., 1952, *Bull. Astro. Netherlands*, No. 433.
Blaauw, A., and Morgan, W. W., 1953, *Bull. Astro. Netherlands*, No. 448.
Delhaye, J., and Blaauw, A., 1953, *Bull. Astro. Netherlands*, No. 448.

FREUNDLICH, E. F., 1953, *Göttinger Nachrichten*, 95 ; 1954 a, *Proc. Phys. Soc.* A, **67,** 192 ; 1954 b, *Phil. Mag.*, **45,** 303.
McCREA, W. H., 1954, *Phil. Mag.*, **45,** 1010.
MORGAN, W. W., WHITFORD, A. E., and CODE, A. D., 1953, *Ap. J.*, **118,** 318.
PLASKETT, H. H., 1947, *Mon. Not. R. Astro. Soc.*, **107,** 117 (p. 139).
PLASKETT, J. S., 1930, *Mon. Not. R. Astro. Soc.*, **90,** 616, 621.
PLASKETT, J. S., and PEARCE, J. A., 1929, *Amer. Astro. Soc.*, **6,** 277.
POPPER, D. M., 1950, *Ap. J.*, **111,** 495.
SMART, W. M., and GREEN, H. E., 1936, *Mon. Not. R. Astro. Soc.*, **96,** 568.
TRUMPLER, R. J., and WEAVER, H. F., 1953, *Statistical Astronomy* (Berkeley: University of California Press).
WEAVER, H. F., 1953, *Pub. Astro. Soc. Pacific*, **65,** 132 ; 1954, *Vistas in Astronomy* (London: Pergamon Press).

CXIII. *Some more Remarks on Freundlich's Red-Shift*

By D. ter Haar
St. Salvator's College, University of St. Andrews*

[Received June 23, 1954]

Abstract

It is pointed out (i) that there seem to exist certain definite line-shifts in stellar spectra which can not be accounted for by existing astrophysical theory ; (ii) that in those cases where one would expect to be able to find the relativistic gravitational red-shift, only an effect which is much smaller has been observed ; (iii) that apart from McCrea's arguments against photon–photon scattering as the explanation of the Freundlich effect one can adduce other arguments against this explanation.

The recent paper by Freundlich (1954) on red-shifts in the spectra of celestial bodies is the subject of discussion in the preceding two papers by McCrea and by E. M. and G. R. Burbidge. The Editors of the *Philosophical Magazine* have asked me in the absence of Professor Freundlich to comment on these papers and it is the purpose of the present note to do this briefly. I should like to mention the following points.

(*a*) It should be mentioned that the main purpose of Freundlich's paper was not so much to explain the various red-shifts which he discusses as well to draw attention to a great amount of observational material which has not been explained by current astrophysical theory. In this connection it should also be mentioned that Freundlich himself did not attach great weight to his formula (1) but only put it forward as a possibility to fit the various data.

(*b*) McCrea states that Freundlich's red-shift could only be due to photon–photon scattering and bases this conclusion essentially on Freundlich's formula (1). However, if Burbidge and Burbidge are right in their statement that the value of the K-effect is much smaller than the one used by Freundlich, and if one uses a much larger value for the temperature of the Wolf–Rayet stars (in view of our very limited knowledge about these stars, any value of their effective temperature must be viewed with great suspicion) one can only conclude that red-shifts occur which increase with increasing effective temperature of the star. In that case the effect might be due, for instance, to photon–electron scattering, as the electron pressure increases with increasing effective temperature. Moreover, as long as we do not have any idea as to the wave-length dependence of the scattering cross section for this particular effect—if it exists—it is rather rash to say anything at all about the temperature dependence to be expected.

(*c*) As far as Born's explanation (1954) is concerned, it should be mentioned that this particular process runs into the following difficulty. His effect has a cross section which is about equal to the square of the Compton wave-length, that is, about 10^{-24} m^2 which in the solar atmosphere with a

---

* Communicated by the Author.

photon density of about 10^{18} m^{-3} would lead to a mean free path of about 10^{6} m which is ten times as long as the depth of the solar atmosphere. (This corresponds to McCrea's remark that only one in 30 of the emerging photons would be effected.) Born's effect would thus never lead to a red-shift but only to a broadening of the spectral lines.

(*d*) Even if one accepts the new value of 2·5 km/sec for the K-effect, there still remains an unexplained red-shift corresponding to at least 1 km/sec, since the gravitational red-shift can only amount to about 1 to 1·5 km/sec (see, e.g., Freundlich 1954, table 1).

(*e*) Even if one accepts the plausible explanation of Burbidge and Burbidge that the Orion Nebula due to one-sided ionization is moving relative to the Orion Nebula group, there still remains a red-shift of at least 5 km/sec of the O-stars relative to the B-stars.

(*f*) The fact that the red-shift varies along the solar disc might be due to the fact that the absorption is produced in different layers of the atmosphere. However, it must be remarked, that McCrea in his § 3.1 gets the same dependence on θ as Freundlich does, but with a different numerical constant. This last point, however, is not of great importance if one treats Freundlich's formula (1) as being only a very rough approximation (compare the arguments under (*a*)).

(*g*) An effect which should possibly be studied in more detail is the so-called Lindholm effect. This is pressure broadening accompanied by a red-shift. Unfortunately any influence of this effect, which in any case seems to be smaller than the red-shifts observed on the sun (Margenau, private communication), will increase the discrepancy between the observed solar red-shifts and the expected gravitational red-shift.

(*h*) It is interesting to mention in this connection that there are indications that spectra taken from hot gases behind fast shocks show spectrum lines which are broadened as well as shifted to the red (Laporte, private communication*).

(*i*) Finally, there remains the fact that in those cases where one would expect to find the full gravitational red-shift (McCrea's argument in favour of the full effect is very strong) only a fraction of the effect is found. This is especially disturbing in the case of the sun, as one might argue with McCrea that our knowledge of the atmospheric conditions in white dwarfs is very limited.

Concluding, I would like to repeat McCrea's statement that " the actual phenomena to which Freundlich directs attention call for much further investigation, both observational and theoretical ".

References

Born, M., 1954, *Proc. Phys. Soc.* A, **67**, 193.
Freundlich, E. F., 1954, *Phil. Mag.*, **45**, 303.

---

* Laporte writes in this connection : " It is certainly not improbable that Professor Freundlich's red-shift is of a similar nature."

Note added in Proof.—It is interesting to note that O. Struve (*Sky and Telescope*, May 1954) arrives at the essentially same conclusion, namely, that Freundlich's formula (1) is unlikely to be correct, but that the effects to which he draws attention merit closer consideration.

CXIV. *Measurements of Forty-four Charged V-Events*

By J. S. Buchanan, W. A. Cooper, D. D. Millar* and J. A. Newth
The Physical Laboratories, The University, Manchester†

[Received May 26, 1954]

Abstract

The measurements made on 44 charged *V*-events are reported and discussed. Arguments are presented to show that most of the events are *not* the decays of τ- or K_μ-mesons, nor are they ‘ cascade ’ decays. The simplest explanation of the majority of the events is that they are decays of a heavy meson into a light charged meson and two light neutral particles. From the results of other experiments the charged secondary particles are probably μ-mesons.

The primary particle in one event has a mass of at least $(1184 \pm 90)m_e$. This event is discussed in detail.

On the assumption that all the events are of the same type, the mean lifetime of the primary particles is found to be greater than 2×10^{-9} sec. Attempts to distinguish a group of particles with a shorter mean lifetime have failed.

Twenty-nine of the primary particles are positively charged, thirteen negatively; the signs of two particles cannot be determined. The positive excess is attributed, in the main, to a statistical fluctuation.

§ 1. Introduction

In this paper the measurements made on 44 charged *V*-events are reported, interpreted and discussed. The events were observed in a large magnet cloud chamber at the Jungfraujoch (Astbury *et al.* 1952, Page and Newth 1954). Some of the events have been reported previously (Astbury *et al.* 1952, 1953, Newth 1954) but in view of the difficulties that are arising in the synthesis of all the experimental results on charged heavy mesons we consider it necessary to present a detailed account of our observations. A typical event is shown in Plate 31.

In considering the significance of our results we have used the survey by Rochester and Butler (1953) as a summary of all the early work on heavy mesons. The discussion at the Bagnères de Bigorre Cosmic Ray Congress (1953) and the recent work of Gregory *et al.* (1954) have shown that the subject is, if anything, growing in complexity.

---

* Now at the School of Physics, The University, Sydney, Australia.

† Communicated by Professor P. M. S. Blackett, F.R.S.

The decay schemes that have been suggested for the charged heavy mesons are

$$\tau^{\pm} \rightarrow \pi^{\pm}+\pi^{+}+\pi^{-}+75\ \text{Mev} \quad . \quad . \quad . \quad . \quad . \quad . \quad (1)$$

$$\tau^{\pm} \rightarrow \pi^{\pm}+\pi^{0}+\pi^{0}+86\ \text{Mev} \quad . \quad . \quad . \quad . \quad . \quad . \quad (2)$$

$$\mathrm{K}^{\pm} \rightarrow \pi^{\pm}+?^{0} \quad . \quad . \quad . \quad . \quad . \quad . \quad . \quad . \quad . \quad (3)$$

$$\mathrm{K}^{\pm} \rightarrow \mu^{\pm}+\mathrm{n}^{0}+\mathrm{n}^{0} \quad . \quad . \quad . \quad . \quad . \quad . \quad . \quad . \quad (4)$$

$$\mathrm{K}_{\mu}{}^{+} \rightarrow \mu^{+}+\mathrm{n}^{0}, \quad . \quad . \quad . \quad . \quad . \quad . \quad . \quad . \quad . \quad (5)$$

where n^0 is used to indicate a light neutral particle (probably a neutrino or γ-ray). Decay scheme (1) is well established. (2) has been discussed theoretically by Dalitz (1953) and an example of such a decay has been reported by Crussard *et al.* (1954). Schemes (3) and (4) are those proposed by the Bristol workers (Powell 1952) to account for their observations in the emulsion experiments. Good evidence for (5) has been presented by the Ecole Polytechnique group (Gregory *et al.* 1954) but the number of neutral secondary particles involved is not yet certain. From the results obtained at the Massachusetts Institute of Technology (Rossi and Bridge 1953) it seems certain that some, but not all, of the n^0 particles among the decay products must be γ-rays.

The masses of the K-mesons remain rather uncertain. The most accurate measurements have been quoted by Gregory *et al.* (1954) who find a mass of $(914 \pm 20)m_e$ for the $\mathrm{K}_{\mu}{}^{+}$-particles ; this value is significantly less than the mass of the τ-meson $(967 \pm 3)m_e$. There is also strong evidence for the existence of mesons with mass greater than $1000\, m_e$ (see, for example, Daniel and Perkins 1954 and the discussion at the Bagnères Congress) but how such mesons decay is not known.

There is evidence that some of the V-events seen in cloud chambers show the decay of charged hyperons and such decays have also been observed in photographic emulsion. The frequency of these decays seems to be small and, as we have no evidence to suggest that any of our events should be interpreted in this way, we attempt to correlate our measurements with the decay schemes (2 to 5) of the heavy mesons.

§ 2. MEASUREMENTS

(*a*) *Momenta*

The cloud chamber is photographed on 35 mm film at a mean magnification of 1/20. Stereoscopic photographs are taken, the angle between the two views being 9°. The curvatures of track images are measured on both photographs using a travelling microscope with a micrometer eyepiece. The coordinates found with the microscope are plotted on a large scale and a curve is fitted to them by eye. Momenta are derived from these curvatures after allowing for the variation of the magnification with the depth of the track in the cloud chamber. For steeply dipping tracks this correction can be large but the illuminated volume of the cloud chamber is only 15 cm deep and steeply dipping tracks are always short.

For tracks inclined at an angle of less than 30° to the plane of the chamber the correction to the mean curvature measured on the film is always less than 20%.

The precision of momentum measurement is limited, at present, by convective distortion of the tracks in the cloud chamber. This distortion is almost certainly the result of temperature differences inside the chamber although these are certainly not greater than *c.* 0·1°c. Under normal conditions the maximum detectable momentum (m.d.m.) has been measured to be about 4×10^9 ev/c for tracks 25 cm long. However, the temperature conditions are not constant and the amount of distortion can vary markedly.

By inspection it is possible to observe gross distortions (corresponding to the magnetic curvature of particles of momentum 2×10^9 ev/c). In the absence of such gross distortions the m.d.m. assumed for tracks more than 25 cm long has been 4×10^9 ev/c. For shorter tracks we have made the extremely pessimistic assumption that the m.d.m. varies as l^2 where l is the length of the track. In no case has significance been attached to measurements giving momenta greater than 2×10^9 ev/c.

As a result of this unsatisfactory situation the only accurate measurements of magnetic curvature are those leading to momenta less than 5×10^8 ev/c. Fortunately, all the heavily-ionizing K-mesons have momenta below this value and the measurements of their tracks give valuable information. The only use made of the decays of fast particles has been in the determination of their mean lifetime. The inherent statistical error in this determination is so large that large random errors in the momenta of the particles can be tolerated.

(*b*) *Angles*

Each event is reconstructed in space by stereoscopic projection of the photographs through lenses similar to those used for photography. From this reconstruction the angle in space between the primary and secondary tracks is found. To find the angle between the trajectories of the two particles a simple correction is made for the uniform dilation of the gas in the cloud chamber during expansion.

(*c*) *Ionization Densities*

Eleven of the *V*-events were produced by slow primary particles. The velocities of these particles were estimated from the density of the ionization in their tracks. To do this, four observers independently examined the tracks and compared them with the tracks of protons whose momenta had been measured. Attention was concentrated on the track structure, that is, the frequency of gaps and unresolved clusters of drops along the track, and on the numbers of energetic δ-rays. From this comparison each observer gave an estimate of the velocity. The results are discussed in § 4.

§ 3. CLASSIFICATION OF *V*-EVENTS

In table 1 we give the measurements of P_1 and P_2, the momenta of the primary and secondary particles in each *V*-event. The angle (ϕ) is the angle between the secondary track and the continuation of the primary track through the point of decay. In general, the events have

Table 1. Measurements on 44 Charged *V*-Events

1 Event	2 Sign	3 Angle ϕ (deg.)	4 P_1 (10^8 ev/c)	5 $\Delta(1/P_1)$ (%)	6 P_2 (10^8 ev/c)	7 $\Delta(1/P_2)$ (%)	8 t (10^{-10} sec)	9 T (10^{-10} sec)
AE 7	+	15±2	6·0*	100	—	—	0·7*	0·7*
JB 127	−	95±7	2·3	20	—	—	7·5	20·2
JK 23	+	80±7	2·1	25	—	—	5·9	13·4
JS 23	+	89±3	6·0	100	0·41	10	1·3	1·9
NJ 93	−	53±2	3·5	15	2·8	20	12·8	14·2
NN 13	?	35±2	9·0*	100	—	—	1·0*	1·3*
NC 75	+	57±2	5·5*	100	—	—	4·5*	9·4*
NS 61	−	11±1	9·5*	100	4·3	60	4·1*	4·8*
NT 249	+	28±2	10·0*	100	4·9	20	0·8*	2·4*
NR 194	+	18±2	11·0*	300	5·1	15	0·5*	3·0*
NZ 357	+	45±5	15·0	50	—	—	1·9	3·7
OD 557	−	43±3	12·0	20	4·3	40	3·8	4·2
OE 316	+	14±1	5·8	75	—	—	9·7	9·7
OE 483	+	38±3	5·4*	150	3·1	70	1·2*	4·2*
OE 489	+	36±1	10·0*	100	5·8	100	1·3*	2·1*
PB 100	+	22±2	15·0	80	—	—	2·2	2·5
PE 65	−	29±1	15·0	80	—	—	1·9	2·1
PL 93	−	19±3	20·0	100	2·6	25	1·0	2·4
QD 138	+	47±3	1·9	15	2·3	15	18·5	31·1
QE 854	+	15±1	11·0*	250	5·0	20	0·4*	5·1*
QF 635	+	58±2	12·0	30	3·0	50	3·4	4·5
QG 284	−	20±2	8·0*	150	—	—	3·0*	6·6*
QH 425	−	55±2	7·0	25	1·4	15	2·5	5·0
QL 707	+	32±2	2·2	25	3·0	10	9·9	18·6
QM 861	+	82±2	3·5	30	0·67	15	11·8	15·0
QR 720	−	20±3	12·0*	150	5·3	15	0·5*	4·8*
QR 979	−	89±2	1·2	15	0·51	10	8·1	8·1
QT 937	+	31±3	1·2	10	—	—	12·6	13·4
QU 1046	+	57±2	3·2	30	—	—	5·5	7·8
QW 557	+	41±3	8·0*	100	4·5	30	0·4*	3·7*
RC 290	+	62±2	3·2*	100	3·1	40	2·4*	10·9*
RC 886	+	11±2	29·0*	100	13·0	40	0·0	1·7*
RC 941	+	18±1	13·0*	100	—	—	1·2*	3·2*
RD 25	+	31±2	8·0	100	2·5	80	2·4	7·2
RD 264	−	14±1	6·0	70	2·6	50	3·7	9·2
RD 473	−	40±1	7·0	14	2·1	25	5·2	7·6
RE 410	+	11±1	21·0*	100	9·6	25	0·2*	2·6*
RF 254	+	37±1	11·4*	50	2·0	50	1·2*	4·3*
RF 2000	+	19±1	22·0*	70	10·0	100	1·6*	2·4*
RG 585	+	75±1	3·2	16	1·2	16	3·6	15·4
RH 478	?	17±1	6·0*	100	—	—	0·6*	1·4*
RM 253	+	45±2	6·0*	100	3·6	10	1·2*	6·7*
RM 541	−	23±1	4·4*	70	2·0	30	0·6*	9·5*
RP 993	+	117±2	2·1	5	2·5	8	25·0	27·8

The measurements made on 44 charged *V*-events. Column 3 gives the angle between th primary and secondary tracks. Columns 4 and 6 give the momenta of the primary and secondar particles. The errors in these momenta (columns 5 and 7) are expressed as a fraction of $1/P$ sinc the error in $1/P$ is approximately symmetrical. Those values marked with an asterisk have bee estimated as described in § 6.

Columns 8 and 9 contain information needed for the lifetime determination; this is discusse in the text (§ 6).

The first eleven events in the table were reported by Astbury *et al.* (1952) and a reproductio of event QD 138 was published by Newth (1954).

been classified as V-events by considering only the three quantities P_1, P_2 and ϕ. In 9 of the 44 events the difference between the velocities of the primary and secondary particles (estimated from the ionization they produced) provided additional evidence. In this section we discuss the criteria used for classification. This subject has been considered in detail by Armenteros *et al.* (1952) and we have made only slight modifications to their criteria.

An event with a heavily-ionizing primary particle is easily identified as a decay since the mass of the primary may be directly estimated. The characteristic difference between the primary and secondary tracks well shown in event RP 993 (Plate 32). Such events may sometimes allow interpretation as neutral V-decays with upward-moving primaries. Usually the geometrical association of the event with a shower above the chamber makes this interpretation unlikely.

The decays of fast charged V-particles have been selected by examining all the sharp deflections in the tracks of fast particles and excluding those that could be attributed to other known processes. These other processes are the decay of light (π- or μ-) mesons, large angle scattering in the gas of the cloud chamber or a nuclear interaction in the gas giving a one-prong star.

In the decay of light mesons the momentum (p^*) of the charged secondary particle in the centre of mass system is small. For $\pi \rightarrow \mu$ decay the value is 29 MeV/c and for $\mu \rightarrow$ e decay $p^* \leqslant 55$ MeV/c. In the laboratory system the transverse component ($P_2 \sin \phi$) of the secondary momentum is always less than p^*. An event for which $P_2 \sin \phi$ is greater than 55 MeV/c cannot therefore be the decay of a light meson.

To discriminate against Coulomb or nuclear scattering it is necessary to decide under what conditions a recoiling argon nucleus would produce a recognizable ‘ blob ’ of ionization. Information on this point is scanty but from the measurements of Blackett and Lees (1932) it appears that an argon nucleus with a momentum of 100 MeV/c should have a visible track of length 0·5 mm in argon at atmospheric pressure. Assuming that a track of this length would be recognized, we have identified as charged V-events all those for which the vector difference between the primary and secondary momenta is larger than 100 MeV/c and in which no recoil track is visible. To use this criterion it is not necessary to know the values of both P_1 and P_2 since either $P_1 \sin \phi$ or $P_2 \sin \phi$ gives a lower limit to the vector difference between P_1 and P_2.*

---

* When both P_1 and P_2 were measured we were able to use a simple dynamical argument to discriminate against events due to large angle elastic scattering. When a fast light particle is scattered by a heavy nucleus the change in momentum of the scattered particle is small for small angles of scattering. For example, when a proton of momentum 10^9 eV/c is scattered through a small angle ϕ by an argon nucleus it loses a fraction of its momentum given by $\delta P/P = 0{\cdot}03\ (1-\cos\phi)$. For a fast meson the fraction is even smaller. The difference between P_1 and P_2 need not, therefore, be as large as 100 MeV/c to exclude interpretation of some events as scatters.

Before selecting events for analysis as *V*-decays we have assumed the measured momenta and angles to be simultaneously altered by one standard deviation in such a way as to make the event fit best an alternative interpretation. Only if the altered measurements were incompatible with a different interpretation was any event accepted as a *V*-decay.

Any one of our events can be interpreted as a single-pronged nuclear ‘ star ’ in the gas of the cloud chamber. For such a star to simulate a *V*-decay the recoil momentum must be carried by one or more neutral particles leaving the nucleus. The number of stars of this type can be roughly estimated in the following way. In all, we have identified 150 stars in the gas of the chamber. Among these there are 3 which superficially resemble charged *V*-events but for the presence of a single low-energy proton emitted from the interaction. In each of these three events there is a detectable ‘ blob ’ of ionization produced by the recoiling nucleus. We expect stars from which neutrons are emitted to have similar characteristics and therefore think it unlikely that any of our events are single-prong stars.

§ 4. DYNAMICS OF THE DECAYS

(*a*) *Direct Mass Estimates*

The primary particles in 11 events had momenta below 350 MEV/*c*. The velocities of these particles were estimated by the rather unsatisfactory procedure described in § 2 (*c*). The results are shown in table 2.

Table 2. Direct Estimates of the Masses of Slow *V*-Particles

Event	Sign	Primary momentum (10^8 ev/c)	Primary velocity ($\beta = v/c$)	Primary mass (m_e)
JB 127	−	1·9 to 2·9	0·40 to 0·46	710 to 1300
JK 23	+	1·6 to 2·7	0·31 to 0·40	740 to 1600
NJ 93	−	3·0 to 4·0	0·40 to 0·60	790 to 1900
QD 138	+	1·6 to 2·2	0·37 to 0·43	670 to 1100
QL 707	+	1·7 to 2·8	>0·46	<1020
QM 861	+	3·0 to 6·0	0·43 to 0·52	970 to 2500
QR 979	−	1·0 to 1·3	<0·31	>610
QT 937	+	1·1 to 1·3	0·24 to 0·34	600 to 1000
QU 1046	+	2·2 to 4·2	0·46 to 0·60	580 to 1600
RG 585	+	2·7 to 3·7	>0·52	<1190
RP 993	+	2·0 to 2·2	0·29 to 0·40	920 to 1440

The momenta quoted in column 3 are one standard deviation above and below the measured value. The velocities (β) were obtained by comparing visually the ionization density in the tracks with that produced by protons of known velocity. In column 4 the range of values of β includes the estimates made by four observers. The masses in column 5 result from combining extreme values of momentum and velocity from the preceding columns.

The limits to the momenta given in column 3 have been obtained by altering the measured value of P_1 (table 1) by one standard deviation. The error includes convective distortion of the tracks, multiple Coulomb scattering of the particles and uncertainty in the strength of the magnetic field. The values of β given in column 4 were obtained from the comparison with proton tracks ; the range of values includes the estimates made by each of the four observers. The mass values given in column 5 were obtained by combining the values of momentum and velocity in the previous columns.

It is clear that no great faith can be put in subjective estimates of β made in this way. However, we think that we are justified in concluding from the results shown in table 2 that all 11 particles could have a unique mass in the range from 900 m_e to 1100 m_e. There is no reason to think that any of these particles are hyperons.

(*b*) *The Transverse Momentum Distribution*

Some information about the decay processes can be obtained from the distribution of the 'transverse' momenta ($P_t = P_2 \sin \phi$) of the secondary particles. The transverse momentum is unaltered by a transformation from the laboratory system to the centre of mass system and thus $P_2 \sin \phi = p^* \sin \theta$ where p^* and θ are the momentum and angle of emission of the secondary in the centre of mass system. For a two-body decay p^* is constant and the distribution of the values of p_t is easily calculated (Podolanski and Armenteros 1954). Butler (1954) has summarized the earlier results obtained from charged *V*-events and has compared the experimental distribution with that to be expected for two-body decay.

In 15 of the events reported here the measured values of P_2 have an error of 20% or less ; since the errors in the values of ϕ are usually negligible, the errors in p_t for these 15 events are also 20% or less. In fig. 1 (*a*) the distribution of these values is shown as a histogram. In fig. 1 (*b*) we have added to our 15 events 17 events observed at the Pic du Midi and reported by Butler for which the values of p_t were measured with the same accuracy. Unfortunately, there is a strong experimental bias against including events with values of p_t less than 100 MeV/*c* since many fast charged *V*-decays are classified as such because p_t is greater than this value. An unbiassed distribution can be obtained by using only those events where the primary particle is heavily ionizing. These are identified without reference to the transverse momentum. In fig. 1 (*c*) the distribution of p_t for 8 events of this type is given (7 are events reported here and 1 is from the Pic du Midi data).†

In fig. 1 the interrupted lines show, for comparison, the distribution

---

† The requirement of 20% accuracy in the values of p_t means that a slight bias is introduced into the distribution. This is because long secondary tracks are confined to directions nearly in the plane of the cloud chamber. With a large sample of events it would be easy to avoid this bias. In our distribution it is, in fact, negligible.

Fig. 1

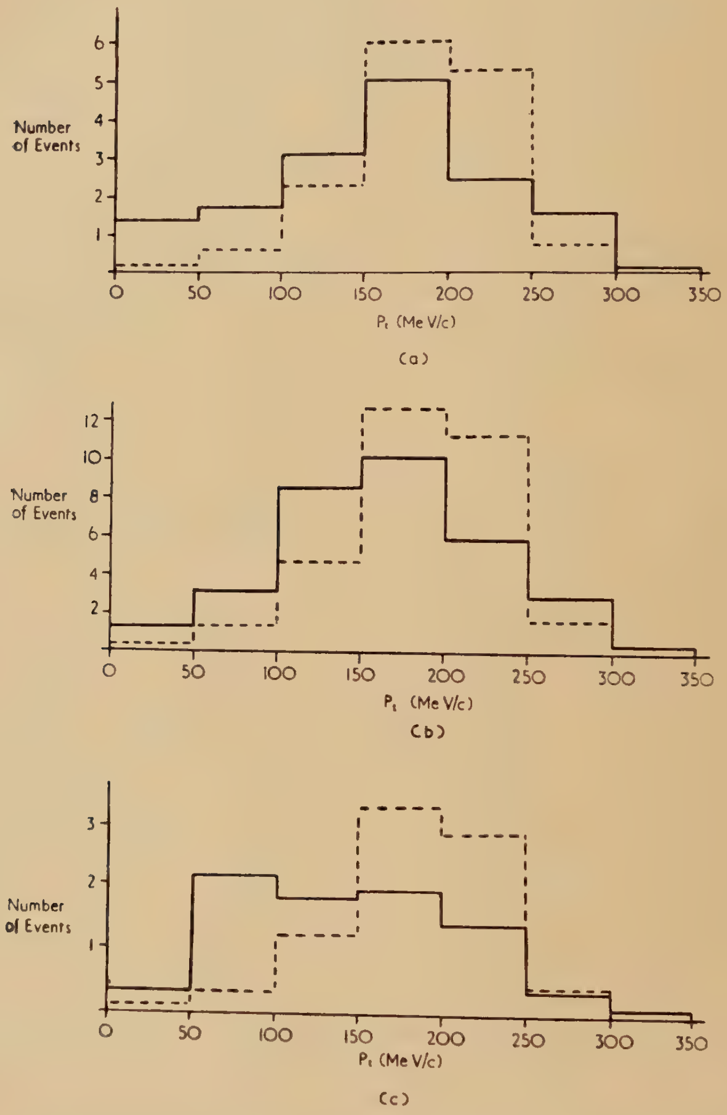

The transverse momenta of secondaries in charged *V*-events.

Histograms giving the distribution of the transverse momenta ($p_t = P_2 \sin \phi$) in charged *V*-events. (*a*) gives the distribution obtained from 15 events reported in this paper where the error in measurement is 20% or less. In (*b*) these 15 values have been added to 17 values of similar accuracy reported by Butler (1954). (*c*) is the distribution obtained by considering only the 8 events where the primary particle was heavily-ionizing.

The interrupted lines show the distribution to be expected if all the events were two-body decays with $p^* = 220$ Mev/c.

that would be expected if all the events were produced by a two-body decay process with $p^*=220$ MeV/c. This value is chosen since it gives reasonable agreement with the experimental histogram.

The histograms of fig. 1 do not provide convincing evidence for or against the existence of a two-body decay process. They are presented partly to show the difficulty of interpreting the measurements and partly to enable other experimental data to be added to our results.

(c) *Further Dynamical Analysis*

For an event where P_1, P_2 and ϕ are all measured it is possible to make a further dynamical analysis. If the masses of the charged primary and secondary particles are assumed, the momentum (p^*) of the secondary in the centre of mass frame of reference can be calculated. Alternatively, if a specific two-body decay process (such as that suggested for the K_μ-particles) is assumed, the mass of the primary particle may be calculated.

We have made these calculations for 11 events and the results are given in table 3. Although the errors are large, the figures in table 3 are not compatible with a single value of p^* and we are forced to conclude that our events can only be interpreted by a three-body decay process or by more than one type of disintegration. We defer discussion of this conclusion until § 7.

In calculating the values of p^* quoted in table 3 we have assumed masses of $1000\,m_e$ and $209\,m_e$ for the primary and secondary particles. With this assumption it is energetically impossible for the value of p^* to exceed 233 MeV/c. Event RP 993 cannot, therefore, be a decay of this type ; it is discussed fully below.

§ 5. EVENT RP 993

Event RP 993 is of exceptional interest since it cannot be interpreted as the decay of a particle of mass $<1000\,m_e$ into a light meson. The event is reproduced in Plate 32.

The primary particle has a mass which is estimated (table 2) to be between $920\,m_e$ and $1440\,m_e$. The secondary particle has a momentum of (250 ± 20) MeV/c and its ionization is near to minimum (i.e. $\beta>0{\cdot}6$). From these values its mass must be less than about $700\,m_e$—allowing interpretation as a light meson or an electron.

If the event is assumed to be a two-body decay, the values of P_1, P_2 and ϕ, together with two secondary masses, determine uniquely the value of the primary mass. By choosing the rest-mass of the neutral secondary to be zero (a neutrino or γ-ray) a *minimum* value for the primary mass is found. When this calculation is made for event RP 993 the minimum primary mass is found to be $1184\,m_e$ on the extreme assumption that the charged secondary is as light as an electron.

The results of the calculation are set out in table 4. The charged secondary particle has been assumed, in turn, to be an electron, a

μ-meson and a π-meson. The calculated primary mass is insensitive to the value of P_1 assumed and its variation with P_2 is shown in the table. The angle (ϕ) is measured to ±2° and this error has a completely negligible effect on the calculation.

Table 3. Dynamical Analysis of 11 Charged *V*-Events

	Event	Sign	p^* (mev/c)	Mass of primary (assuming K_μ-decay) (m_e)
Group A	QR 979	−	56 (+26) (− 4)	420 (+35)
	QM 861	+	102 (+40) (−21)	620 (+125)
	RG 585	+	133 (+33) (−20)	680 (+97)
	RD 473	−	145 (+60) (−29)	720 (+146)
Group B	QH 425	−	161 (+55) (−34)	780 (+130) (− 95)
	QD 138	+	182 (+39) (−28)	740 (+170) (−100)
	QL 707	+	209 (+38) (−36)	840 (+190) (−170)
	NJ 93	−	224 (+65) (−37)	920 (+230) (−135)
Group C	RP 993	+	329 (+30) (−28)	1220 (− 80)
	OD 557	−	387 (+343) (−126)	1310 (−280)
	QF 635	+	440 (+670) (−180)	1360 (−350)

The results obtained from two methods of analysing the decay events. p^* is the momentum of the charged secondary in the centre of mass frame of reference; the values have been calculated by assuming the masses of the primary and secondary particles to be 1000 m_e and 209 m_e respectively.

The values of the primary mass in the last column have been calculated by assuming that each event is a two-body decay into a charged μ-meson and a neutral particle of zero rest-mass (the K_μ-decay scheme).

The errors given in parentheses are *larger than* standard errors. They have been obtained by altering simultaneously the values of P_1 and P_2 by one standard deviation in such a way as to produce the greatest variation in p^*. This procedure is desirable since the errors in P_1 and P_2 are not independent and their effect on the values of p^* and M is complicated.

The importance that is attached to this event clearly depends upon the reliability of the measurement of P_2. The quoted error of ±20 mev/c is based on the maximum detectable momentum measured for near-vertical tracks in the cloud chamber while the secondary of RP 993 is inclined at 60° to the vertical. Tracks at this inclination are likely to suffer more from distortion than do those near to the vertical. However, the secondary track in event RP 993 is 30 cm long and shows no irregularity in its curvature. Neighbouring photographs show no evidence of abnormal convective distortion. For these reasons we consider the quoted error to be a realistic estimate and conclude that the event provides very strong evidence for the existence of K-mesons with mass greater than 1000 m_e.

Two other interpretations of the event are possible. First, it could be the decay of an upward-moving neutral *V*-particle—decaying, presumably, into a K^--meson and a light positive meson. If this is so, the energy released in the decay must be *c.* 110 MEV. Second, the event could be a neutron-produced star whose only charged products are a negative heavy meson and a positive light meson. The association of the event with a nuclear interaction above the cloud chamber is evidence against both these interpretations and, as pointed out in § 3, the absence of a recoil nucleus is strong evidence against the event being a star.

Table 4. The Mass of the Primary Particle in Event RP 993

Assumed nature of charged secondary	Mass (m_e) of primary particle for various values of P_2		
	P_2=250 MEV/*c*	P_2=225 MEV/*c*	P_2=200 MEV/*c*
Electron	1184	1091	998
μ-meson	1225	1135	1047
π-meson	1253	1167	1083

The masses given in the table are derived by assuming that the decay is a two-body process and that the neutral secondary particle has zero rest-mass. If the decay is, in fact, a three-body process or if heavy neutral secondaries are produced the values given in the table are lower limits to the primary mass.

The measured value of P_2 is (250 ± 20) MEV/*c*. The direct estimate of the primary mass from momentum and ionization is 920 m_e to 1440 m_e.

It is impossible for the event to be a star produced by a slow proton since the kinetic energy of such a proton would be far less than the energy of the light secondary particle.

§ 6. LIFETIME ESTIMATES

The mean lifetime of the *V*-particles has been estimated from the distribution of their decay points in the cloud chamber. In columns 8 and 9 of table 1 two times (t, T) are given for each event. t is the observed proper time of flight in the cloud chamber of each primary particle and T is the potential observable time of flight (limited by the size of the cloud chamber). These times have been obtained from the corresponding distances (l, L) by using the relation $l=(P_1/M)t$ where M is the mass of the primary particle.

In measuring l and L we have used the correction procedure described by Newth (1954) to ensure that allowance is made for the length of track necessary to identify an event. In finding the times of flight we have, in every event, assumed a value of $1000\,m_e$ for the mass of the primary particle. For those events where P_1 could not be measured directly (marked with an asterisk in table 1) we have made a rough estimate of its value by assuming some features of the decay process. This procedure is justified by the fact that the inherent statistical uncertainty in the calculated mean lifetime is large; it is better to include inaccurately measured events than to ignore completely the information that they provide.

To estimate P_1 we have assumed that every unmeasured event is the decay of a meson of mass $1000\,m_e$ into a μ-meson with a value of p^* of 200 Mev/c. On this assumption an upper limit can be set to P_1 from the value of ϕ alone. Blaton (1950) has shown that the inequality

$$\sin\phi \leqslant p^* M/P_1 m$$

must hold. Substituting the values we assume, we find the upper limit to P_1 to be 920 cosec ϕ Mev/c. A lower limit to P_1 is always obtained from the measurement of track curvature or from the estimate of ionization density. In those cases where only ϕ could be measured accurately we have taken the harmonic mean of the upper and lower limits to P_1 as our assumed value. This corresponds to taking the direct average of the corresponding limits to the time of flight. How accurate this procedure is can be seen from table 1; the error in $1/P_1$ is, for these estimated values, made to include the upper and lower limits.

When both ϕ and P_2 were measured a better estimate of P_1 was made. The longitudinal momentum ($P_2\cos\phi$) of the secondary particle in the laboratory system is related to the corresponding quantity ($p^*\cos\theta$) in the centre of mass system by

$$P_2\cos\phi = \gamma(p^*\cos\theta + \beta E^*),$$

where E^* is the total energy of the secondary in the centre of mass system and γ and β are the usual constants of the Lorentz transformation. In general, we are biased towards the selection of events where p_t ($=p^*\sin\theta$) is large. $p^*\cos\theta$ will therefore be small (its average value is, in any case, zero). If we assume it to be zero we find

$$P_2\cos\phi = \gamma\beta E^*$$

or, since $\gamma\beta = P_1/M$,

$$P_1 = (M/E^*)\times P_2\cos\phi$$

which leads to

$$P_1 = 2{\cdot}2\times P_2\cos\phi$$

when the numerical values corresponding to our assumptions are inserted.[†]

[†] It is interesting to compare this result with the empirical relation used by Barker *et al.* (1952). These workers found the relation $P_1 \sim 2{\cdot}5 P_2$ from a number of events where both momenta were measured and used it to estimate P_1 for events where only P_2 was measurable.

In this way times of flight have been assigned to all the 44 V-particles listed in table 1. The statistical analysis due to Bartlett (1953) has been used to estimate the value of the decay constant $(1/\tau)$ of the particles. The value of $1/\tau$ is found to be very small and the approximate expression for $1/\tau$

$$\frac{1}{\tau} \sim \frac{\Sigma(\frac{1}{2}T-t)}{\Sigma T^2/12} \pm \frac{1}{\sqrt{(\Sigma T^2/12)}}$$

(eqn. 6 of Bartlett's paper) has been used. If all our events are analysed together the resulting value of $1/\tau$ is $(-0\cdot6\pm0\cdot5)\times10^9$ sec^{-1}. A negative value of $1/\tau$ has, of course, no physical meaning and our result means only that the time scale of our observations is too short to obtain more than a lower limit to the mean lifetime of the particles. Such a lower limit is obtained by increasing the value of $1/\tau$ by two (or three) standard deviations. The resulting values of τ are $2\cdot5\times10^{-9}$ sec and $1\cdot1\times10^{-9}$ sec for two and three standard deviations respectively.

This analysis assumes that all the events we consider are decays of the same type of particle. If particles with different mean lifetimes have been included in our classification of V-particles the result of our lifetime determination must be taken to mean that the majority of the particles have a mean lifetime which is considerably greater than 10^{-9} sec; the presence of a component with a shorter mean lifetime is not excluded.

To search for any such component we have divided our events into different classes and made an estimate of the mean lifetime of the particles in each class. These estimates are given in table 5. The separation of positive and negative particles was suggested by the positive excess among our events. Heavily-ionizing particles were treated as a group

Table 5. Estimates of the Mean Lifetime of Charged V-Particles

Class of events	Number and sign	Mean T (10^{-10} sec)	Estimate of $1/\tau$ (10^9 sec^{-1})	$\tau_{2\sigma}$ (10^{-10} sec)
All events	29+ve 13−ve 2?	7·6	$-0\cdot6\pm0\cdot5$	20
Positive particles	29+ve	8·1	$-0\cdot6\pm0\cdot6$	16
Negative Particles	13−ve	7·5	$-0\cdot5\pm1\cdot1$	6
Slow particles (Heavily-ionizing)	6+ve 3−ve	17·0	$-1\cdot2\pm0\cdot6$	∞
Fast Particles ($P_1>10^9$ ev/c)	12+ve 5−ve	3·2	$+1\cdot8\pm2\cdot5$	1·5
Events with $p^*>133$ Mev/c	13+ve 3−ve	9·4	$-0\cdot3\pm0\cdot7$	9

The results obtained from estimating the mean lifetimes of various groups of charged V-particles. Column 3 shows, in effect, the time scale of the observations for each group; column 4 gives the estimate of $1/\tau$ with the statistical error. $\tau_{2\sigma}$ (column 5) is obtained by increasing $1/\tau$ by two standard deviations to find a lower 'limit' to τ. No group of particles provides a finite upper limit to τ.

since their identification as K-mesons is unambiguous. The events with fast primary particles were analysed separately since unstable particles with a very short lifetime might only enter our cloud chamber if their momenta were large. Finally, all the decays in which p^* was significantly greater than 133 Mev/c were treated as a class. This criterion was chosen since a decay with $p^* \leqslant 133$ Mev/c can be interpreted as a τ-meson decaying according to scheme (2).

For none of these groups of particles do we obtain a finite upper limit to the mean lifetime. In fact, all our events are effectively evenly distributed throughout our cloud chamber. To demonstrate this more clearly we show in fig. 2 the distribution of the values of t/T for our events. It is evident that there is no significant departure from a uniform distribution for either positive or negative particles. Thus we find no evidence to support the conclusion of Leighton (1953) that some of the positive V-particles have a mean lifetime as short as c. 10^{-10} sec.

Fig. 2

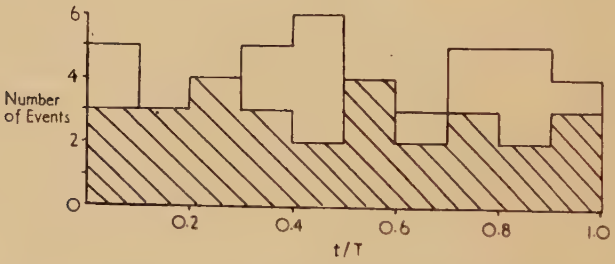

The spatial distribution of charged V Events

The distribution of t/T for the 44 charged V-events showing that the events are evenly distributed throughout the cloud chamber. The contribution to the histogram from the positive V-particles is shaded.

The mean value of t/T for all the events is 0·53 ; the value to be expected from a uniform distribution is $0{\cdot}50 \pm 0{\cdot}04$.

§ 7. Discussion

(*a*) *Decay Processes*

The values of p^* given in table 3 are clearly incompatible with any single unique value. We are forced to the conclusion that our events cannot be interpreted as examples of a single two-body decay process. We consider here the possibility of explaining them by the different processes listed in § 1.

Any one of the events with p^* less than 133 Mev/c (Group A in table 3) can be interpreted as a τ-meson decaying into a single charged π-meson (2). However, Dalitz (1953) has shown on theoretical grounds that the branching ratio between decay schemes (1) and (2) is of the order of unity. We observed only two τ^+-decays of type (1) during our experiments ; therefore not more than two or three of our 44 V-events are likely to be a

τ-decay of type (2). If table 3 includes a representative sample of events there should be at least 10 decays with low values of p^* in all our data. Clearly, most of these must be due to some process other than (2).

The events in group B of table 3 are, dynamically, compatible with the K_μ-decay (5) identified by Gregory *et al.* (1954). Some of the events in groups A and C could also be interpreted in this way. The objection to this interpretation is the strong evidence that Gregory *et al.* produce for the K_μ-mesons being positive only. It is unreasonable to assume that the positive particles in Group B are all K_μ^+-mesons leaving the negative particles to be explained in some other way. While some of our events may be K_μ^+-decays, there is no evidence from the sample in table 3 that many are.

A third process that cannot account for many of our events is the 'cascade' type of decay first observed by Armenteros *et al.* (1952). One of the secondaries in this type of decay is a neutral *V*-particle which can, in favourable circumstances, be observed to decay. From the results of Cowan (1954) it is probable that the neutral *V*-particles produced are Λ^0-particles with a mean lifetime of about 4×10^{-10} sec (Page 1954). The probability of seeing the decay of a neutral *V*-particle coming from each of our events has been calculated.† Excluding only those events for which the direct estimate of the primary mass makes cascade decay impossible, the *average* time for which a neutral *V*-particle would have been inside the illuminated volume of the cloud chamber is $8{\cdot}6 \times 10^{-10}$ sec. Thus if more than two or three of our events were cascade decays we should have observed a neutral *V*-decay; in fact, we observed no such decay.

From these arguments we consider that few of our events can be τ-meson decays, K_μ^+-decays or cascade decays. The simplest explanation is that the great majority are K-meson decays into more than two secondary particles. We cannot say whether the charged secondary particles are π- or μ-mesons but the results of other experiments suggest that our events are of type (4) giving secondary μ-mesons (see discussion at the Bagnères de Bigorre Congress).

The single event RP 993 is convincing evidence for K-mesons with a mass greater than 1000 m_e. If we assume that this event is of the same type as the majority of our events we find that the minimum mass of the primary particles is $(1225 \pm 90)m_e$. It may be, of course, that event RP 993 is an example of a different, rarer, decay process.

(*b*) *Mean Lifetimes*

The conclusion that the majority of charged *V*-particles have a mean lifetime much greater than 10^{-9} sec is confirmed by our analysis. This conclusion evidently applies to particles other than the K_μ^+-mesons and τ-mesons since it holds for negative particles and for particles which decay with large values of p^* (table 5). We conclude that the K-meson that undergoes three-body decay has a mean lifetime $\geqslant 10^{-9}$ sec.

---

† We are grateful to Mr. R. A. Salmeron for making these calculations.

The mean lifetime of charged *V*-particles previously estimated by Astbury *et al.* (1953) was based on observations of negative particles and cannot therefore have referred to K_μ^+-mesons. This estimate

$$(\tau > 4 \times 10^{-9}\ \text{sec})$$

probably remains valid for the particles we consider here.

From our results there is no evidence for particles with a mean lifetime shorter than 10^{-9} sec. We can find no explanation that accounts for our disagreement with Leighton (1953) on this point. Most of our observations were made under circumstances which favoured the observation of short-lived particles (the high yield of neutral *V*-events is good evidence for this) but we find no indication of such particles among the charged *V*-particles.

(*c*) *The Positive Excess*

The positive excess amongst our events is common to all the groups separated in table 5. Unfortunately, it is not reflected by the events in table 3 that could be accurately measured. Therefore it is very difficult to find a satisfactory reason for the excess.

The chance of obtaining a more marked asymmetry if the 44 events were chosen at random from a symmetrical population is *c.* 3%. Thus an explanation of our result as a statistical fluctuation is not unreasonable. In fact, if all the results reported by Butler (1954) and Leighton (1953) are added to ours the total numbers of positive and negative charged *V*-particles are 75 and 70.

Another explanation which could account for the difference between our results and those of Butler (1954) is in the different time scale of the observations. The mean traversal time for the *V*-particles reported by Butler was $2{\cdot}5 \times 10^{-10}$ sec and the numbers of positive and negative particles were 10 and 20. The corresponding time for our observations was 8×10^{-10} sec. Thus, long-lived positive particles such as the K_μ^+-mesons might form a higher proportion of our *V*-particles.

This interpretation is not borne out by more detailed analysis. First, we observe a positive excess among our fast *V*-particles whose mean traversal time is only $3{\cdot}2 \times 10^{-10}$ sec. Second, we should expect to find the K_μ^+-mesons among the slow particles with long traversal times. The positive excess for these particles is no greater than that for our data as a whole.

For these reasons we think that a statistical fluctuation is the most likely cause of the charge asymmetry we observe. In addition, there may be a small proportion of K_μ^+-decays among our events.

§ 8. CONCLUSIONS

We find that the majority of our charged *V*-events are *not* due to τ-meson decays, to K_μ^+-meson decays or to 'cascade' decays. They can most easily be explained by a decay scheme of the form

$$K^{\pm} \rightarrow L^{\pm} + n^0 + n^0,$$

where L represents a charged π- or μ-meson and n^0 is a light neutral particle. From the results of other experiments it is probable that the charged secondary particles are μ-mesons.

The mean lifetime of the K-mesons that decay in this way is considerably greater than 10^{-9} sec and the earlier estimate by Astbury *et al.* (1953) which gave a lifetime greater than 4×10^{-9} sec probably applies to these particles.

The positive excess among the charged *V*-particles we have observed may well be the result of a statistical fluctuation. It cannot be explained entirely by the presence of K_μ^--decays amongst our events.

Event RP 993 provides evidence for the existence of K-mesons with a mass greater than 1000 m_e. If the secondary particle from this event is a μ-meson, the mass of the primary particle must be at least $(1225 \pm 80)m_e$. If the secondary is a π-meson the corresponding minimum primary mass is $(1250 \pm 80)m_e$.

ACKNOWLEDGMENTS

We should like to thank our colleagues, Mr. A. H. Chapman, Mr. G. D. James, Miss P. Miles, Mr. D. I. Page and Mr. R. A. Salmeron, for assistance in obtaining and analysing the results presented in this paper.

We have had several invaluable discussions with members of the Ecole Polytechnique group in Paris and we have drawn heavily on their results and suggestions in writing this paper.

Our work has been supported and directed by Professor P. M. S. Blackett of Imperial College, London: we are deeply indebted to him for guidance.

We record our thanks to Mr. H. Wiederkehr and to the Administration of the Hochalpine Forschungsstation, Jungfraujoch, for making our work in Switzerland possible. Two of us (J. S. B. and W. A. C.) have received grants from the Department of Scientific and Industrial Research during our work.

REFERENCES

Armenteros, R., Barker, K. H., Butler, C. C., Cachon, A., and York, C. M., 1952, *Phil. Mag.*, **43,** 597.

Astbury, J. P., Chippindale, P., Millar, D. D., Newth, J. A., Page, D. I., Rytz, A., and Sahiar, A. B., 1952, *Phil. Mag.*, **43,** 1283.

Astbury, J. P., Buchanan, J. S., Chippindale, P., Millar, D. D., Newth, J. A., Page, D. I., Rytz, A., and Sahiar, A. B., 1953, *Phil. Mag.*, **44,** 241.

Barker, K. H., Butler, C. C., Sowerby, M. G., and York, C. M., 1952, *Phil. Mag.*, **43,** 1201.

Bartlett, M. S., 1953, *Phil. Mag.*, **44,** 249.

Blackett, P. M. S., and Lees, D. S., 1932, *Proc. Roy. Soc.* A, **134,** 658.

Blaton, J., 1950, *K. danske Vidensk. Selskab. Mat-fys. Medd.*, **24,** no. 20, p. 25.

Butler, C. C., 1953, *Report of the Bagneres Congress on Cosmic Radiation*; 1954, *Proc. Roy. Soc.* A, **221,** 339.

Cowan, E. W., 1954, *Phys. Rev.*, **94,** 161.
Crussard, J., Kaplon, M. F., Klarmann, J., and Noon, J. H., *Phys. Rev.*, **93,** 253.
Dalitz, R. H., 1953, *Proc. Phys. Soc.* A, **66,** 710.
Daniel, R. R., and Perkins, D. H., 1954, *Proc. Roy. Soc.* A, **221,** 351.
Gregory, B., Lagarrigue, A., Leprince-Ringuet, L., Muller, F., and Peyrou, C., 1954, *Nuov. Cim.*, **11,** 292.
Leighton, R. B., 1953, *Report of the Bagneres Congress on Cosmic Radiation.*
Newth, J. A., 1954, *Proc. Roy. Soc.* A, **221,** 406.
Page, D. I., 1954, *Phil. Mag.*, **45,** 863.
Page, D. I., and Newth, J. A., 1954, *Phil. Mag.*, **45,** 38.
Podolanski, J., and Armenteros, R., 1954, *Phil. Mag.*, **45,** 13.
Powell, C. F., 1952, *Report of Copenhagen Conference*, June 1952.
Rochester, G. D., and Butler, C. C., 1953, *Rep. Prog. Phys.*, **16,** 364.
Rossi, B., and Bridge, H. S., 1953, *Report of the Bagneres Congress on Cosmic Radiation.*

CXV. *Evidence for the β-Decay of a K-Meson*

By M. W. Friedlander, D. Keefe,* M. G. K. Menon† and L. van Rossum‡
H. H. Wills Physical Laboratory, University of Bristol§

[Received July 8, 1954]

Summary

The decay at rest of a K-meson in which the secondary particle appears to be an electron of ~90 mev has recently been observed. The secondary particle, after traversing a distance of 2·3 cm in the emulsion, appears to have been sharply deviated ; thereafter, the track is closely similar to that of a slow electron. The grain density in the track, before and after the deviation, is indistinguishable from the ' plateau value '. The most plausible explanation of this behaviour is that it is due to the sudden loss of energy of an electron through the production of *bremsstrahlung*. Alternatively, the secondary particle could be assumed to be (*a*) a π-meson which interacts with a nucleus and undergoes change exchange, the product nucleus subsequently suffering β-decay, or (*b*) a μ-meson which decays in flight. The last two possibilities have been considered and appear very improbable.

§ 1. Introduction

During the past three years, more than a hundred examples of the decay of heavy charged mesons, each of which produces a single secondary charged particle, have been observed in photographic emulsions. In a few of these events the secondary particle has been arrested in a stack of plates and has then been identified, in some cases as a π- in others as a μ-meson ; in a few others, reliable measurements of mass have been carried out by observations of grain density and multiple scattering. When the grain density is appreciably above the plateau value, the particle must necessarily be a light meson, but whether a π- or a μ-particle could not always be established. In most of the events, however, the grain density of the secondary track is equal to g_p, the plateau value, to within the statistical fluctuations, and the possibility cannot be excluded that the secondary particle is an electron. Hitherto however, there has been no positive evidence in favour of the presence of electrons among the secondary particles.

---

* On leave of absence from University College, Dublin.

† Senior Scholar of the Royal Commission for the Exhibition of 1851.

‡ On leave of absence from the Faculté des Sciences, Paris.

§ Communicated by Professor C. F. Powell, F.R.S.

In order to identify a particle as an electron, it is necessary to show that the grain-density of the track is indistinguishable from that at plateau, and that the value of $p\beta$ is significantly lower than that for a μ-meson of the same grain density. Alternatively, a sudden reduction in the energy of the particle may occur—detectable by a deviation in the track, and a significant change in the value of $p\beta$—as a result of the creation of *bremsstrahlung*. The probability of such a process varies inversely as the square of the rest mass of the particle and therefore occurs very rarely for particles other than electrons.

In this laboratory we have recently observed the transformation of a K-meson in which the secondary particle makes a collision in which it appears to lose energy by *bremsstrahlung*. Certainly the charged particle after the collision is an electron. Although other possibilities cannot be excluded, the evidence strongly suggests the β-decay of a K-meson. Details of the measurements are described in § 2, and the various possible interpretations and conclusions discussed in § 3.

The results of preliminary measurements on this event were presented at the Padova Conference (April 1954).

§ 2. EXPERIMENTAL DETAILS

The event shown in Plate 1, was found in the course of general scanning for slow heavy mesons. The track of the primary particle is $190\,\mu$ long in the emulsion in which the meson decayed. It was traced through four emulsions for a total length of 8·7 mm and was found to have originated in a star of type $4+0n$. Of the other three tracks from the star, two were traced to their ends in the emulsion and were probably due to protons ; the third particle left the stack.

2. 1. *The Heavy Meson*

Mass determinations on the K-particle were made by two independent methods :

(i) *Multiple Scattering and Range*

Scattering measurements were carried out on the last 6·7 mm of track recorded in four emulsions including the one containing the point of decay. The mass values obtained were : $800\pm150\,m_e$ $(\bar{\alpha}R)$ and $720\pm190\,m_e$ (constant sagitta method). The usual cut-off procedure was employed in which all signals greater than $4\bar{D}$, where $\bar{D}$ is the mean, are removed, but there was only one signal greater than this value when using the $(\bar{\alpha}R)$ method, and none in the ' constant sagitta ' method. Since the nuclear disintegration from which the K-particle was emitted is close to the edge of the emulsion, no measurements were made on the first 1·3 mm of track near the star.

(ii) *Photometric Measurements of Track-density*

The apparatus used for these measurements will be described in detail in a later publication, but the main features of the method are outlined in the Appendix. The mass of the K-particle as determined by this method was $1050 \pm 100\ m_e$.

2. 2. *The Secondary Particle*

The secondary track is 100 μ long in the emulsion in which the decay was observed, but it could be traced through 11 emulsions, its average length in each being 2 mm. After 710 μ in the 12th emulsion there is a sudden deviation in the track (see B, Plate 33) ; thereafter the track has all the characteristics of a low energy electron (∼5 MeV). The total length of the track from the point of decay to ‘ B ’ is 2·3 cm. Details of the measurements on the secondary track are given in the table.

Plate number	Projected length (mm)	$\bar{\alpha}_{100\mu}$ ‡			Normalized grain density g^*
		(*a*) without cut-off	(*b*) $4\bar{D}$ cut-off	(*c*) $4\bar{D}$ cut-off with replacement	
31†	0·10	—	—	—	—
30	2·38	0·32	0·32	0·32	1·06
29	2·09	0·35	0·24	0·33	0·92
28	2·06	0·22	0·22	0·22	1·05
27	1·91	0·19	0·19	0·19	0·94
26	1·95	0·24	0·24	0·24	0·97
25	1·92	0·33	0·33	0·33	1·01
24	1·81	0·17	0·17	0·17	1·11
23	1·80	0·32	0·32	0·32	0·93
22	1·70	0·21	0·21	0·21	1·07
21	1·85	0·48	0·30	0·42	0·97
20	1·67	0·38	0·30	0·37	1·08
19	0·70	—	—	—	—
Average over all plates :		0·293 ± 0·021	0·261 ± 0·019	0·275 ± 0·020	1·01 ± 0·02

† Plate 31 contains the decay of the heavy meson.

The errors in the individual values of g^* and $\bar{\alpha}_{100\mu}$ are ∼6% (±0·06) and ∼20% (±0·06) respectively.

‡ The values in this table have been obtained after elimination of noise between different cell sizes, and are in perfect agreement with those calculated using the method of cross products. It is known that the latter method is very sensitive to the presence of distortion ; the agreement therefore provides strong evidence against the presence of any appreciable distortion on the track.

The values of the scattering parameter in the individual plates, $\bar{\alpha}_{100\mu}$, are given in the table. They have been calculated, using three different procedures : (*a*) with no ‘cut-off’ (column 3) ; (*b*) with a $4\bar{D}$ cut-off (column 4), those signals being removed which exceed four times the mean of the second differences taken from observations in all the emulsions; (*c*) with a $4\bar{D}$ replacement cut-off (column 5). In this last procedure, those signals removed as described in (*b*) are replaced by values equal to four times the mean of the second differences. When appropriate scattering constants, as derived from Molière's theory, are used in conjunction with these three procedures, the corresponding values of $p\beta$ agree to within $2\frac{1}{2}\%$. The mean value of $p\beta$ is $88{\cdot}5 \pm 6$ MeV/c assuming the particle to be an electron, and $90{\cdot}0 \pm 6$ MeV/c if it is an L-meson. Values of the normalized grain density, g^*, obtained for each emulsion strip are given in the table. In each plate the counts were made on a segment of track in the central layer of the emulsion, and about 300 grains counted. The normalization was made by comparison with the tracks of high energy electron pairs. The mean value of g^* was found to be $1{\cdot}01 \pm 0{\cdot}02$, which is not significantly different from the plateau value. A π-meson of this ionization would have a value of $p\beta$ of $\gtrsim 130$ MeV/c and a μ-meson $\gtrsim 100$ MeV/c. The grain density and scattering measurements are therefore consistent with the assumption that the secondary particle was an electron or a μ-meson, but make it very improbable that it was a π-meson.

Although the mass measurements do not allow a definite identification of the secondary particle, the appearance of the track at B (Plate 33) strongly favours the view that it was an electron. At the point B, while still at plateau ionization and in a region of the emulsion free from processing or manufacturing defects, the secondary particle suddenly changes direction, and this deviation is accompanied by a large increase in multiple scattering without any change in grain density. After the point B, the track is almost certainly due to an electron with an energy of ~ 5 MeV. This observation strongly suggests the reduction in energy of a high energy electron through a collision involving the production of *bremsstrahlung*. We therefore suggest that this event is probably an example of the decay of a K-meson into an electron. If so, it is the first example yet observed of such a process.

In view of the importance of such a conclusion, especial care has been taken to ensure that no error could have occurred in following the track through the emulsion strips. This has been done by carefully matching successive plates, using suitable neighbouring grey and black tracks. In every case, the continuation of the secondary track from the heavy meson was found within a few microns of its predicted position, and not once was an alternative track found. The values of the various measured parameters in the individual plates, shown in the table, display the expected degree of internal consistency.

§ 3. DISCUSSION

It is known that the charged secondary particles arising in the decay of K-mesons are in some cases μ-mesons and in others π-mesons, and one may therefore attempt to interpret the present event in terms of:

(*a*) a π-meson secondary arising from (i) the decay of the χ-meson, $\chi^{\pm}\rightarrow\pi^{\pm}+N^{\circ}$; (ii) the alternative mode of decay of the τ-meson, $\tau^{\pm}\rightarrow\pi^{\pm}+2\pi^{\circ}$; (iii) the nuclear interaction of a K^{-}-meson; or

(*b*) a μ-meson secondary produced by the decay of a K-particle.

The behaviour of the track at B (see Plate 33), could be explained in terms of the nuclear interaction in flight of a charged π-meson, with the production of a slow β-particle. The cross sections for processes of this type are known from work on artificially generated particles. The probability of our observing such a process is 5×10^{-2} for π^{-}-mesons, and 2×10^{-3} for π^{+}-mesons. In obtaining these estimates, we have taken into account the *total* track length of all *possible* π-meson secondaries in emulsions arising in the decay of K-mesons. These considerations taken in conjunction with the independent grain density and scattering measurements, make it very improbable that the observed secondary particle is a π-meson.

This conclusion may be supported by the following arguments. The energy of the secondary particle at emission, as deduced from the measured scattering, and assuming it to be a π-meson, was ~57 MEV, a value consistent with the maximum energy (54 MEV) for a π-meson arising in the alternative mode of decay of the τ-meson. If so, however, the value of g^{*} in the track should change from $\sim1{\cdot}4$ at emission, to $\sim1{\cdot}7$ towards the end of the observed 2·3 cm of track. Such an increase of grain density certainly does not occur. On the other hand, if the π-meson is assumed to arise in the decay of the χ-particle, the observed value of $p\beta$ is widely different from that reported earlier.

A possible alternative explanation, though a very improbable one, is that the secondary particle is a μ-meson which at point B, undergoes decay in flight into an electron. This would not be inconsistent with the grain density and scattering measurements. The probability of observing such a process is, however, only 4×10^{-4}, when one considers the integrated path length of all *possible* μ-meson secondaries arising from the decay of K-mesons hitherto observed in emulsions.

The Decay Scheme $K\rightarrow\beta$

The above considerations make it very improbable that the secondary particle is a L-meson. We therefore suggest that the event corresponds to a mode of decay: $K^{\pm}\rightarrow e^{\pm}+$ one or more neutral particles. The grain density and scattering measurements, and the behaviour of the particle as shown in Plate 33 (Point B) are completely consistent with the interpretation that it is an electron which loses energy in producing *bremsstrahlung*. It is known that in such a process, at high energy, it is very probable that the electron will lose most of its energy. It may be remarked that the radiation length in emulsion is 2·9 cm, and that the secondary particle had travelled a distance of 2·3 cm up to point B. If an electron, it was therefore probable that the secondary particle would produce radiation by *bremsstrahlung* in its observed length of path.

If the decay is a two-body process involving a known neutral particle, a θ°-particle (of mass $\sim 966\,m_e$) must have been emitted. The mass of the primary would then be $1175\,m_e$, which is not inconsistent with the photometric mass measurement. No evidence for the transformation of the neutral particle was discovered in a scan of the available 6·7 mm along its expected line of motion.

On the other hand, if the primary particle is assumed to have a mass close to $1000\,m_e$, then in order to avoid the introduction of a new type of neutral particle it is necessary to interpret our event in terms of a decay involving more than two bodies. It is then possible that the event represents an alternative mode of decay of a type of K-meson of which the existence is already established.

ACKNOWLEDGEMENTS

We wish to thank Professor C. F. Powell for the hospitality and facilities of his laboratory. We are grateful to Miss Rosemary Mitchell who found the event and Mr. A. R. Gattiker and Miss P. Dyer for the photograph. Certain of us wish to thank the following bodies : National University of Ireland for a Travelling Studentship and University College, Dublin, for additional assistance and leave of absence (D.K.) ; the Royal Commission for the Exhibition of 1851 for a Senior Studentship (M.G.K.M.), Centre Nationale de la Recherche Scientifique for financial assistance (L.v.R.) and also Professor M. Morand in whose laboratory the photometric apparatus was constructed.

APPENDIX

The main features of the photometric method used in the determination of the mass of the primary particle are as follows :

(*a*) The residual ranges in emulsion of two particles having the same velocity are in the ratio of their masses. At points of the same velocity along both tracks the photometric track density must be the same for each, provided one ensures that all the physical conditions governing the formation of the track and the measurement of its density, are identical at these two points. Two factors which influence the photometric track density to a serious extent are the variation both in the degree of development and in the contrast of the image, as one proceeds from the top to the bottom of the emulsion-strip. But for two particles which cross a given layer of emulsion, with the same velocity at the centre of this layer, the mean photometric densities along both track segments must be the same, independent of their respective angles of dip and no matter what the variation with depth of contrast and development. It is thus possible to choose the position of calibration proton tracks such that the photometric density along the comparison segments are affected to exactly the same degree by these factors as the density at the corresponding segment on the track of the K-particle. This of course is valid only if the track segments are straight and if the variation of ionization along them can be supposed to be linear. The layer thicknesses in the present case were chosen such that these conditions were satisfied. It may also be pointed out that the variation of contrast with depth in an emulsion strip was less than 5% and this may be compared with the variation of development with depth of about 10%.

The contraction of emulsion upon processing causes foreshortening of all inclined tracks, resulting in an increase in the measured density, and a simple geometrical correction is necessary to arrive at the true mean track density. This is the only effect for which a correction to the measured density is required.

(*b*) The two emulsion strips which contained that part of the track of the K-particle between residual ranges $200\,\mu$–$5\,200\,\mu$ were divided into four suitable horizontal layers and the mean track density was measured in each. A selection was made of nine convenient proton tracks which had mean track densities within 10% of that of the K-particle in the same layer, and density measurements were carried out on these along a total length of 28 mm. Most of the proton tracks were suitable for measurements in more than one layer. By interpolation, those proton ranges were found which corresponded to the measured mean densities in the four sections of the K-particle track.

In the present instance, the situation was complicated by the fact that the track segment measured was from 2·4 mm to 5·1 mm from the edge of the emulsion and so the degree of development was expected to depend, in addition, on the distance from the edge. For this reason, the calibration proton tracks were chosen even more carefully in order to eliminate this further effect.

The mass of the K-particle as stated before, was found to be,

$$1050\,m_e \pm 100\,m_e.$$

The main contribution to the error comes from the statistical fluctuation in the density. The error quoted includes, however, a cautious estimate of the uncertainties arising from the fact that in the neighbourhood of an edge the surfaces of constant degree of development are no longer horizontal. No significant abrupt changes in velocity were observed along the track.

CXVI. *Counters with Random Dead Time*

By Alladi Ramakrishnan
Department of Physics, University of Madras*

[Received in revised form March 8, 1954]

Summary

The problem of determining the probability distribution function $\pi(n, t)$ of the number of registered events n in a time interval t when the dead times following the registered and unregistered events are themselves stochastic variates is solved using a method developed recently by the author and P. M. Mathews (Ramakrishnan and Mathews 1953).

§ 1. Statement of the Problem

Events occur at random in time according to the Poisson distribution, $\exp[-\lambda t]\,(\lambda t)^n/n!$ representing the probability that n events occur in time t. Due to resolving time a counter does not register all events and two types of counters have been considered by many authors.

Type I. Every registered event is followed by a dead time τ during which no event is registered. An unregistered event is not followed by a dead time.

Type II. Every event, registered or unregistered is followed by a dead time τ during which no event is registered.

We shall here solve the stochastic problem of determining $\pi(n, t)$, the probability that n events are registered in time t given that an event was registered at $t=0$, when the dead time has a probability distribution $R(\tau)$ in the case of both Type I and Type II counters. The probability distribution $\pi(n, t, a)$ when the dead time is exactly a, i.e., $R(\tau)=\delta(\tau-a)$ where δ is the Dirac delta function is well known in the two cases.

The above problem will illustrate in a striking manner the nature of the difficulty involved in assuming a probability distribution for a parameter occurring in a probability distribution function. In such cases we have to examine how the parameter enters into the distribution. In the present problem when we say the dead time has a distribution function we obviously mean that the dead times following the events are independent stochastic variates but have the same probability distribution function as distinguished from the case when we require that all the dead times following the events are *equal* but the dead time is a stochastic variable. It is only in the latter case the problem is quite simple involving elementary integration of $\pi(n, t, a)$ over the parameter a.

---

* Communicated by the Author.

§ 2. DESCRIPTION OF THE METHOD

We are given that an event is registered at $t=0$. Let $\omega(t)dt$ be the probability that the *next* registered event occurs between t and $t+dt$ and $f_1(t)dt$ the probability that a registered event occurs in dt irrespective of what happens between 0 and t. Then according to Ramakrishnan and Mathews, $\omega(t)$ or $f_1(t)$ uniquely determines $\pi(n, t)$, the probability that n registered events occur in time t. If $\eta(s)$, $\psi(s)$, $p(n, s)$ are the Laplace Transforms* of $\omega(t)$, $f_1(t)$ and $\pi(n, t)$ respectively,

$$p(n, s)=\frac{1}{s}\frac{[\psi(s)]^n}{[1+\psi(s)]^{n+1}}=\frac{[\eta(s)]^n[1-\eta(s)]}{s} \quad . \quad . \quad . \quad . \quad . \quad (1)$$

In any stochastic problem we must determine $\omega(t)$ *or* $f_1(t)$.

§ 3. TYPE I COUNTER

In type I counter it is easier to compute $\omega(t)$ rather than $f_1(t)$.

At $t=0$ an event is registered. The joint probability that the dead time following this event lies between τ and $\tau+d\tau$ and the next registered event occurs between t and $t+dt$ is

$$R(\tau) \exp [-\lambda(t-\tau)]\lambda \, dt \, d\tau \quad (t>\tau). \quad . \quad . \quad . \quad . \quad . \quad (2)$$

Thus the total probability that the next registered event occurs between t and $t+dt$ is

$$\omega(t) \, dt=\int_0^t R(\tau) \exp [-\lambda(t-\tau)] \, d\tau \, \lambda \, dt \quad . \quad . \quad . \quad . \quad . \quad (3)$$

$$\eta(s)=\lambda \frac{\rho(s)}{s+\lambda} \quad . \quad . \quad . \quad . \quad . \quad . \quad . \quad . \quad . \quad . \quad . \quad . \quad . \quad (4)$$

where $\rho(s)$ is the Laplace Transform of $R(\tau)$.

Thus
$$p(n, s)=\frac{1}{s}\left[\lambda\frac{\rho(s)}{s+\lambda}\right]^n\left[1-\lambda\frac{\rho(s)}{s+\lambda}\right]. \quad . \quad . \quad . \quad . \quad . \quad (5)$$

If $R(\tau)=\delta(\tau-a)$, i.e., in the case of the counter with fixed dead time a, we get the result already obtained by Ramakrishnan and Mathews. $\pi(n, t)$ is obtained by inverting $p(n, s)$.

§ 4. TYPE II COUNTER

In this type, it is very difficult to compute $\omega(t)$. We shall obtain $f_1(t)$ by using the following argument.

We first note that

$$\lambda^{n+1} \exp [-\lambda t] \, d\tau_1 \, d\tau_2 \ldots d\tau_n \, dt$$

is the joint probability that the first event occurs between τ_1 and $\tau_1+d\tau_1$, the second between τ_2 and $\tau_2+d\tau_2$, . . . , the n-th between τ_n and $\tau_n+d\tau_n$ and the $(n+1)$th between t and $t+dt$. If the $(n+1)$th event is to be registered it should be ‘ beyond ’ the dead time ‘ range ’ of *all* the previous events including the initial registered event at $t=0$. Therefore the joint probability that the $n+1$th event occurs in dt and is registered is :

---

* In this paper the Laplace transform of a function $F(x)$ is defined as $\int_0^\infty F(x) \exp [-sx] \, dx$ where s is a complex variable.

$$f_1^{(n+1)}(t)dt=dt\int_0^t\int_{\tau_1}^t\dots\int_{\tau_{n-1}}^t\lambda^{n+1}\exp[-\lambda t]\,\kappa(t)\,\kappa(t-\tau_1)\,\kappa(t-\tau_2)\dots$$

$$\dots\kappa(t-\tau_n)\,d\tau_1\,d\tau_2\dots d\tau_n \qquad . \quad . \quad . \quad . \quad . \quad . \quad . \quad (6)$$

where $$\kappa(\tau)=\int_0^\tau R(\tau')\,d\tau'.$$

$\kappa(\tau)$ represents the probability that the dead time following an event is less than τ. Noticing that the integrand in (6) is symmetrical in $\tau_1, \tau_2, \dots, \tau_n$ we obtain

$$f_1^{(n+1)}(t)=\frac{\lambda^{n+1}}{n\,!}\int_0^t\int_0^t\dots\int_0^t\kappa(t)\,\kappa(t-\tau_1)\,\kappa(t-\tau_2)\dots\kappa(t-\tau_n)\,d\tau_1\,d\tau_2\dots d\tau_n \qquad . \quad . \quad . \quad (7)$$

$$=\kappa(t)\,\frac{\lambda\exp[-\lambda t]}{n\,!}\left[\lambda\int_0^t\kappa(\tau)\,d\tau\right]^n. \qquad . \quad . \quad . \quad . \quad . \quad . \quad . \quad . \quad (8)$$

Thus $f_1(t)dt$ the probability that an event is registered between t and $t+dt$ is given by

$$f_1(t)dt=\sum_{n=0}^{\infty}f_1^{(n+1)}(t)\,dt=\lambda\kappa(t)\exp\left[-\int_0^t\lambda[1-\kappa(\tau)]d\tau\right]dt. \qquad . \quad . \quad . \quad (9)^*$$

The formal solution of the problem is now complete since $p(n, s)$ is uniquely determined by $\psi(s)$, the Laplace Transform of $f_1(t)$.

REFERENCES

Hammersley, J. M., 1953, *Proc. Camb. Phil. Soc.*, **49,** 623.

Ramakrishnan, Alladi, and Mathews, P. M., 1953, *Phil. Mag.*, **44,** 1122.

Takacs, Lajos, 1952, *Math. Rev.*, **13,** 1956.

---

* In a private communication, J. Mackenzie (Division of Tribophysics, University of Melbourne) has informed me that he has arrived at the expression for $f_1(t)$ independently by using identical arguments.

CXVII. *On the Molecular Distribution Functions of a One-Dimensional Fluid : II*

By Alladi Ramakrishnan and P. M. Mathews
Department of Physics, University of Madras*

[Received March 22, 1954]

Abstract

The method of ‘ basic functions ’ developed by one of us (Ramakrishnan 1954) in a previous contribution to this Journal† is used to derive the molecular distribution functions of a one-dimensional fluid with an intermolecular potential defined recently by Sells, Harris and Guth (SHG 1953). It is shown that in the approach to the asymptotic form there is an essential difference between positive and negative potentials.

§ 1. Introduction

In Paper I one of us (R) developed a method of derivation of the molecular distribution functions of a one-dimensional fluid. It consists in first deriving the ‘ basic function ’ of the distribution, given the inter-molecular potential, and obtaining the molecular distribution functions in terms of the ‘ basic function ’. To illustrate the use of the method we shall apply it to the case of a one-dimensional fluid with an inter-molecular potential $V(t)$ defined by

$$\left.\begin{array}{ll} V(t)=\infty, & 0<t<a \\ V(t)=\epsilon, & a<t<b \\ V(t)=0, & t>b \end{array}\right\} \quad . \quad . \quad . \quad . \quad . \quad . \quad (1)$$

when t is the distance of a particle from the previous one.

§ 2. Derivation of the ‘ Basic Function ’

As there is no point in reproducing details of the method already elaborated in Paper I, we proceed directly with the derivation of the ‘ basic function ’, which is defined by

$$\omega(t)=\frac{1}{\Omega(\lambda)}\exp\{-\lambda t-\beta V(t)\} \quad . \quad . \quad . \quad . \quad . \quad (2)$$

where

$$\Omega(\lambda)=\int_0^\infty \exp\{-\lambda t-\beta V(t)\}dt, \quad . \quad . \quad . \quad . \quad . \quad (3)$$

---

* Communicated by the Authors.

† Hereafter we refer to it as Paper I.

λ is the parameter of the 'free' distribution and β the familiar constant in the partition functions. If $V(t)$ is defined by (1) then

$$\Omega(\lambda)=\frac{1}{\lambda}[c\exp\{-\lambda a\}+(1-c)\exp\{-\lambda b\}] \quad . \quad . \quad . \quad (4)$$

where $c=\exp\{-\epsilon\beta\}$, i.e.

$$\omega(t)=\frac{\lambda\exp\{-\lambda t\}[cH(t-a)+(1-c)H(t-b)]}{c\exp\{-\lambda a\}+(1-c)\exp\{-\lambda b\}} \quad . \quad . \quad . \quad (5)$$

where H denotes the Heaviside unit function, i.e. $H(x)=0$ if $x<0$, $H(x)=1$ if $x>0$.

§3. THE MOLECULAR DISTRIBUTION FUNCTIONS

If $f_n^{(F)}(t_1, t_2, \ldots, t_n)$ is the product density of degree n (it is called a molecular distribution function) of molecules in a 'free' distribution, then, recalling the earlier results,

$$f_n^{(F)}(t_1, t_2, \ldots, t_n)=f_1^{(F)}(t_1)f_1^{(F)}(t_2-t_1)\ldots f_1^{(F)}(t_n-t_{n-1}) \quad . \quad . \quad (6)$$

and

$$f_1^{(F)}(t)=\sum_{n=1}^{\infty}\omega(n, t), \quad . \quad . \quad . \quad . \quad . \quad . \quad . \quad (7)$$

where $\omega(n, t)\,dt$ is the probability that the nth particle (omitting the particle at $t=0$) occurs between t and $t+dt$. If $\eta(n, s)$ is the Laplace transform of $\omega(n, t)$,

$$\eta(n, s)=[\eta(s)]^n, \quad . \quad . \quad . \quad . \quad . \quad . \quad . \quad . \quad (8)$$

where $\eta(s)$ is the Laplace transform of $\omega(1, t)\equiv\omega(t)$, the 'basic function'. If $\omega(t)$ is given by (5),

$$\begin{aligned}\eta(s)&=\frac{\Omega(s+\lambda)}{\Omega(\lambda)}\\ &=\frac{1}{\Omega(\lambda)}\frac{1}{\lambda+s}[c\exp\{-(\lambda+s)a\}+(1-c)\exp\{-(\lambda+s)b\}], \quad . \quad . \quad (9)\end{aligned}$$

$$\begin{aligned}\eta(n, s)=\frac{1}{[\Omega(\lambda)]^n(\lambda+s)^n}\sum_{r=0}^{n}c^r(1-c)^{n-r}\binom{n}{r}\exp\{-r(\lambda+s)a\}\\ \times\exp\{-(n-r)(\lambda+s)b\}. \quad . \quad . \quad . \quad (10)\end{aligned}$$

Inverting $\eta\,(n, s)$ we immediately obtain

$$\begin{aligned}\omega(n, t)=\sum_{r=0}^{n}\frac{c^r(1-c)^{n-r}}{[\Omega(\lambda)]^n}\binom{n}{r}\exp\{-\lambda t\}\frac{(t-ra-\overline{n-r}b)^{n-1}}{(n-1)!}\\ \times H(t-ra-\overline{n-r}b). \quad . \quad . \quad . \quad (11)\end{aligned}$$

Our object is to obtain $f_n^{(c)}(t_1, t_2, \ldots, t_n)$ the product density of degree n of the 'constrained' distribution, i.e. when we are given that the $N+1$th particle occurs at L. By arguments now familiar, we have

$$f_n^{(c)}(t_1, t_2, \ldots, t_n)=\sum_{m_i}\frac{\omega(m_1, t_1)\omega(m_2, t_2-t_1)\ldots\omega(m_{n+1}, L-t_n)}{\omega(N+1, L)}. \quad (12)$$

where $\sum\limits_{m_i}$ denotes summation over all m_i such that $\sum\limits_i m_i = N+1$, $m_i \neq 0$. $\omega^{(c)}(n, t)\,dt$ the probability that the nth particle lies between t and $t+dt$ when the distribution is ‘ constrained ’, is given by the equation

$$\begin{aligned}
\omega^{(c)}(n, t) &= \frac{\omega(n, t)\omega(N+1-n, L-t)}{\omega(N+1, L)} \\
&= \left\{ \sum_{r=0}^{n} c^r(1-c)^{n-r} \binom{n}{r} \frac{(t-ra-\overline{n-r}b)^{n-1}}{(n-1)\,!} H(t-ra-\overline{n-r}b) \right\} \\
&\quad \times \left\{ \sum_{r=0}^{N+1-n} c^r(1-c)^{N+1-n-r} \binom{N+1-n}{r} \right. \\
&\quad \left. \times \frac{(L-t-ra-\overline{N+1-n-r}b)^{N-n}}{(N-n)\,!} H(L-t-ra-\overline{N+1-n-r}b) \right\} \\
&\quad \div \left\{ \sum_{r=0}^{N+1} c^r(1-c)^{N+1-r} \binom{N+1}{r} \frac{(L-ra-\overline{N+1-r}b)^N}{N\,!} \right. \\
&\quad \left. \times H(L-ra-\overline{N+1-r}b) \right\}. \qquad \qquad (13)
\end{aligned}$$

The product density of degree one in the case of the ‘ constrained ’ distribution is therefore given by

$$f_1^{(c)}(t) = \sum_{n=1}^{N} \omega^{(c)}(n, t). \qquad \qquad (14)$$

§4. ASYMPTOTIC FORMS OF $f_1^{(c)}$ AND $f_n^{(c)}$

We shall obtain the asymptotic forms of $f_1^{(c)}$ and $f_n^{(c)}$ as N and L are made very large such that $N \gg 1$, $L \gg a, b, t$ but L comparable to Na. We have now to distinguish between two cases.

Case I : $c<1$

This case occurs if ϵ is positive. From elementary probability theory we know that for $N \gg 1$, $\binom{N+1}{r} c^r(1-c)^{N+1-r}$ has a sharp maximum in the neighbourhood of $r=(N+1)c$. Using this simple result and proceeding in the same manner as for deriving a Poisson approximation from a binomial distribution we obtain

$$\begin{aligned}
\omega^{(c)}(n, t) &\sim \sum_{r=0}^{n} \frac{c^r(1-c)^{n-r}\binom{n}{r}}{[\Omega(\lambda_1)]^n} \exp\{-\lambda_1 t\} \\
&\quad \times \frac{(t-ra-\overline{n-r}b)^{n-1}}{(n-1)\,!} H(t-ra-\overline{n-r}b), \qquad (15)
\end{aligned}$$

where

$$\lambda_1 = \frac{N}{L-Na-N(1-c)(b-a)}.$$

Hence we have

Lemma I :

In the asymptotic case when $N \gg 1$, $L \gg a, b, t$ but L is comparable to Na if the intermolecular potential is defined by (1) with ϵ positive, we can replace the 'constrained' distribution by a 'free' distribution with the parameter

$$\lambda = \frac{N}{L-Na-N(1-c)(b-a)}.$$

$f_n^{(c)}$ and $f_1^{(c)}$ are obtained by using (6) and (7).

Case II : $c>1$

This occurs when ϵ is negative. In such a case the procedure adopted above is not valid and we employ the following device.

In (13) we write $c^r(1-c)^{N+1-r}$ as $c^{N+1}(1/c-1)^{N+1-r}$ and $c^r(1-c)^{N+1-n-r}$ as $c^{N+1-n}(1/c-1)^{N+1-n-r}$. We notice that $|1/c-1|<1$ since $c>1$. Consequently $|1/c-1|^{N+1-r}$ decreases rapidly as $N+1-r$ increases. Thus in the denominator only terms involving values of r in the neighbourhood of $N+1$ are significant. Similarly we note that in the numerator as regards the summation $\sum\limits_{r=0}^{N+1-n}$ only terms involving r in the neighbourhood of $N+1-n$ are significant. Using this device we now obtain

$$\omega^{(c)}(n, t) = \sum_{r=0}^{n} \frac{c^r(1-c)^{n-r}\binom{n}{r}}{[\Omega(\lambda_2)]^n} \exp\{-\lambda_2 t\} \times \frac{(t-ra-\overline{n-r}b)^{n-1}}{(n-1)!} H(t-ra-\overline{n-r}b), \quad . \ . \ (16)$$

where

$$\lambda_2 = \frac{N}{L-Na}.$$

Hence we have :

Lemma II :

In the asymptotic case for $N \gg 1$, $L \gg a, b, t$ but L comparable to Na, if the potential is defined by (1) with ϵ negative, we can replace the 'constrained' distribution by a 'free' distribution with parameter

$$\lambda = \frac{N}{L-Na}.$$

§ 5. DISCUSSION OF RESULTS

The main result of Paper I and the present paper is that in the asymptotic case a 'constrained' distribution can be replaced by a 'free' distribution if the value of λ is properly chosen. In Paper I, where we assumed a hard-core model with

$$V(t) = \infty \qquad t<a$$
$$V(t) = 0, \qquad t>a$$

we obtained $\lambda=N/(L-Na)$. The expression for $f_1^{(F)}(t)$ with $\lambda=N/(L-Na)$ is in agreement with that of Salzburg, Zwanzig and Kirkwood (SZK 1953). For the present model we have obtained the 'proper' values of the parameter λ as

$$\frac{N}{L-Na-N(1-c)(b-a)} \quad \text{or} \quad \frac{N}{L-Na}$$

according as ϵ is positive or negative.

The mean density $f_1^{(F)}(t)$ assumes a very simple asymptotic form if $t \gg a$, but $L \gg t$. In such a case $f_1^{(F)}(t) \sim \lambda$. Therefore $f_n^{(F)}(t_1, t_2, \ldots, t_n)$ which is given by (6) reduces to $\lambda f_1^{(F)}(t_2-t_1) \ldots f_1^{(F)}(t_n-t_{n-1})$ if we assume $t_1 \gg a$, $L \gg t_1, t_2, \ldots, t_n$ but $t_2-t_1, \ldots, t_n-t_{n-1}$ are comparable to a.

It is only in regard to the particular asymptotic value of $f_1^{(F)}(t)$, $t \gg a$, that we are not in agreement with SZK and SHG who assume N/L to be the mean density. According to us the mean density is λ which has to be evaluated by finding the asymptotic form or by using the following simple physical argument justifiable in the light of our results.

(1) In the case of a hard core potential the space 'available' is only $L-Na$, since Na is the 'excluded' volume and so the mean density of 'centres' of the spheres is $N/(L-Na)$ at a large distance from the boundary. This value is higher than N/L but it should be remembered that integration over the range 0 to L is not valid since $N/(L-Na)$ is only an asymptotic form. Near the boundary, i.e. for t finite and comparable to a, the density is given by (7) with $\lambda=N/(L-Na)$ or more rigorously by (14) and this is less than N/L.

(2) Considering the SHG potential, it is to be noted that a negative potential cannot increase the 'available' space and so $\lambda=N/(L-Na)$ while a positive potential in the range (a, b) reduces the 'available' space $L-Na$ still further to $L-Na-N(1-c)(b-a)$. We can state therefore that a positive potential of magnitude ϵ in the range $(b-a)$ can be replaced by a hard core potential with range $(b-a)(1-c)$ where $c=\exp(-\epsilon\beta)$. If $c=1$ $(V=0)$ the available space tends to $L-Na$. If $c=0$ $(V \to \infty)$, i.e. if the hard core extends to b, the available space tends to $L-Nb$ as should be expected.

We hope to extend these ideas to any potential function $V(t)$ which can be approximated to a sum of discrete potentials.

APPENDIX

There is an alternative method of deriving the expression for $\omega(n, t)$ in the case of the 'free' distribution. From Paper I we know

$$\omega(n, t)=\int_0^t \omega(\tau)\omega(n-1, t-\tau)\, d\tau.$$

If $\omega(\tau)$ is defined by (2) it is a discontinuous function of τ and the differential form of the above equation is

$$\frac{\partial\omega(n,t)}{\partial t}=-\lambda\omega(n,t)+\frac{c\exp\{-\lambda a\}}{\Omega(\lambda)}\omega(n-1,t-a)H(t-a)$$
$$+\frac{(1-c)\exp\{-\lambda b\}}{\Omega(\lambda)}\omega(n-1,t-b)H(t-b).$$

In the domain $0<t<a$ we know that $\omega(n,t)=0$ for all n except $n=0$ and $\omega(0,t)=\exp\{-\lambda t\}$. The above equation can be solved in two ways.

(i) By a Laplace transformation with respect to t. In such a case it reduces to the method used in this paper.

(ii) Since $\omega(n,t)$ is known in the domain 0 to a for all values of n it can be analytically continued into the entire domain of t.

It is clear that $f_1(t)=\sum_{n=1}^{\infty}\omega(n,t)$ has discontinuities at points $t=k_1a+k_2b$ where k_1 and k_2 are non-negative integers and $k_1+k_2\geqslant 1$. This is also apparent from our solution (11). But if we use this method of analytical continuation we are faced with the problem of defining the successive domains since it is a very difficult task to order the points $t=k_1a+k_2b$ except by actually computing their values. This difficulty is obviated by using the Laplace transform technique.

REFERENCES

RAMAKRISHNAN, ALLADI, 1954, *Phil. Mag.*, **45,** 401.

SALZBURG, Z. W., ZWANZIG, R. W., and KIRKWOOD, J. G., 1953, *J. Chem. Phys.*, **21,** 1098.

SELLS, R. L., HARRIS, C. W., and GUTH, E., 1953, *J. Chem. Phys.*, **21,** 1617.

CXVIII. *A Cloud Chamber Study of the Interactions of Fast μ-Mesons*

By V. Appapillai, A. W. Mailvaganam and A. W. Wolfendale*
The Physical Laboratories, University of Ceylon†

[Received May 20, 1954]

Abstract

A cloud chamber operating in a magnetic field has been used to investigate the production of penetrating secondaries by μ-mesons at sea level. No definite events in which single penetrating secondaries are produced (APP) have been observed. Some possible explanations for the high cross sections for production of APP found by earlier workers are discussed. Events in the cloud chamber attributed to the nuclear interaction of μ-mesons can be explained in terms of the virtual photon interaction postulated by George and Evans (1950).

§ 1. Introduction

The early experiments of Braddick and Hensby (1939) using a cloud chamber operated underground showed the existence of pairs of apparently associated particles (APP) penetrating the lead plate in the cloud chamber. Later, the results of a counter hodoscope experiment by George and Trent (1951) were interpreted in terms of the same phenomenon and assuming that the APP consist of a μ-meson and a single secondary produced in a nuclear interaction, a cross section of 4×10^{-29} cm^2/nucleon was derived for the production of single penetrating secondaries by μ-mesons. Cloud chamber experiments by Braddick, Nash and Wolfendale (1951) gave a similar value for the cross section. These values were an order of magnitude higher than that found by George and Evans (1950) for the production of stars and showers by μ-mesons in nuclear emulsions exposed underground. The discrepancy was ascribed to the lack of nuclear evaporation products in the process of production of single penetrating secondaries and the consequent large reduction in the scanning efficiency for detecting such events in the emulsion. A possible theoretical explanation of the production of APP's was given by Hayakawa (1952). The mechanism allowed penetrating secondaries to be produced without frequent nuclear evaporation, but the theory was later shown to be very improbable by Amaldi *et al.* (1952 a).

---

* On leave from the University of Manchester, England.
† Communicated by Professor P. M. S. Blackett, F.R.S.

A counter hodoscope experiment by Amaldi *et al.* (1952 b) first gave disagreement with the cloud chamber experiments, an upper limit to the cross section for production of APP's of

$$(13 \pm 3) \times 10^{-30} \text{ cm}^2/\text{nucleon}$$

being found.

The present experiment was carried out to clarify the situation. Since its commencement further experiments by Walker (1953), Amaldi *et al.* (1952 c), Deutschmann (1953), Lovati *et al.* (1953 a, b) and Braddick and Leontic (private communication) have all given values much lower than 4×10^{-29} cm²/nucleon for the production of APP's. On the other hand experiments by George, MacAnuff and Sturgess (1953) and George, Redding and Trent (1953) appear to support the original high cross section.

The relation of these results to ours will be considered.

A preliminary account of the results of this experiment has already been given (Wolfendale 1953).

§ 2. The Experimental Arrangement

2.1. *The Apparatus*

The arrangement used to 'trigger' the cloud chamber is shown in fig. 1. The 100 cm lead filter was used to eliminate nucleons from the particle beam and to ensure that only μ-mesons were accepted. A coincidence ABC was then usually due to a μ-meson traversing the filter and cloud chamber. The interactions of μ-mesons in Σ, a 10 cm lead absorber placed immediately above the cloud chamber, were studied.

The cloud chamber was 32 cm in diameter and had an illuminated depth of 6 cm. It contained a single lead plate 2·0 cm in thickness, placed just below the centre of the chamber so that a longer length of track was available above the plate for accurate momentum measurements. In order to reduce track distortions, a rather short delay between expansion and photography—40 msec—was used.

The cloud chamber was operated in a magnet field of 7500 gauss produced by a Blackett-type electromagnet mounted with its 'baseplate' vertical.

2.2. *The Accuracy of Measurement*

Measurements of small curvatures were made using a prism curvature compensator of the type devised by Blackett (1937). Large curvatures were measured using a microscope. The maximum detectable momentum was found to be about 6×10^9 ev/*c*.

§ 3. Experimental Results

6880 photographs showing at least one particle penetrating the lead plate were taken. Photographs showing more than one apparently contemporary particle were carefully examined and the stereoscopic photographs were reprojected to determine the degree of coplanarity of the tracks. The events were classified in the following categories.

Fig. 1

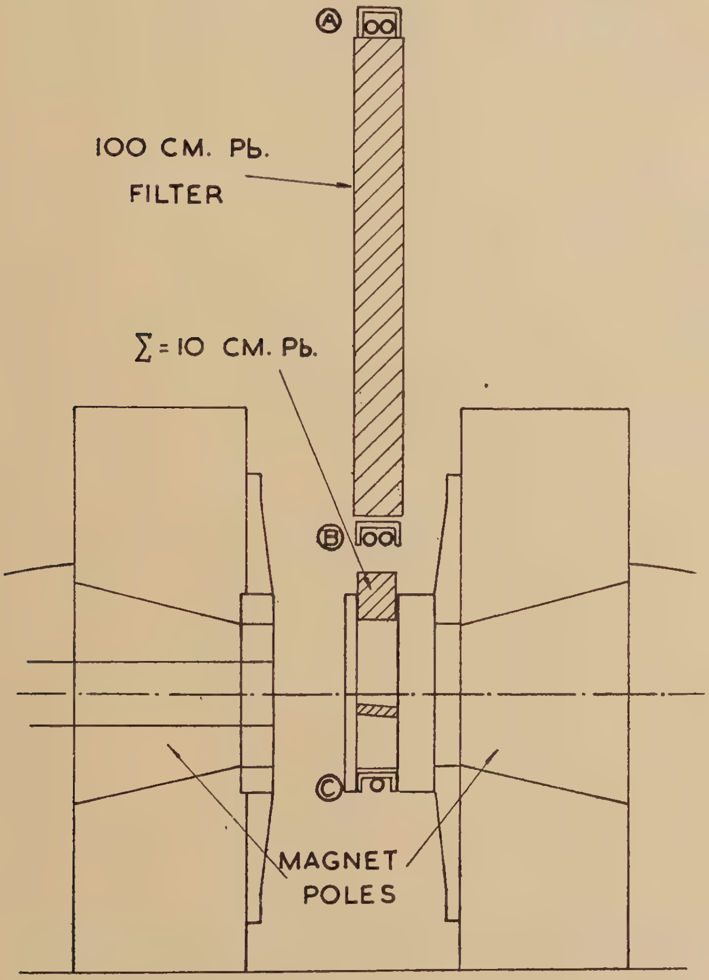

Diagram of the apparatus.

μ-mesons traversing the counter system ABC and the cloud chamber were recorded and their interactions in Σ investigated.

3.1. *Pairs of Tracks Traversing the Plate Unaccompanied and without Multiplication*

The 39 photographs in this category were accurately reprojected and the spatial coordinates of the tracks determined. The heights, above the surface of the plate, of the intersections of the projections of the tracks in the plane of the cloud chamber, H, and the perpendicular plane, h, were determined. The lack of coplanarity θ was defined as the angle, in the perpendicular plane, subtended by two points on one track at heights H and h above the plate, at the point of intersection of the other track with the plate. The height H or h in the plane in which the accuracy of determination was greater (usually the plane of the chamber) is given for each value of θ in fig. 2. It is obvious from the distribution of points in fig. 2 and the fact that almost as many pairs of tracks converge to points

Fig. 2

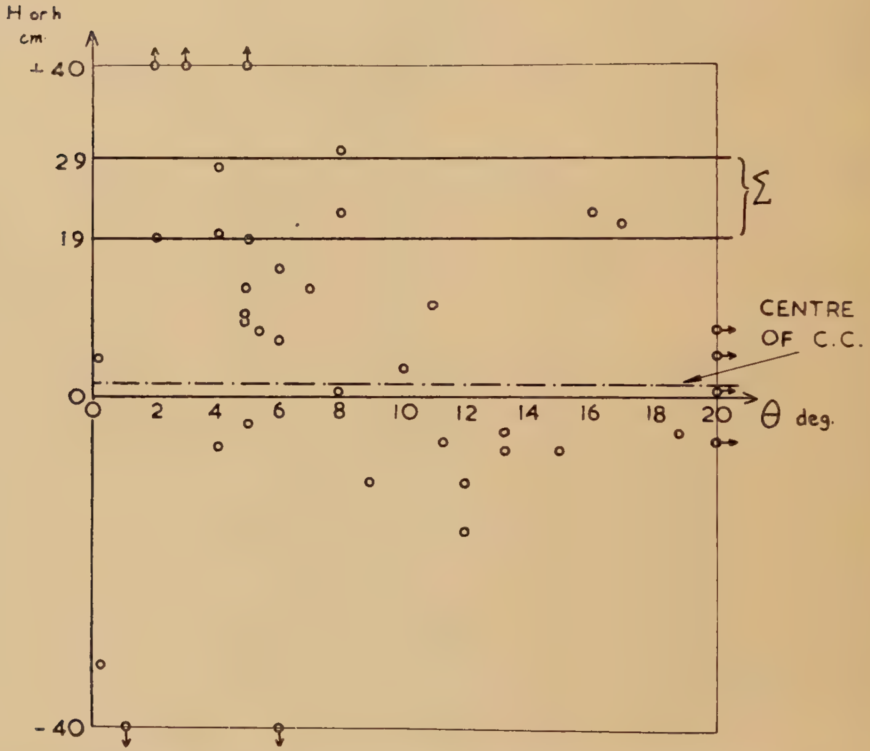

Random associations of pairs of μ-mesons in the cloud chamber. The apparent height of intersection of tracks above the plate (H or h) and the lack of coplanarity θ is given for all apparently contemporary pairs of particles traversing the cloud chamber and penetrating the lead plate.

below the centre of the chamber as diverge from points above it, that most of the events were due to the random association of the particle producing the expansion with another particle passing through the chamber within the resolving time. Only one event was observed where two tracks diverged from Σ and were coplanar to within 2° (the limit for a similar geometrical arrangement used by Braddick, Nash and Wolfendale 1951). In this event the particles had the following properties: (a) negatively charged, $p=(4\cdot2\pm1\cdot5)\times10^9$ ev/c and (b) positively charged,

$p=(1\cdot8\pm0\cdot5)\times10^9$ ev/*c*. However, it is obvious from the density of points in fig. 2, that even this event may be a random association. If μ-mesons produced single penetrating secondaries at small ejection angles and with momenta in the region of 1 Bev/*c* as postulated by Braddick, Nash and Wolfendale (1951), then the effect of scattering in Σ and loss of secondaries from geometrical effects would not be very important and most of the secondaries would have been observed in the cloud chamber having θ less than about 3°.

It is concluded that the number of such secondaries produced in Σ during the experiment was very probably less than 3, and possibly zero.

3.2. *Knock-on Electrons and Positrons from Σ reaching the Plate*

Thirty-eight photographs showed a fast penetrating particle accompanied by a single low momentum secondary from Σ, reaching the plate. The secondaries were all produced in the bottom few mm of the lead absorber and their ionization was equal to the minimum value—(the single case of a secondary having ionization significantly above the minimum value is discussed in § 3.3). Thirty-two of the secondaries were negatively charged and are interpreted as knock-on electrons, the remaining 6 are interpreted as positrons produced in knock-on showers originating in Σ. All the secondaries appeared to stop in the plate. The momentum distribution of the single secondaries is given in table 1.

Table 1. The Momentum Distribution of Knock-on Electrons and Positrons from Σ reaching the Plate

Momentum range in Mev/*c*	0–50	50–100	100–150	150–200	200–250	250–300	300–350	350–400	400–450	>450
No. of electrons	6	17	4(1)	2	2	1	(1)	0	0	0
No. of positrons	2	3(2)	1	(1)	0	0	0	0	(1)	0

The figures in brackets are the numbers of accompanied secondaries. The reduction in number of electrons with momentum less than 50 Mev/*c* is due to the curvature of their trajectories in the magnetic field.

In addition to the photographs showing single secondaries, a number showed small showers produced in Σ. Six particles from showers reached the plate of which only 2 gave rise to observable particles below the plate. The momentum distribution of the accompanied secondaries is also given in table 1. One electron of momentum 136 ± 20 Mev/*c* gave rise to a single positron of momentum 43 ± 7 Mev/*c* below the plate and another electron of 440 ± 70 Mev/*c* produced a single electron of 7 ± 1 Mev/*c* below the plate. In both events the electron above the plate was accompanied by a positron from Σ.

3.3. *Nuclear Interactions of μ-Mesons in Σ*

The expected number of stars and penetrating showers produced in Σ either by protons which have penetrated the filter or by nuclear interacting particles arising from interactions in the filter, has been calculated and found to be negligible. The calculations are based on the sea level proton spectrum given by Mylroi and Wilson (1951). It is considered then, that the interactions observed were due to μ-mesons. Two events were observed in this category.

Event 1 showed a fast μ-meson of momentum $\gtrsim 3\times 10^9$ ev/*c* and probably positive sign accompanied by a positive particle of momentum 425 ± 60 Mev/*c* and estimated ionization in the region of 3× minimum.* A proton of the latter momentum would have an ionization of 4× minimum and the event is thus consistent with an interaction in Σ in which a fast μ-meson produced a proton (with possibly evaporation particles which would be absorbed in Σ before reaching the cloud chamber).

Event 2 showed 4, minimum ionization particles diverging from a point in Σ about 2 cm above the top of the cloud chamber.

Table 2. Momenta and Signs of the Shower Particles in Event 2

Particle	Sign	Momentum in Bev/*c*
a	+	$0{\cdot}63\pm 0{\cdot}07$
b	−	$1{\cdot}4\ \pm 0{\cdot}3$
c	+	$0{\cdot}85\pm 0{\cdot}2$
d	+	$0{\cdot}9\ \pm 0{\cdot}2$

The data for all the particles are given in table 2. Two of the particles, a and b, penetrated the plate without interaction and one particle, c, which reached the plate at the edge of the chamber was accurately coplanar with a positive particle below the plate, of momentum ~170 Mev/*c* and dense ionization consistent with its being a proton. The fourth particle, d, traversed the chamber obliquely and did not reach the plate, its relatively high momentum and large angle with the other particles show that it was very probably not an electron. The event is interpreted as a shower of penetrating particles—probably π-mesons—produced by the nuclear interaction of a μ-meson in Σ.

§ 4. DISCUSSION OF RESULTS AND COMPARISON WITH OTHER OBSERVATIONS

4.1. *Results on Knock-on Electrons*

The results of § 3.2 on the penetration (and otherwise) of the 2 cm lead plate in the cloud chamber by knock-on electrons can be compared with the behaviour expected on the basis of the Monte Carlo calculations of Wilson (1952). Wilson gives the average number of electrons of all energies (and the number with energy >8 MeV) expected below a lead absorber for an incident electron of energy up to 500 MeV. The average number of electrons of all energies expected below our 2 cm lead plate varies from about 1·0 for an incident electron of 100 MeV to about 4·7 for a 400 MeV incident electron. The expected number of electrons having energy greater than 8 MeV varies from about 0·6 to 2·7 between the same limits. An estimate of the probability of only a single electron emerging from the plate can be made assuming that the fluctuations in number obey the Poisson statistical distribution, and using the mean number of emergent electrons given by the Monte Carlo method. We expect accordingly about 10 electrons to give rise to single electrons below the plate, compared with the observed number of 2 such events. It is probable, however, that the expected number is overestimated for two reasons.

---

* The true minimum and plateau ionizations were indistinguishable.

(*a*) Wilson has shown that for primary photons incident on an absorber the probability of a single electron emerging is appreciably less than that calculated on the Poisson distribution, on account of the mechanism of the cascade process. A similar, though smaller, reduction in probability should be expected for incident electrons.

(*b*) The fluctuations in cascade showers are represented better by the Polya distribution, calculations of the Polya probability of electron penetration having been made by Arley (1943). For incident electrons of energy in the range 50–100 MeV (the region in which most of the knock-on electrons detected by us, occurred) the Polya probability of a single electron emerging is only about 50% of the corresponding Poisson probability.

A more realistic estimate of the expected number of ‘penetrating’ knock-on electrons is then about 5, i.e., about 1 knock-on penetrating the 2 cm plate per 1400 traversals of Σ.

The observed number of electrons emerging from the plate is reduced by the loss of low energy electrons due to their increased path in the lead produced by magnetic curvature (e.g., an electron of momentum 2·25 MeV/*c* has a radius of curvature in the magnetic field equal to half the thickness of the plate) and the geometrical loss of secondaries out of the rather small illuminated depth of the chamber. Consequently it is concluded that there is agreement with theory to within at least an order of magnitude.

4.2. *Results on APP's*

The upper limit to the cross section for production of single penetrating secondaries by μ-mesons in lead derived from our experiment is about 6×10^{-30} cm^2/nucleon. This value is not inconsistent with the cross sections found by Amaldi *et al.*, Lovati *et al.*, etc. (see § 1) and indicates that the cross sections found by George *et al.* and Braddick *et al.* are seriously in error. These experiments will now be considered in some detail and an attempt will be made to explain the large cross section found by these workers.

4.2.1. *George and Trent* (1951) *Counter Hodoscope Experiment*

In this experiment the discharge of two separated counters below a block of lead was interpreted in terms of the production of single penetrating secondaries in the lead. Similar events were observed in an experiment carried out by Leontic and Wolfendale (1952). These events were, however, attributed to the following mechanism. A penetrating meson produces a knock-on electron shower in the lead absorber from which low energy photons of energy in the region of 3 MeV penetrate considerable distances, on account of their small attenuation length, and discharge distant counters by Compton-recoil electrons produced locally. It appears likely that some if not all of the events observed by George and Trent can be explained in this manner.

4.2.2. *Leontic and Wolfendale* (1952) *Counter Hodoscope Experiment.*

This experiment indicated that the single secondaries from μ-meson interactions were nuclear interacting particles, a value of about 14 cm Pb being found for the interaction length. Most of the APP events consisted of two pairs of adjacent counters discharged, narrow pairs of particles being presumed responsible. Similar events in which pairs of adjacent counters were discharged but which could not be explained by narrow pairs have been found by Amaldi *et al.* (1952 c) and by Argan *et al.* (1953). The origin of these events is presumably electronic and the majority of the events are presumably not due to penetrating secondaries but the mechanism is rather uncertain. The interaction length calculated by Leontic and Wolfendale from the much smaller number of events in which the counters discharged were not adjacent was of a similar magnitude and it is probable that the conclusion from the experiment is correct—that the single penetrating secondaries are nuclear interacting particles. A very approximate evaluation of the cross section for these events shows that they are not inconsistent with the showers observed by George and Evans (1950).

4.2.3. *Braddick, Nash and Wolfendale* (1951) *Cloud Chamber Experiment*

Most of the quantitative results on APP come from the experiment of Braddick, Nash and Wolfendale 1951 in which a cloud chamber containing one plate was used to examine secondaries accompanying μ-mesons from a lead absorber immediately above the chamber (Series II and III). It is likely that an appreciable number of the events were due to knock-on electrons penetrating the plate without multiplication, for example the two events found by us and detailed in § 3.2 would have been classified as APP events if observed in a chamber without a magnetic field. We have shown in § 3.2 that about 1 knock-on per 1400 traversals of a lead absorber is expected to traverse a 2 cm lead plate without multiplication. Applying this analysis to Series II and III of Braddick, Nash and Wolfendale 1951, we expect about 10 events to be due to penetrating knock-on electrons. Recent accurate reprojection measurements on the original photographs have shown that 7 of the 16 events classed as apparent pairs originated within 5 mm of the bottom of the 3 cm lead absorber above the chamber (a characteristic of knock-on electrons). It seems likely therefore that the 7 events were due to knock-on electrons. Some of the remaining events may have been due to random associations, especially in Series II where the contemporaneity of the particles was uncertain due to the relatively poor resolving time of the chamber. In the experiment reported here the number of random associations, where the lack of coplanarity was only a few degrees, was appreciable (see fig. 2) so that in a cloud chamber of longer resolving time (e.g., Braddick, Nash and Wolfendale (1951) Series II) the number of random associations satisfying the geometrical conditions for acceptance as pairs of APP might be appreciable (in spite of the background rate of μ-mesons being lower than in the present sea-level experiment). The relatively large rate of events found by Braddick, Nash and Wolfendale with the multiplate chamber (Series IV and V) may have been due to a statistical fluctuation, since the total number of events observed was small. In addition, in two cases the APP appeared to originate in the top plate of the chamber and their interpretation in terms of random associations is just possible. It is concluded, therefore, that most of the APP events found by Braddick, Nash and Wolfendale can be explained by knock-on electrons and random associations.

4.2.4. *George, Redding and Trent* (1953) *Cloud Chamber Experiment*

In this experiment 8 cases of APP were found for 7311 traversals of a producing layer. In 6 cases the secondary was observed to traverse a 2 cm lead plate without multiplication. We would expect in the region of 6 events due to knock-on electrons penetrating one plate and it seems likely that most of the APP events found by George *et al.*, were due to this cause.

4.3. *Results on the Nuclear Interactions of μ-Mesons*

The two events observed by us in this category (§ 3.3) are similar to the events observed in nuclear emulsions exposed underground by George and Evans (1950). These workers found a cross section of about 5×10^{-30} cm^2/nucleon for the production of stars and showers by μ-mesons at a depth of 60 m.w.e., the value agreeing with that expected from the interaction of the virtual photons accompanying μ-mesons with nuclear matter. The underground shower particles are thought to be π-mesons (George 1952) since the frequency of slow π-mesons underground is consistent with that calculated on this assumption. The approximate cross section found by us (from 2 events) agrees with the value found by George and Evans and the nature of the secondary shower particles is probably identical since we have shown that the secondaries observed by us could be π-mesons.

It is of interest to note here that the two penetrating showers observed to cross the multiplate chamber in Series V of Braddick, Nash and Wolfendale, were also of the same type. In both events 3 fast contemporary particles were seen in the chamber diverging from a point in the overlying rock; the total length of absorber traversed by the particles being 29 cm lead. One of the fast, penetrating particles in each event suffered a large angle deflection in one of the plates, indicating that the particles were probably π-mesons or protons.

§ 5. Conclusions

The conclusions of the experiment can be summarized as follows :—

(i) No evidence has been found for the production of single penetrating secondaries by μ-mesons (APP) with a cross section of the order of 5×10^{-29} cm^2/nucleon.

(ii) The frequencies of knock-on electrons penetrating the absorber in the cloud chamber and the random association of penetrating particles indicate that most of the APP events reported by previous workers were probably due to a combination of these two effects.

(iii) The existence of the nuclear interaction of μ-mesons with matter has been confirmed, the cross section for the interaction being about 5×10^{-30} cm^2/nucleon in lead.

Acknowledgments

The cost of the electromagnet and associated equipment was provided by a special grant from the Council of the University of Ceylon.

The Authors wish to thank Professor P. M. S. Blackett for his continued interest and encouragement, Professor J. G. Wilson for much helpful advice in the choice of equipment, the staff of the Research Department Metropolitan Vickers Electrical Co. (in particular Messrs. P. P. Starling and W. E. Edgar) for their helpfulness during the construction of the apparatus, Professors E. O. E. Pereira and R. H. Paul of the Faculty of Engineering, University of Ceylon, for advice during the installation, and the technical staff of the Physical Laboratories, University of Ceylon (in particular Messrs. P. A. S. Perera and S. D. Samuel) for their share of assistance in the construction and maintenance of the equipment.

The authors are specially grateful to Dr. H. J. J. Braddick for his helpful criticisms in connection with the present investigation.

References

Amaldi, E., Castagnoli, C., Sciuti, S., and Gigli, A., 1952 a, *Proc. Phys. Soc.* A, **65,** 556 ; 1952 b, *Nuovo Cimento*, **9,** 453 ; 1952 c, *Ibid.*, **9,** 969.

Argan, P. E., Gigli, A., and Sciuti, S., 1953, Cagliari Conference (*Nuovo Cimento*, in the press).

Arley, N., 1943, *Stochastic Processes and Cosmic Radiation* (Copenhagen : G. E. C. Gads Forlag).

Blackett, P. M. S., 1937, *Proc. Roy. Soc.* A, **159,** 1.

Braddick, H. J. J., and Hensby, G. S., 1939, *Nature, Lond.*, **14,** 1012.

Braddick, H. J. J., Nash, W. F., and Wolfendale, A. W., 1951, *Phil. Mag.*, **42,** 1277.

Deutschmann, M., 1953, *Zeits. f. Naturfor.*, **8** a, 308.

George, E. P., 1952, *Progress in Cosmic Ray Physics*, edited by J. G. Wilson, p. 436 (Amsterdam).

George, E. P., and Evans, J., 1950, *Proc. Phys. Soc.*, **63,** 1248.
George, E. P., MacAnuff, J. W., and Sturgess, J. W., 1953, *Proc. Phys. Soc.* A, **66,** 346.
George, E. P., Redding, J. L., and Trent, P. T., 1953, *Proc. Phys. Soc.* A, **66,** 533.
George, E. P., and Trent, P. T., 1949, *Nature, Lond.*, **164,** 838 ; 1951, *Proc. Phys. Soc.*, **64,** 1134.
Hayakawa, J., 1952, *Proc. Phys. Soc.* A, **65,** 215.
Leontic, B., and Wolfendale, A. W., 1952, *Phil. Mag.*, **43,** 1335.
Lovati, A., Mura, A., Succi, C., and Tagliaferri, G., 1953 a, *Nuovo Cimento,* **10,** 105 ; 1953 b, *Ibid.*, **10,** 1201.
Mylroi, M. G., and Wilson, J. G., 1951, *Proc. Phys. Soc.* A, **64,** 404.
Walker, W. D., 1953, *Phys. Rev.*, **90,** 234.
Wilson, R. R., 1952, *Phys. Rev.*, **86,** 261.
Wolfendale, A. W., 1953, Cagliari Conference (*Nuovo Cimento*, in the press).

CXIX. *Notes on Soft X-ray Spectra, particularly of the* Fe *Group Elements*

By H. W. B. Skinner, F.R.S., T. G. Bullen and J. E. Johnston*
The University, Liverpool†

[Received May 17, 1954]

Abstract

The paper describes some old unpublished work on the L and M bands of the Fe group metals, and compares the results with new work by Cauchois and Gyorgy and Harvey. A number of differences are discussed. Our results support Farineau's old curves for Cu as against Cauchois', and we are unable to find evidence for the sharp M-emission edges found by Gyorgy and Harvey. Some comment is also given about various suggestions on the general interpretation of soft x-ray levels.

§ 1. Introduction

Recently Gyorgy and Harvey (1952 and 1954) have published results on M bands of a number of Fe group metals, and also of Cu. Also Cauchois (1953) has published work on the L bands of Cu and Ni. Since both these M and L bands represent transitions of valence electrons‡ into p type x-ray levels, they should give similar results as regards the form of the band. In fact there is very little correspondence and both sets of results are in some respects difficult to understand.

It happened that just before the war, we had completed a study at Bristol of the M and L bands of the Fe group metals. For various reasons this was not published. But the recent interest in the subject seems to make it desirable to publish the more important data now. We think that they will be found to throw some light on the discrepancies and difficulties, although we cannot claim to have settled all the problems.

§ 2. Experimental Method

The methods employed were those of Skinner (1940) and O'Bryan and Skinner (1940). We had two vacuum grating spectrographs, one with a grating with a 1 metre radius of curvature and an angle of incidence of 6°, and the other with a grating of 7 metres radius and an angle of incidence of $1\frac{1}{2}°$. The first was used for the M radiations in the region of 150–400 Å, the second for the L radiations from about 13 to 40 Å.

---

* Dr. Bullen (now at Iona College, New Rochelle, N.Y.) cooperated with the experimental work on the L spectra of the Fe group elements, and Dr. Johnston (now at A.E.R.E., Harwell) on the M spectra. Professor Skinner (University of Liverpool) is alone responsible for the writing of the paper.

† Communicated by Professor Skinner.

‡ We use the term ‘ valence electrons ’ to mean, for the elements considered, either 3d electrons or 4s electrons.

Glass x-ray bulbs were used, pumped out by oil diffusion pumps, and liquid air traps were employed. In this way, after careful degassing, running pressures of the order of 10^{-6} mm could be obtained. The targets were layers of metal evaporated in the high vacuum onto a square copper anticathode, which could be rotated so that either of the four sides could be bombarded by the electrons. The evaporation could be repeated at will. The anticathode was always heated to a dull red by electron bombardment before evaporation was begun. We consider that this evaporation technique is the best way of ensuring an uncontaminated surface, and that any other technique can only give doubtful results. This, of course, applies especially in the longer wavelength region, but we feel that evaporation is essential at least for some metals even in the short wavelength region. We also think that a glass x-ray bulb is to be preferred to a metal one (as used by Gyorgy and Harvey) because it can be heated for outgassing by a flame.

The bombarding voltage for the x-ray tube serving the 1 metre spectrograph was 3000 v, and currents up to 200 mA could be used. The bombarding voltage for the other equipment was 5000 v, with currents up to 150 mA. Ilford Q 1 plates were used for recording and the exposures in both cases ran into several hours. During this time a fresh surface was evaporated every 15–20 min, in order to ensure freedom from contamination.

The alternative method is that described by Piore, Harvey, Gyorgy and Kingston (1952) of recording by means of a photo-multiplier. This has the advantage that the time needed to record a band is diminished, even using a much lower input into the x-ray tube then we did. We shall compare the results of this method with ours in § 4.

We made no attempt to determine wavelength accurately. In the case of the M bands, the wavelengths were found in terms of C K radiation which is diffracted in many orders ; in the case of L radiation the values of Tyrén (1937) were used.

§ 3. L Bands

In fig. 1, actual photometric traces of the L bands of the metals Ca to Cu (except Sc) are given, together with certain of the corresponding oxide bands.* These are the bands which represent the transitions valence → $2p_{1/2}$ and valence → $2p_{3/2}$. The bands valence → 2s do not occur, as in the case of the second group metals (Skinner 1940). Other spectra, such as $M_1(3s) \rightarrow L_{23}(2p_{1/2}, 2p_{3/2})$ were also observed, but since these only represent internal atomic transitions, we will not refer to them here.

The photometric records of fig. 1 show $L_2(2p_{1/2})$ and $L_2(2p_{3/2})$ clearly resolved. The L_2 band in the case of metals is always weaker than the

---

* The oxides were simply dusted as fine powder onto the surface of the Cu anticathode.

L_3 band. The ratio of the intensities is considerably less than the ratio 1 : 2 which might be expected statistically. This is interpreted as due to a $2p_{3/2} \rightarrow 2p_{1/2}$ Auger transition causing the de-excitation of the L_2 level. On the other hand, the oxides (except CaO) all show apparent L_2 bands of much greater strength. Just why this should be so is not certain. Possibly the transition of the Auger electron from the valence band into the continuum of levels is in the case of the oxides made improbable either by a low density of states corresponding to its final energy, or by some selection rule. An alternative would be to regard these apparent L_2 bands as L_3 satellites, but this would not explain why they should occur exactly in the position of the L_2 bands. At any rate, it seems a clear experimental fact that we normally get apparent L_2 bands of considerably greater strength in oxides than in metals.

Fig. 1

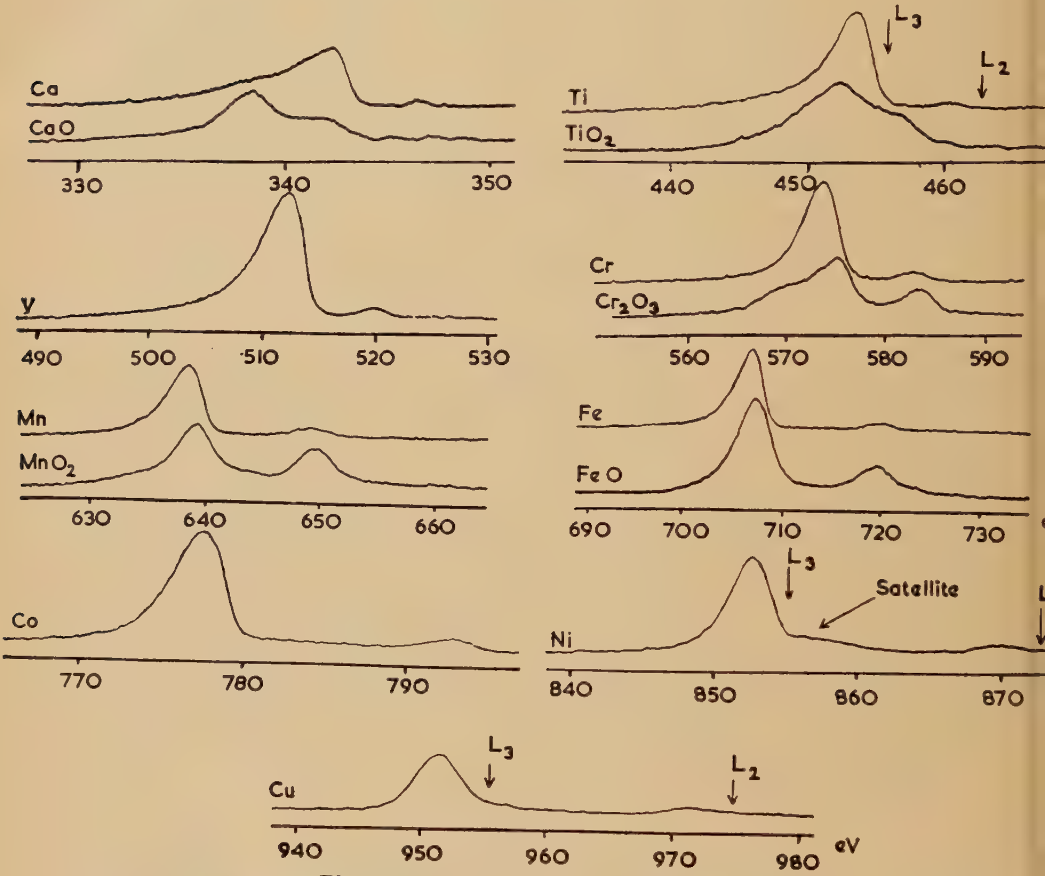

Photometer Traces of L_2 and L_3 Bands.
The arrows marked L_2 and L_3 represent the high energy limits of the respective emission bands.

We did not manage to get Ca completely uncontaminated by oxide, as the results show, but there is no sign of oxide in the case of the other metals.

The spectrograph was more suited to the elements of lower atomic number, and the resolution became rather poor in the case of Cu. It is therefore possible that we may have missed some detail in this case. But for the earlier elements, the lack of any sharp feature cannot be instrumental. There are no really sharp emission edges, the sharpest being that for Ca ($\sim$1) ev. The slight inflection on the down-slope in Co is probably genuine since it also occurs, more obviously in the M spectrum.

We may compare the bands for Ni and Cu with those published by Cauchois (1953). Our band for Ni is practically identical with hers. By comparison with the absorption spectrum, she was able to show that the projection on the high energy side of the L_3 edge is a satellite. Our results show that this is stronger for Ni than for the other bands. Cauchois also found that the L_2 band was quite weak. But she claims that it is narrower than the L_3 band. This, on general grounds, would seem most unlikely, since the bands should be identical in shape. Also there is no evidence from our spectra of any difference.

In the case of Cu, Cauchois claims a fairly marked disagreement with the band published by Farineau (1938) (although agreeing with some records left by Farineau which he had rejected). Her band also agrees more closely with the work of Saur (1939) and Gwinner (1938). But Cauchois' curves show, contrary to the case of Ni, a very strong L_2 band, comparable in intensity with L_3. From what we have said earlier, this is a strong indication of impurity, such as oxide. This is not improbable because no method of ensuring an uncontaminated surface seems to have been used. Our band, though, as we have remarked, its resolution may be imperfect, is practically identical with Farineau's, and we think it is much more likely to give the true form of the band of Cu metal than the more complicated curve given by Cauchois.

Our L bands (and also as we shall see our M bands) show evidence of considerable 'tailing' towards low energies. In this respect they are similar to the L spectra of the second group elements (Skinner 1940).

§ 4. M BANDS

The M bands of the Fe group elements, lying in the range of several hundred Å, are weak. Unfortunately, in this range of the spectrum, they are superposed upon a quite appreciable continuum. This consists of continuous radiation mostly of shorter wavelength, diffracted in high orders by the grating. The intensity of the radiation is modified by absorption in the surface layer of the glass of the grating, and therefore the continuous background is by no means smooth in distribution. Especially for the lower members of the Fe group, the background is quite comparable in intensity with the band itself. This may partly be due to the fact that the sensitivity of the Q plate is tending to fall off with increasing wavelength, whilst the background, being of shorter wavelength, is less affected. For this reason we were not able to get satisfactory results below V. In all cases, some form of background correction was essential in order to avoid spurious kinks in the bands. This was accomplished by having two metals (different in atomic number by 2 or 3) available in the X-ray bulb for evaporation onto the target. Two exposures were taken, one for each metal, using a shutter over the photographic plate, without breaking the vacuum. In this way, two well-separated M bands were obtained on the same plate. The exposure times being equal, each exposure served to provide the background correction for the M band on the other exposure. Usually a certain amount of adjustment of the background had to be done through the densities of the exposures not turning out to be exactly equal. But this is not of much importance, because any irregularities in the background are clear. Photometric curves of this process in the case of Ni and Co are shown in fig. 2, in which the photometer zero has been shifted vertically in between the two traces. The densities being small, that of the background could simply be subtracted to give fairly accurately the relative intensities of the various parts of the band.

Fig. 2

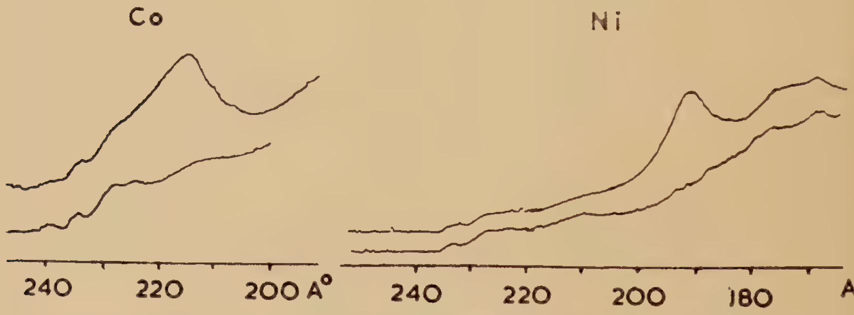

Band and Background Traces for Ni and Co.

The results* for the bands *valence* M_{23} are shown in fig. 3, in which we have plotted the intensity $I(E)$ divided by ν^3, which quantity is proportional to the density $N(E)$ of the states as a function of the energy.† In going from a curve plotted against wavelength, we have to apply another factor of ν^2, making ν^5 in all. This correction makes a slight difference to the overall shape of the M bands. (It would make very little difference in the case of the L bands.) We also give, in the cases of Zn, Cu and Ni, the corresponding M absorption curves as determined by Skinner and Johnston (1937) and Johnston (1939). In view of our rather inaccurate emission wavelength, the relative positions of the

---

* Exactly similar results have been obtained recently at Liverpool by Jacob and Wood. As for the L bands, there are no observed spectra corresponding to *valence* $\rightarrow M_1$.

† This correction follows Skinner (1940). It may be better theoretically to plot $I(E)/\nu^2$, but the difference would be scarcely appreciable.

Fig. 3

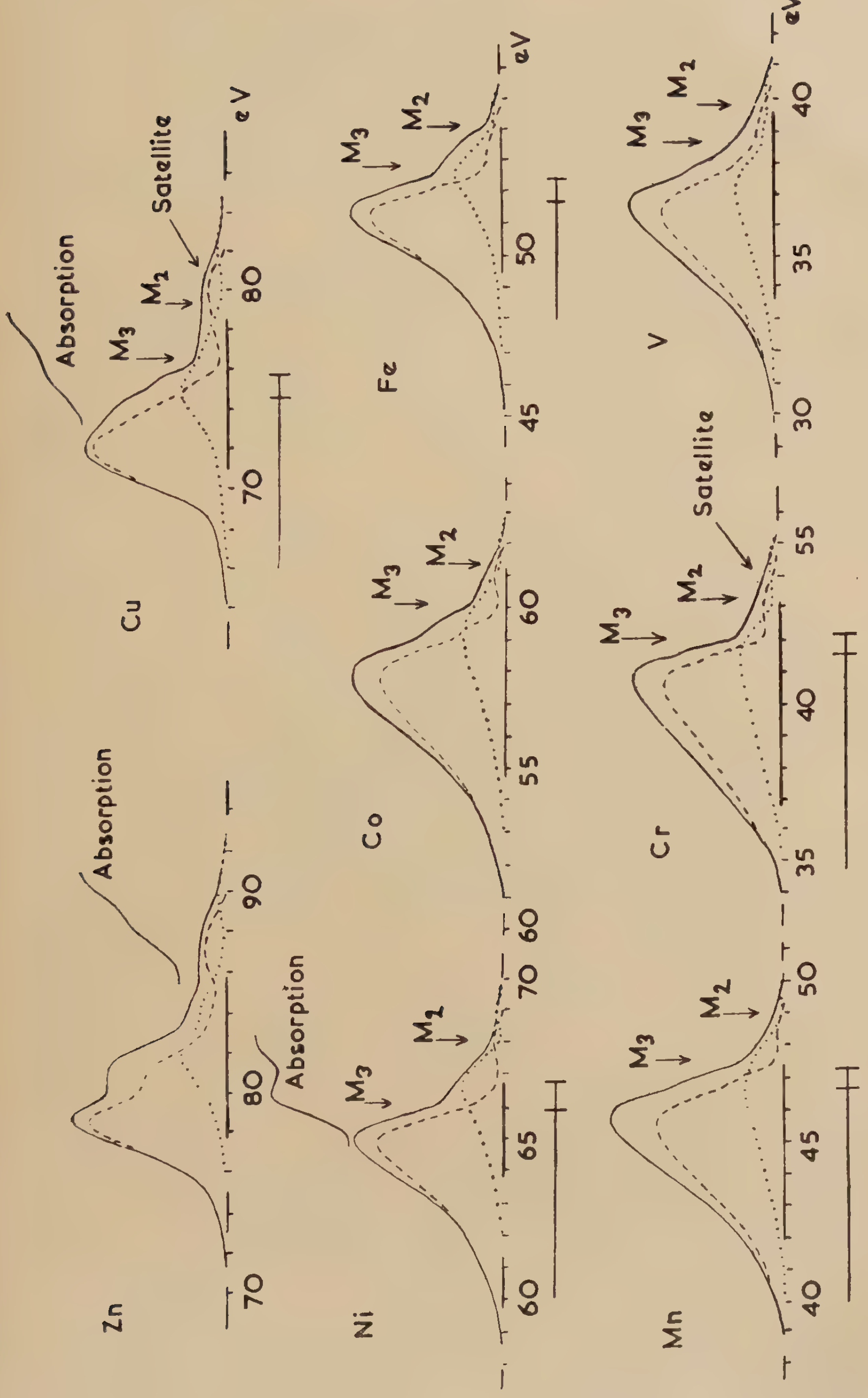

——— Total Band, - - - - M_3 Band, and . . . . . . M_2 Band.
—|—|— Band Widths and Emission Edges of Gyorgy and Harvey.
The arrows marked M_2 and M_3 represent the extreme high energy limits of the respective emission bands without satellites.

emission and absorption curves cannot be set with an accuracy better than perhaps 1/2 ev. Even taking this into account, there would seem in the cases of Cu and Ni to be an overlap between the emission bands and the regions of absorption. This, of course, could occur if the M levels are broadened, and the overlap seems to suggest that this is the case. In the case of Zn, the end of the emission band is too indefinite for us to make a similar comparison. The extent of the M emission bands obtained by Gyorgy and Harvey (1952 and 1954) are also indicated, together with the positions of the ‘ edges ’ they have found (see below).

Figure 3 also attempts a separation of the emission bands into the M_3 and M_2 components. As is found for the L spectra, we assume that the M_2 band must be less than half the strength of the M_3 band. The band for Ni seems to be easily split up into two simple components with a separation of about 2·0 ev. This difference also corresponds to the energy difference between what appear to be the M_3 and M_2 absorption edges. A similar procedure is possible for Cu and Zn. In the other cases, we have only the emission curve with which to work. In this way the M_2–M_3 energy differences are found which are listed in table 1.

Table 1

Zn	Cu	Ni	Co	Fe	Mn	Cr	V
2·5	2·8	2·0	1·6	1·4	1·2	1·0	0·9

Obviously considerable errors are involved, and the value for Cu, taken from the absorption results, appears to be too high. One cannot claim that the M_2–M_3 differences are established with certainty in this way, but the analysis appears reasonable.

We thus get a set of M_3 bands to be compared with the L_3 bands with which, except for differences in resolution (either instrumental or inherent), they should be identical. We see that in fact the bands are very similar both in width and shape. However, certain inflections in the M bands appear on the steep slope at their high energy ends. These are near the limits of observation except in the case of Co, but all the bands except for Ni seem to show them. Also all the bands appear to show weak high energy satellites.

The band widths as obtained from L_3 and M_3 bands may be compared. We define the band width by extrapolating the straight portions of the band, both to the high and low energy sides of the maximum, except in the case of Zn, where the high energy end-point is very indefinite. The values agree fairly well, those from the L bands being the more reliable. The errors are of the order of ±0·5 ev.

Table 2

Element	Ca	Ti	V	Cr	Mn	Fe	Co	Ni	Cu	Zn
L_3 band width, ev	7·0 (?)	6·0	7·8	7·2	6·0	5·7	6·5	5·5	6·8	—
M_3 band with, ev	—	—	7·0	7·2	6·5	5·0	6·5	5·0	7·5	10·4 (?)

None of the M_3 bands show a really sharp emission edge. In the case of Co, where the kink is undoubtedly real, we might assume that the curve is falling from a maximum and then shows an edge of approximately 1/2 ev in width. Edges of the same order of width can also be assumed in most of the other cases, but not in Zn or Ni. The resolution is better than for the L_3 bands, but the edge widths compare unfavourably with those which could be obtained for the L spectra of the second group metals (about 0·1 ev at room temperature). It is also to be noted that the absorption edges are not sharp, and that this is not due to lack of experimental resolution because the same method gave sharp edges for LiK, MgL and AlL. Although the M emission spectra were taken at a considerably higher power input into the target than was generally used for the L spectra of Na, Mg and Al, calculation shows that the surface temperature rise should be much too small to account for this difference. The worse resolution of the L bands as compared with the M bands may perhaps be accounted for by the effects of broadening of the x-ray levels due to radiation damping. In order to explain the worse resolution of the M bands as compared with that of the L bands of the second group elements (which are in the same energy region) we might possibly assume that the transitions of the 3d electrons into the M_2 and M_3 levels can occur with a high probability as Auger transitions, as well as by radiation.

Fig. 4

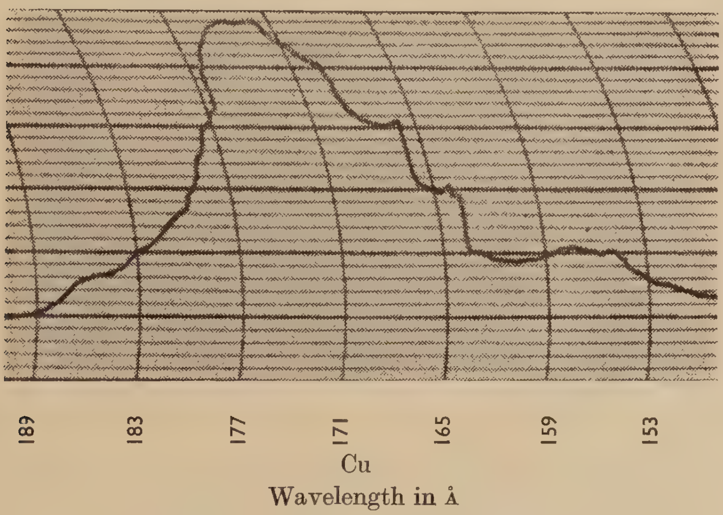

Cu M Radiation after Gyorgy and Harvey.

Although they show general similarity in shape as well as a close correspondence in band width and in the energy of the band head (omitting satellites), the M spectra obtained by Gyorgy and Harvey for Cu, Ni, Fe, Mn and Cr differ from ours by showing very sharp breaks which are interpreted as emission edges. A typical example of their pen-recording traces is shown in fig. 4 for Cu, in which it is seen that there are two sharp breaks, of the order of 1/10 ev in breadth, which they interpret as the M_3 and M_2 edges. The M_3–M_2 differences which they obtain are only about half of those which we have given in table 1. In addition, their curves are distinctly irregular in shape as compared with our smooth bands. This might partly be due to poor counting statistics, and possibly partly to the presence of unsuspected kinks in the background. But the difference in the edges is clearly fundamental.

Apart from the difference between the photographic and photomultiplier methods of recording, the techniques used by Gyorgy and Harvey and ourselves are very similar. It is true that the power input used by them is much lower than ours and that they have stressed the effects of contamination, stating that they had to run the evaporating furnace continuously. But even if contamination were present in our case, one would not expect it to mask the sharpness of the edges, unless very serious. Also the conditions we used were nearly the same as for the L_2 bands of Na, Mg and Al which showed very sharp edges. In fact, a curve by the photo-muiltiplier method for the Al L band, published by Piore, Harvey, Gyorgy and Kingston (1952) is certainly considerably inferior to the curve of Skinner (1940), both in general smoothness and in resolution of fine detail. It is difficult to see why contamination should be more effective for the Fe group metals than for the second group metals. The cause for the discrepancy therefore remains mysterious and should be investigated. A suggestion which might possibly be worth putting forward is that the sharp kinks might actually be produced spuriously by the method of continuous evaporation. They might be phenomena of the vapour phase, either in emission or in absorption. Alternatively, they might be due to an unstable surface layer, before crystallization had time to take place.*

We would like to point out certain serious difficulties in the interpretation given by Gyorgy and Harvey of their bands :

(1) The M_2 bands are always at least as strong as the M_3 bands and are given in two cases as twice as strong. It seems impossible to understand this, because statistically, as we have pointed out already, the ratio 2 should be the other way round, and, though the M_2 level can be de-excited by an Auger effect, there appears to be no mechanism for de-exciting an M_3 level relative to an M_2 level. This fact alone must throw serious doubt on Gyorgy and Harvey's interpretation.

(2) The fact that they obtain sharp emission edges for Cu is very surprising. For Cu consists of a full band of ten 3d electrons and one 4s electron. Any sharp edge must therefore represent a sudden break in the number of occupied 4s levels. The observed band must therefore be made up of an appreciable number of 4s→3p transitions as well as 3d→3p transitions. This is most unexpected because not only is the number of

---

* *Note added in proof.*—Cf. Shinonda *et al.*, *Phys. Rev.*, 1954, **95**, 840.

3d electrons much greater, but also the transition probability for 4s→3p transitions may be calculated to be smaller. Instead of this, in the manner in which Gyorgy and Harvey break up their band in fig. 9 of their second paper, the 4s→4p would have to be about 50 times more probable. This difficulty is recognized by them, but we believe that such a discrepancy is impossible to understand. In our case, it will be seen from fig. 3 that there might be an edge of small intensity for Cu, but there is none for Zn and therefore we believe the apparent edge for Cu is not real.

If this interpretation is correct, it would follow that our bands represent in all cases substantially the structure of the 3d band of the metals with only small or negligible contributions from the s band, especially for the heavier elements.* Ni would be expected to have only a very small (probably unobservable) emission edge, and this would increase in strength as we go to metals of lower atomic number with less complete d shells. Our results, if the kinks in the observed curves are real, are quite consistent with such a picture. They seem to show that the 3d band, contrary to what has been suggested on theoretical grounds, is without any appreciable structure up to Ni, though possible showing some sign of structure in Cu (namely the apparent ‘ edge ’), and a clear doublet in the case of Zn. Indeed, this general conclusion would probably hold, however the discrepancy with regard to the emission edges is settled.

§ 5 GENERAL REMARKS

(*a*) We would like in conclusion to refer to some ideas in a paper by Friedel (1952), which to a certain extent queries generally the direct interpretation of soft x-ray spectra. Friedel takes the case of Li K radiation. When an electron is removed from the K shell, one of the electrons has its energy lowered by the altered screening and becomes an ‘ atomic electron ’. This was realized, but Friedel points out that this electron might be either in a 2s or a 2p state. Obviously, however, this would lead to a double emission edge, which does not exist. We believe that this difficulty is easily removed by assuming that the state Li^+ ($1s^1$, $2p^1$) is only transient ; it will certainly be de-excited in the case of a metal (though not necessarily for an insulator) by an Auger transition into the state Li^+ ($1s^1$, $2s^1$). In absorption there are two possibilities, (i) that the K electron is thrown into the unoccupied continuum of states and a valence electron is ‘ sucked in ’ by the altered screening into a 2p level (instead of the normal 2s level), (ii) that the K electron makes a direct transition into the 2p level. The first gives a second absorption edge and the second, according to Friedel, an absorption line. Although the two processes would appear to be physically identical when the transition (i) occurs to the lowest unoccupied level, Friedel believes that the line absorption really exists. If so, the line, as well as the edge, would be expected to be very much broadened by possibility of the Auger transition, and therefore it seems doubtful whether either can play any significant part in the absorption spectra of metals.

---

* If so, there would be no point in trying to relate the M band widths to the number of s electrons per atom as has been done for example by Cauchois (1953), in spite of the fact that this procedure seems to give reasonable values.

(*b*) In a recent paper, Jones and Schiff (1954) have questioned whether soft x-ray bands give an accurate indication of the electron bands of a metal. They base their argument on the fact that the x-ray emission occurs from an atom ionized in an x-ray shell, and therefore, in a sense, an ‘ impurity ’. The field outside such an atom is certainly different from the field outside a normal atom of the metal, although this effect is greatly reduced by the ‘ sucking in ’ of a valence electron into a 2s level as described under (*a*) and therefore may be quite small. Thus one might certainly not be surprised if there would be some slight distortion of the electron band in the neighbourhood of such an atom. But Jones and Schiff require more. Schiff (1954) has carried out a calculation showing that in the Li valence electrons of highest energy have p-symmetry, whilst the observed Li K band seems to show a considerable proportion of electrons with s-symmetry at the head of the band. This follows from the fact that the intensity drops from a maximum before the emission edge is reached. To account for the disagreement, Jones and Schiff postulate that the x-ray band does not represent the band of levels, except very roughly in width. With regard to width, Schiff has calculated a value for Li of 2·69 ev, as compared with Skinner's (1940) observed ‘ reduced ’ width of 3·7 ± 0·5 ev. The ‘ reduced ’ widths for Li and Na are both at least 0·5 ev smaller than the calculated Sommerfeld widths, which assume s-symmetry. The case of Na has been recently discussed by Raimes (1954) and he has been able to go a long way towards explaining the discrepancy. He uses a more recondite model than Sommerfeld's, and his work leads to the conclusion that the ‘ empirical ’ widths, roughly 0·5 ev larger than the ‘ reduced ’ widths, are of greater physical significance. It would therefore appear likely that the experimental evidence excludes Schiff's width for Li, and supports the evidence of the band-shape, which suggests s-symmetry for the conduction electrons of highest energy.

REFERENCES

Cauchois, 1953, *Phil. Mag.*, **44**, 173.
Farineau, 1939, *Journ. de Phys.*, **10**, 327.
Friedel, 1953, *Phil. Mag.*, **43**, 1115.
Gwinner, 1938, *Zs. f. Phys.*, **108**, 523.
Gyorgy and Harvey, 1952, *Phys. Rev.*, **87**, 861 ; 1954, *Ibid.*, **93**, 365.
Johnston, 1939, *Proc. Camb. Phil. Soc.*, **35**, 108.
O'Bryan and Skinner, 1940, *Proc. Roy. Soc.* A, **176**, 229.
Piore, Harvey, Gyorgy and Kingston, 1952, *Rev. Sci. Inst.*, **23**, 8.
Raimes, 1954, *Phil. Mag.*, 7, **45**, 727.
Saur, 1936, *Zs. f. Phys.*, **103**, 421.
Schiff, 1954, *Proc. Phys. Soc.* A, **67**, 1.
Jones and Schiff, 1954 *Proc. Phys. Soc.* A, **65**, 217.
Skinner, 1940, *Phil. Trans.*, **239**, 95.
Skinner and Johnston, 1937, *Proc. Roy. Soc.* A, **161**, 420.
Tyren, 1937, *Arkiv f. Nat. Astr. och Fys.*, 25A, No. 32.

CXX. CORRESPONDENCE

The Mechanism of Rolling Friction

By D. Tabor
Research Laboratory for the Physics and Chemistry of Surfaces,
Department of Physical Chemistry, Cambridge

[Received August 3, 1954]

When a hard steel ball rolls, under moderate loads, over a flat metal specimen, it initially deforms the surface plastically, and the resistance to rolling is primarily due to plastic displacement of the metal. With repeated traversals of the same track, the groove grows in width until an equilibrium stage is reached at which the deformation is primarily elastic. The rolling resistance under these conditions is of great interest since it is probable that, for the greater part of their lives, practical ball bearings operate under these conditions.

The most widely accepted theories of equilibrium or elastic rolling friction in the past have been based on some type of interfacial microslip between the roller and the surface. Reynolds in 1875 attributed interfacial slip to differential stretching of the surface layers within the region of contact. Heathcote in 1921 pointed out that in the rolling of a ball in a groove a more important source of slip arises from the fact that, for each rotation of the sphere, the central band on the ball measures out a full circumference whilst the outermost bands measure out a smaller circle. This could lead to microslip within the ellipse of contact. Finally Tomlinson in 1929 suggested that rolling friction was primarily due to interfacial adhesion.

In a recent communication (Tabor 1952) it was shown that for hard cylinders or spheres rolling on *rubber* the Reynolds slip is trivial, and for a hard sphere rolling in a rubber groove (excepting very deep grooves) the Heathcote slip contributes very little to the rolling friction. It was shown that the primary source of the rolling resistance is the elastic hysteresis losses in the rubber, and there was close agreement between the observed and the calculated values of the rolling force. Finally it was suggested, by analogy, that a similar mechanism might apply to the rolling of a sphere in the equilibrium groove formed in a *metal* surface.

The investigation has now been carried a stage further and the main conclusions may be summarized as follows :—

1. If the rolling resistance is attributed primarily to the type of slip described by Heathcote its magnitude may be calculated in terms of the coefficient of friction between the ball and the ellipse of contact where microslip occurs (Eldredge 1952), and the results at first sight appear

reasonable. There are however two overriding objections to this theory. (i) The rolling friction is the same whether the surfaces are clean or are lubricated with a very good boundary lubricant. (ii) This, in itself, might not be objectionable but for the fact that the coefficient of friction that must be invoked is of the order of $\mu \approx 1$–2 even for the lubricated surfaces. This is impossibly high since in ordinary sliding the lubricated values are nearer $\mu \approx 0{\cdot}05$–$0{\cdot}1$.

2. The hysteresis loss theory is attractive because it explains the independence of rolling friction on lubrication. The main drawback is that surprisingly high hysteresis loss factors (perhaps $>20\%$) have in some cases to be invoked.

3. This problem has now been resolved by rolling a metal ball over a metal ball of identical material and diameter (see, for example, Tomlinson 1929). The rolling is repeated until any initial plastic deformation is superseded by elastic deformation. By symmetry the region of contact is plane so that the Heathcote type of slip is eliminated. Further, lateral stretching of the surface elements is the same on both balls so that the Reynolds type of slip no longer occurs. Under these conditions it might be thought that, with the elimination of interfacial slip, the rolling friction would fall to a very small value. This is not so. The rolling resistance is about as high as that observed for a hard sphere rolling in the equilibrium groove of the given metal. Further the dependence of rolling friction on load and ball diameter is substantially the same in both cases. In addition lubrication produces no perceptible reduction in the rolling friction of a ball on a ball so that interfacial adhesion (Tomlinson 1929) cannot be the primary source of rolling friction. The losses here can only be due to hysteresis and it is clear that these losses can be very large for metals deformed into the plastic range. This answers the objection raised in 2.

4. If hard copper balls are rolled on one another until elastic equilibrium is reached the rolling friction is very much greater than for hard steel balls under the same conditions and the hysteresis loss factor may be 30 times bigger. If, however, the results are extrapolated back to the conditions at which the copper and the steel balls are both just at their elastic limit (onset of plasticity, Tabor (1951), p. 51) the hysteresis loss factor is almost the same (of the order of 1 to 2%). Similar results are found for other materials. The hysteresis loss factor up to the elastic limit is found to lie between 1 and 2% for materials as diverse as work-hardened copper, ball race steel, workhardened mild steel, phosphor bronze and duralumin. Since hysteresis losses depend mainly on the strains produced this would suggest that hysteresis losses are roughly the same for a wide variety of metals provided the strain to which they are subjected is the same fraction of the strain at their elastic limit. Data of other workers are not generally complete enough to test this but it applies satisfactorily to the results of Rowett (1914) and to those of Robertson and Yorgiadis (1946). If elastic losses below the yield point

are due to reversible slip involving the forward and backward movement of dislocations these results would appear to be reasonable.

5. It is well known that the hysteresis losses first observed when a metal is deformed beyond its elastic limit may be high but that with repeated cyclic loading the hysteresis loop closes up so that, if the metal does not fail by fatigue, the losses diminish (Gough 1922). Similar effects are observed in rolling friction. In a specific experiment, where a hard steel ball $\frac{1}{8}$ in. diameter rolled over a workhardened mild steel surface, equilibrium rolling was reached after 200–300 traversals and the rolling friction had a value of 25 g. After 10 000 traversals it had fallen to 15 g; after 60 000 to 12 g and after 200 000 traversals to 9 g. After this the material within the groove began to flake and fragment presumably as a result of fatigue (see, for example, Jones 1946).

6. Some microslip may occur within the ellipse of contact as proposed by Heathcote but its contribution to the rolling resistance is very small for two main reasons :—(i) The deformation of the surfaces is relatively gentle so that the oxide present on the surface is not appreciably ruptured : slip occurs within the oxide surface layers rather than within the metal itself. This is shown by the fact that if ball races are run at high temperatures *in vacuo* so that the oxide is removed gross seizure occurs (Bell and Findlay 1941). (ii) The amount of slip at any region—if it does occur—is extremely small and, as the work of Cocks (1952) and of Eisner (1954) has shown the friction for minute displacements may be very small indeed. Thus with ordinary oxide-covered metals the slipping process involves only a very small amount of frictional resistance and this is scarcely affected by the presence of lubricants. On the other hand slip between the ball and the groove may play an important part in surface attrition. Consequently although a lubricant may produce little perceptible reduction in friction it may be of very great importance in protecting the surfaces from plucking and wear and so in prolonging their life.

7. Several earlier workers have suggested that rolling friction is primarily due to interfacial slip. The present work however shows that when rolling occurs between metal surfaces covered with their usual oxide films, interfacial slip in most cases contributes very little to the observed rolling resistance. It is true that a lubricant may greatly reduce metallic transfer between the rolling surfaces but it is relatively ineffective in reducing the rolling resistance. In this sense therefore, there is very little conventional friction in rolling. The new point brought out by this work is that the major part of the resistance to rolling arises from elastic hysteresis losses in the metals themselves.

A fuller account of this work is now in course of publication (Eldredge and Tabor, in press).

ACKNOWLEDGMENTS

I wish to thank the Ministry of Supply (Air) for a research grant and Dr. Bowden for his continuous interest.

References

Bell, M. E., and Findlay, J. H., 1941, *Phys. Rev.*, **59,** 922.
Cocks, M., 1952, *Nature, Lond.*, **170,** 203.
Eisner, E., 1954, *Ph. D. Dissertation*, Cambridge.
Eldredge, K. R., 1952, *Ph. D. Dissertation*, Cambridge.
Gough, H. J., 1922, *Engineering*, **114,** 291.
Heathcote, H. L., 1921, *Proc. Inst. Aut. Eng.*, **15,** 569.
Jones, A. B., 1946, Metallographic Observations of Ball-bearing Fatigue Phenomena, *A.S.T.M.*, **46.**
Reynolds, O., 1875, *Phil. Trans.*, **166,** 1.
Robertson, J. M., and Yorgiadis, A. J., 1946, *J. App. Mech.* A, **13,** 173.
Rowett, F. E., 1914, *Proc. Roy. Soc.* A, **89,** 528.
Tabor, D., 1951, *The Hardness of Metals* (Oxford : Clarendon Press) ; 1952, *Phil. Mag.*, **43,** 1055.
Tomlinson, G. A., 1929, *Phil. Mag.*, **7,** 905.

The Thickness of the Saturated Helium Film Above and Below the λ-point

By A. C. Ham and L. C. Jackson
H. H. Wills Physical Laboratory, University of Bristol

[Received August 9, 1954]

The properties of the static helium film have been re-examined for heights between 0·4 and 1·6 cm from 1·2 to 3·8°K, using the optical method of Burge and Jackson (1951). In particular, the results are believed to be free from any systematic error due to radiation, impurities or vibrations in the gas column, and the effects of these perturbing factors on the film thickness have been investigated.

The work of Jackson and Henshaw (1953) had indicated that a thin film existed at 2·3°K, casting doubt on the earlier method of obtaining the zero setting. The apparatus was therefore re-designed as shown in the figure. The mirror is supported from the bottom in a glass tube terminating in copper-glass seals at each end, and the tube is surrounded by a copper radiation shield in which appropriate slits have been cut. The tube is pumped out before and during the early stages of a run, and the zero setting is made when the tube is completely immersed in liquid helium. Specially purified helium is then condensed into the tube from an external reservoir. This arrangement has removed any ambiguity about the zero setting, and has resulted in a greater optical accuracy and much more strictly isothermal conditions. Moreover, the gas close to the mirror now undergoes no mass flow, whereas previously the mirror had been in direct contact with the moving vapour in the cryostat.

The original, provisional calibration of the instrument by Burge and Jackson (1951) was found to be incorrect by about 30%, due primarily to birefringent effects in the strained glass of the Dewar vessels which had not hitherto been considered. All previously published film thicknesses using the optical method (Burge and Jackson 1949, 1951, Jackson and Henshaw 1950, Henshaw and Jackson 1952) were based upon this original calibration, and must now be disregarded in favour of the present results, although the earlier work would have given approximately the same values for the helium II film thickness had a correct calibration curve been available. A completely new calibration curve has been constructed, based on experimentally determined refractive indices of the 1- and 3-areas, which has eliminated the error introduced by assuming the barium stearate to be isotropic. These refractive indices have been shown to be independent of temperature between room temperature and 4·2°K, as had previously been assumed, and the only remaining assumption in the theory is that the refractive indices of film and bulk liquid are the same.

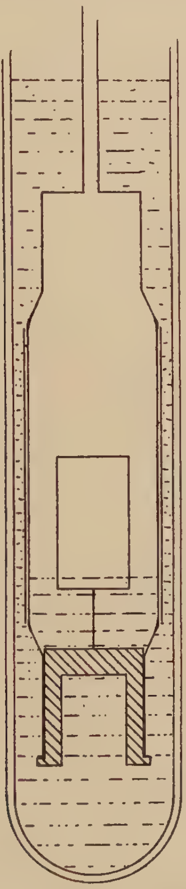

The results, which may subsequently be revised only in the light of a new value for the refractive index of the film, are briefly as follows. At 2·05°K the profile of the film can be expressed in the form $d=k/H^{1/z}$ where $k=3{\cdot}15\times10^{-6}$ cm and $z=2{\cdot}3$. The thickness decreased slightly with temperature, and at 1·32°K was found to be $2{\cdot}96\times10^{-6}$ cm at a height of 1 cm.

Above the λ-point, the thickness of the film at a height of 1 cm was found to be $2{\cdot}85\times10^{-6}$ cm and no significant variation with temperature could be detected between the λ-point and 3·8°K. The thickness increased with decreasing height, but less rapidly than below the λ-point. Using an analysis similar to that suggested by Atkins (1954), it has been shown that if the film at 3°K were 10^{-5} deg. warmer than the vapour close to it, due to radiation absorbed by the mirror, the equilibrium thickness at a height of H cm would be that expected at a height of $(H+1)$ cm in a completely isothermal system. This has accounted semi-quantitatively for the observed difference between the height dependences.

Neither doubling the thickness of Chance ON20 heat-absorbing glass in the incident light beam, nor removing it altogether, had any effect on the thickness of the film below the λ-point. It could, however, be evaporated by holding a small lamp immediately outside the tails of the Dewar vessels, but it reformed completely in a small fraction of a second as the lamp was removed. Above the λ-point the film was readily evaporated by the lamp, but reformed slowly when it was removed, reaching its original thickness after 1–2 min. Whether it condensed from the vapour or rose from the bulk liquid below is not known.

The thickness of the helium II film was greatly increased by the presence of an extremely thin layer of solid air on the surface of the mirror. Films as thick as 20×10^{-6} cm have been observed, but it has been shown that solid air has no effect on the film thickness above the λ-point. This effect on the static helium II film is analogous to the observations of Bowers and Mendelssohn (1950), who showed that the transfer rate through the flowing film was greatly increased by the presence of impurities.

Temperature gradients and spuriously thick films have been observed under certain geometrical conditions, and are believed to have been due to vibrations in the gas column above the mirror (Taconis *et al.* 1949).

As the thickness of the helium I and II films are so nearly equal, it appears that neither radiation nor impurities can have seriously influenced the results, since the helium I film is very much more sensitive to radiation than the helium II film, while the reverse is true of impurities.

It seems clear that the films above and below the λ-point are one and the same, except that the vanishing viscosity of the superfluid, providing a rapid replacement mechanism from bulk liquid, has enabled the film to be readily observed below the λ-point. Above the λ-point extreme temperature homogeneity is necessary in order that the film may form.

These results essentially confirm the predictions of Frenkel (1940) and Schiff (1941), which have recently been reproduced by considering the helium film as an adsorbed layer in equilibrium with a slightly unsaturated vapour (Rice and Widom 1953, Meyer 1954, Atkins 1954). In all these approaches it is the Van der Waals forces of attraction which are regarded as predominant.

Full details, including a comparison of these results with other determinations of the film thickness, will be published later.

We should like to thank Professor N. F. Mott and Dr. E. B. Mendoza for helpful discussions, and we are indebted to the Department of Scientific and Industrial Research, both for a grant in support of a programme of investigation of the helium film, and also for a maintenance allowance to one of us (A.C.H.).

REFERENCES

ATKINS, K. R., 1954, *Can. J. Phys.*, **32,** 347.
BOWERS, R., and MENDELSSOHN, K., 1950, *Proc. Phys. Soc.* A, **63,** 1318.
BURGE, E. J., and JACKSON, L. C., 1949, *Nature, Lond.*, **164,** 660 ; 1951, *Proc. Roy. Soc.* A, **205,** 270.
FRENKEL, J., 1940, *J. Phys., U.S.S.R.*, **2,** 365.
HENSHAW, D. G., and JACKSON, L. C., 1952, *Proc. Natl. Bur. Standards Symposium. Natl. Bur. Standards Circular* 519, p. 183.
JACKSON, L. C., and HENSHAW, D. G., 1950, *Phil. Mag.*, **41,** 1081 ; 1953, *Ibid.*, **44,** 14.
MEYER, L., 1954, *Phys. Rev.*, **93,** 655.
RICE, O. K., and WIDOM, B., 1953, *Phys. Rev.*, **90,** 987.
SCHIFF, L. I., 1941, *Phys. Rev.*, **59,** 839.
TACONIS, K. W., BEENAKER, J. J. M., NIER, A. O. C., and ALDRICH, L. T., 1949, *Physica*, **15,** 733.

Electrical Resistance Minimum in Dilute Copper Alloys

By W. B. PEARSON
Division of Physics, National Research Council, Ottawa, Canada

[Received August 9, 1954]

A MINIMUM in the electrical resistance of metals at low temperatures was first discovered in gold (de Haas, de Boer and van den Berg 1934). Similar minima have subsequently been observed and confirmed in copper, silver, and magnesium (see references in MacDonald 1952). It has been suggested that the resistance minimum was caused by relatively few kinds of solute atoms, perhaps those which could offer impurity levels which were favourably placed so as to lead to resonant scattering effects very close to the top of the conduction band (Gerritsen and Korringa 1951, Korringa and Gerritsen 1953). Work in this laboratory (MacDonald 1952) on dilute copper alloys showed that the minimum could be caused by Sn, Pb, Bi and carbon, while other solutes which were investigated did not appear to give rise to a minimum. This investigation has now been extended to show that the resistance minimum at low temperatures is a fairly general phenomenon for copper as solvent and that those solutes which do not give rise to a minimum are perhaps the more noteworthy. The following elements in dilute solid solution produce a resistance minimum in copper : Mn, Fe, Co, Ga, In, Si, Ge, Sn, Pb, and Bi, while Ag, Au and probably Ni do not give rise to any minimum greater than 0·2% of the residual resistance (MacDonald and Pearson 1954). It has also been reported that zinc causes a resistance minimum in copper (Gerritsen and Linde 1952). Experiments in this laboratory have also shown that samples of ' pure ' polycrystalline copper do or do not show a minimum according as they are prepared under reducing conditions or under oxidizing conditions (which precipitate traces of impurity, particularly iron, as a separate phase). On the other hand, Blewitt, Coltman and Redman (1954) have recently demonstrated that grain boundaries are necessary for the existence of the resistance minimum in copper. In their experiments it was shown that there was no minimum in single crystal copper or in the same crystal following tensile deformation, but that after recrystallization of the deformed material at 1000°c the resulting polycrystalline copper showed a resistance minimum.

The conclusions to be drawn from this evidence would therefore seem to be (i) that the impurities causing a minimum are so diverse that it is unlikely to be the result of the creation of energetically favourable impurity levels due to the presence of a particular impurity atom *per se* ; and (ii) that the resistance minimum is probably not due either to impurities alone or to grain boundaries alone, but rather to a particular impurity distribution in relation to the grain boundaries. Although the presence of grain boundaries in pure copper need not result in a resistance minimum, there is as yet no information on whether the presence of a specific impurity, which causes a minimum in polycrystalline copper, also gives rise to a resistance minimum in single crystal copper.

That the impurities are indeed associated with the grain boundaries is further suggested by the following consideration. The experiments of MacDonald and Pearson (1954) show, for polycrystalline dilute solid solutions of Cu–Ga, Cu–In, Cu–Si, Cu–Ge and Cu–Sn alloys, a critical concentration in the region of 0·005 atomic per cent solute, up to which the size of the minimum taken as $(R_{4\cdot 2^\circ}-R_{T_{\mathrm{min}}})/(R_{T_{\mathrm{min}}})$ increases rapidly and beyond which it decreases again. Smart and Smith (1943) on the other hand have shown that there is for certain alloy systems a critical concentration at which the rate of rise with concentration of an arbitrarily defined ' softening ' temperature shows a rapid increase and subsequent decrease. In Cu–Sn alloys for instance there is a correspondence between these critical concentrations which suggests that the remarkable changes in electrical and mechanical properties have a common origin. The variation of mechanical properties with tin concentration suggests in turn that the effect is caused by the positioning of the lower melting tin atoms about special sites, such as high and low angle grain boundaries or other imperfections which are *limited* in number. There is also a degree of correlation between the probable grain boundary areas and the critical solute concentration involved.

It should be noted however that our conclusion differs from that reached by Blewitt *et al.* who suggested that grain boundaries alone were sufficient to produce the resistance minimum. We believe that their experiments are not conclusive for the following reasons. As mentioned above, oxygen-containing ' pure ' polycrystalline copper samples do *not* show a resistance minimum after straining and recrystallization at

530–600°c (MacDonald and Pearson 1954). Although the values for the residual resistivity of the single crystals which they investigated seem to exclude the possibility of impurities in solid solution, the recrystallized copper gave a ratio $R_{4\cdot2^\circ}/(R_{273\cdot2^\circ}-R_{4\cdot2^\circ})$ of 4 to 7×10^{-3} which considerations of mean free path show is higher than expected for grain boundary scattering alone for specimens recrystallized at 1000°c. It is significant that in the experiments of Blewitt *et al.* the ' pure ' copper was melted in graphite, that is, in reducing conditions which leave traces of impurity present in solid solution. For the same reason we find, for instance, that the residual resistivity of ' pure ' copper samples melted in reducing conditions (under hydrogen or in graphite) is increased by a factor of 3 or 4 compared to vacuum melting the same copper in alumina so that it contains a little oxygen, traces of impurity being precipitated from solid solution.

Finally we suggest a possible mechanism by which a distribution of impurities along grain boundaries might produce a resistance minimum. The distribution of solute atoms in planes along grain boundaries to relieve lattice strain when there is an appreciable difference (say 10% or more) in radius ratio of solute and solvent may be of the order of a unimolecular layer. The resistance due to the solute atoms in this layer is likely to be less than that due to the same number of atoms distributed randomly. This may cause a resistance minimum at low temperatures especially if the interference term is negative and temperature dependent. It is interesting to note that *at room temperature* Bhatia (1949) has shown for Fe–C interstitial solid solutions that distribution of carbon atoms along lines in the lattice (along line dislocations) leads to (i) a decrease of scattering and hence resistivity compared to a normal random distribution of solute atoms and (ii) a negative and temperature dependent interference term (cf. eqn. (27), Bhatia 1949). Furthermore, the resistance minimum in magnesium has recently been interpreted as a decrease of scattering at $T_{\min}\sim6$°K from that given by a T^5 law established at slightly higher temperatures (Rosenberg 1954) rather than an additional anomalous scattering mechanism becoming dominant at low temperatures.

The author wishes to thank Dr. D. K. C. MacDonald and Dr. A. B. Bhatia for their interest and discussions.

REFERENCES

Bhatia, A. B., 1949, *Proc. Phys. Soc.* B, **62,** 229.
Blewitt, J. H., Coltman, R. R., and Redman, J. K., 1954, *Phys. Rev.*, **93,** 891.
Gerritsen, A. N., and Korringa, J., 1951, *Phys. Rev.*, **84,** 604.
Gerritsen, A. N., and Linde, J. O., 1952, *Physica*, **18,** 877.
de Haas, W. J., de Boer, J., and van den Berg, G. J., 1934, *Physica*, **1,** 1115.
Korringa, J., and Gerritsen, A. N., 1953, *Physica*, **19,** 457.
MacDonald, D. K. C., 1952, *Phys. Rev.*, **88,** 148.
MacDonald, D. K. C., and Pearson, W. B., 1954, to be published.
Rosenberg, H. M., 1954, *Phil. Mag.*, **45,** 73.
Smart, J. S., and Smith, A. A., 1943, *Trans. Amer. Inst. Min. Metall. Engrs.*, **152,** 103.

A 7-Second Iridium Isomer

By F. D. S. Butement and A. J. Poë
Atomic Energy Research Establishment, Harwell

[Received August 20, 1954]

In a recent paper (Butement and Poë 1954) we described the properties of five new iridium isotopes, including a 7-second activity emitting Ir K x-rays and gamma-rays of energies 0·125 and 5·6 Mev. Each of the radiations showed individually the same half-life. Owing to the very short half-life no radiochemical identification was possible. Several different mass assignments were possible, and ^{191m}Ir was suggested. The difficulty of fitting the 5·6 Mev γ-ray into a decay scheme was pointed out. We are indebted to Dr. M. Goldhaber for informing us of recent unpublished work carried out at Brookhaven, in which it was found that ^{191}Os is the parent of a 6·9 second ^{191m}Ir emitting radiations similar to our activity (except for the 5·6 Mev γ-ray).

Apparently, therefore, both observations refer to the same isomer but our iridium isomer sources must have contained two activities of almost identical half-lives. We have now found that the 5·6 Mev γ-ray is due to contamination with 7·3 second ^{16}N derived from traces of oxygen combined with or adsorbed on the iridium metal used, since this γ-ray is no longer found if the metal is reduced in hydrogen before irradiation. The remaining radiations may then be attributed to ^{191m}Ir, since this isomer would have been produced by the fast neutron irradiation of iridium in our experiments.

Reference

Butement, F. D. S., and Poë, A. J., 1954, *Phil. Mag.*, **45**, 31.

The Scattering of Deuterons and Protons by Alpha-Particles

By R. G. Freemantle,* T. Grotdal,† W. M. Gibson,
R. McKeague,‡ D. J. Prowse§ and J. Rotblat||

[Received August 20, 1954]

Earlier papers have described the use of a scattering camera in experiments with beams of 19 Mev deuterons, and of 9·5 Mev protons accelerated as molecular hydrogen, from the 60-in. Birmingham cyclotron (Freemantle, Gibson, Prowse and Rotblat 1953, Burcham, Gibson, Hossain and Rotblat 1953). The camera, which is essentially the same as that described by Burrows, Powell and Rotblat (1951), allows the

---

* Physics Department, University of Birmingham.
† Fysisk Institutt, University of Bergen, Norway.
‡ Physics Department, Queen's University of Belfast.
§ H. H. Wills Physics Laboratory, University of Bristol.
|| Physics Department, St. Bartholomew's Hospital, London.

measurement of differential cross sections from 15° to 165° for various types of nuclear process in gaseous targets. In this note, we present preliminary results obtained for the elastic scattering of deuterons and protons in helium gas. Each of these processes has been the subject of previous investigations at several energies, but for neither is the information as complete as could be desired.

Fig. 1

p—α scattering

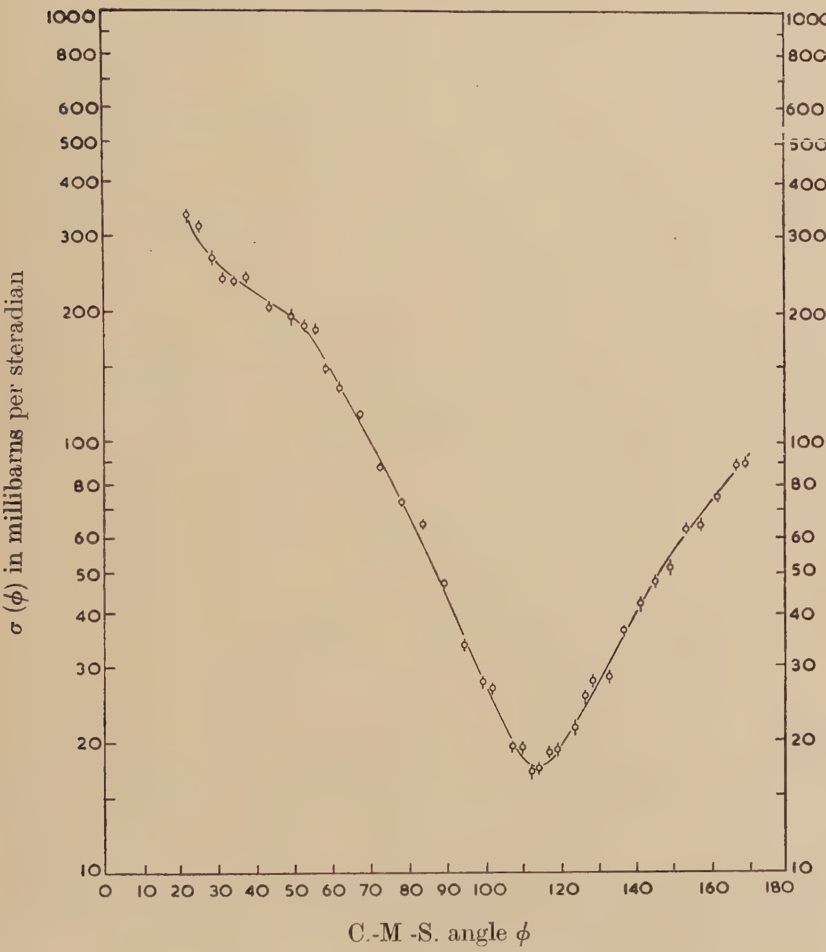

C.-M.-S. angular distribution for elastic scattering of protons by helium (proton energy in laboratory system, 9·55 MeV).

The angular distribution obtained for the elastic scattering of 9·55 MeV protons by helium is shown in fig. 1. The shape of this curve is very similar to that found at 9·48 MeV by Putnam (1952), who used a camera built at Los Alamos; but the absolute values of cross section observed by Putnam are higher than ours by a factor of 1·28. In the phase-shift calculations made by Dodder and Gammel (1952) there are indications that Putnam's values of the cross section are somewhat high. We have reason to believe that our values may be too low by about 5%, but we do not expect any appreciably greater systematic error (Rotblat, Burcham, Gibson, Prowse and Hossain 1954). The relative accuracies of the measurements in the present work are of the order of 4%. Measurements

Fig. 2

d—α scattering

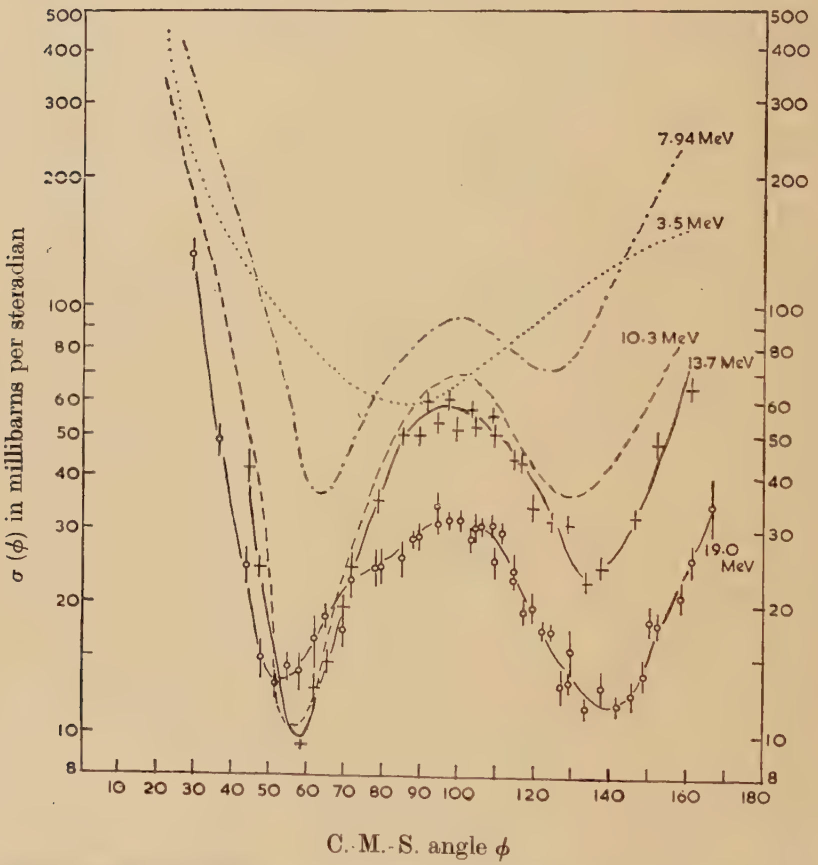

C.-M.-S. angular distribution for elastic scattering of deuterons by helium.
ϕ : experimental points at 19·0 Mev.
+ : experimental points at 13·7 Mev.

Full lines : best curves through experimental points.
Dashed line, thus : – – – – results of Allred, Froman, Hudson and Rosen (1951).
Dot-Dash line, thus : –·–·– results of Burge, Burrows, Gibson and Rotblat (1951).
Dotted line, thus : ········ results of Blair, Freier, Lampi and Sleator (1949).
All energies are for the deuterons, in the laboratory system.

were made independently by several observers, on plates from separate exposures, in order to eliminate errors of observation. Most of the points in fig. 1 are based on at least two separate sets of measurements.

The results for the elastic scattering of deuterons by helium are shown in fig. 2 ; some of the measurements were made on the scattered deuterons and some on the projected alpha-particles. Two sets of exposures were made, one with the normal 19·0 MEV deuteron beam and one with this beam passing through an aluminium foil which reduced its energy to 13·7 MEV. Although this is not an ideal method of obtaining a beam of deuterons of intermediate energy, since the beam leaving the foil diverges somewhat, it was considered that it would provide useful additional information about the dependence of the angular distribution on energy. The divergence made the measurement of the beam current rather unreliable, and the scale of the curve obtained at 13·7 MEV may therefore be in error by as much as 10%, with respect to that for 19 MEV ; it should not have had any appreciable effect on the form of the angular distribution.

Some curves obtained by other workers at lower energies are shown in fig. 2, in order to give a general picture of the variation of the angular distribution with energy. It will be seen that the two minima become more pronounced and more nearly equal in depth as the energy increases. We would emphasize that, apart from the particular uncertainty in the case of the 14 MEV curve, the absolute scale of each of the curves shown in fig. 2 is known with considerably less accuracy than is its form.

In the 19 MEV experiment, as in the earlier work at 8 MEV, indications were found of the occurrence of the reaction ^{4}He(d, p) ^{5}He, with a Q-value of $-3{\cdot}10 \pm 0{\cdot}05$ MEV ; but reliable measurements of the cross section were not possible.

REFERENCES

ALLRED, FROMAN, HUDSON, and ROSEN, 1951, *Phys. Rev.*, **82,** 786.
BLAIR, FREIER, LAMPI, and SLEATOR, 1949, *Phys. Rev.*, **75,** 1678.
BURCHAM, GIBSON, HOSSAIN, and ROTBLAT, 1953, *Phys. Rev.*, **92,** 1266.
BURGE, BURROWS, GIBSON, and ROTBLAT, 1951, *Proc. Roy. Soc.* A, **210,** 534.
BURROWS, POWELL, and ROTBLAT, 1951, *Proc. Roy. Soc.* A, **209,** 461.
DODDER, and GAMMEL, 1952, *Phys. Rev.*, **88,** 520.
FREEMANTLE, GIBSON, PROWSE, and ROTBLAT, 1953, *Phys. Rev.*, **92,** 1268.
PUTNAM, 1952, *Phys. Rev.*, **87,** 932.
ROTBLAT, BURCHAM, GIBSON, PROWSE, and HOSSAIN, 1954, *Proceedings of Glasgow Conference* (London : Pergamon Press).

Polytypism of Cadmium Iodide

By RICHARD S. MITCHELL
Department of Geology, University of Virginia, Charlottesville, Virginia

[Received August 3, 1954]

THOUGH the existence of more than one crystal modification of cadmium iodide has been known for some time, the magnitude of polytypism in this compound has, until recently, been overlooked. From evidence based on a study of the heights of growth steps, Forty (1952) concluded that many polytypes of this compound may exist. The writer has recently begun an x-ray study of this compound with the plan of eventually correlating the various step heights with definite polytypes. The purpose of this present note is to summarize all the types which have been identified by x-ray analysis up to the present time. This includes three types not previously recorded.

Cadmium iodide structures consist of planes of cadmium atoms sandwiched between every other layer of close-packed (0001) planes of iodine atoms. It is obvious that variations in the stacking sequence of these layers would result in different polytypes of the substance. In the remainder of this note the stacking sequence of (0001) layers will be described in the classical A, B, C notation for sphere-packing lattices, in which iodine atoms are represented by Roman letters and cadmium atoms, by Greek letters. In addition, the Ramsdell (1947) zigzag sequence, representing the sequence of succeeding iodine atoms in the $(11\bar{2}0)$ section will be given. The various polytypes will be named according to the number of iodine layers within the length of the *c* axis. In addition to this the letter 'H' will be used since the unit cell is hexagonal. An 'R' can be used to designate rhombohedral if any of these are discovered in the future. This follows the same scheme Ramsdell (1947) suggested for the designation of various polytypes of silicon carbide.

The first structure of cadmium iodide, determined by Bozorth (1922), is that of the simplest type 2H. The atom layers are arranged in the manner $[(A\gamma B)]_n$. The iodine atoms have the Ramsdell zigzag sequence of (11). The space group is $P\bar{3}m1$, $Z=1$, $a_0=4{\cdot}24$ Å and $c_0=6{\cdot}835$ Å. Pinsker (1941 a, b) grew crystals of this same type and confirmed Bozorth's structure. The type, however, is apparently uncommon.

Arnfelt (1932) reported lines in x-ray powder photographs of cadmium iodide which needed a *c* axis double that for 2H. Hassel (1933), Pinsker (1941 a, b), Smirnova *et al.* (1941), Hägg *et al.* (1943, 1949), as well as the writer, have confirmed the 4H structure. This type has a stacking sequence of $[(A\gamma B)(C\alpha B)]_n$, and an iodine zigzag sequence of (22). The space group is $P6_3mc$, $Z=2$, $a_0=4{\cdot}24$ Å and $c_0=13{\cdot}67$ Å. Polytype 4H appears, so far, to be the most common structure of cadmium iodide.

Type 6H, reported by Pinsker (1941 a, b), has layers stacked according to the arrangement $[(A\gamma B)(C\beta A)(C\alpha B)]_n$. This corresponds to an iodine zigzag sequence of (33). The space group is $P\bar{3}m1$, $Z=3$, $a_0=4{\cdot}24$ Å and $c_0=20{\cdot}505$ Å.

Recently the writer discovered a crystal of type 8H which he had grown from an aqueous solution of cadmium iodide at room temperature. Of six possible stacking sequences only $[(A\gamma B)(A\gamma B)(A\gamma B)(C\alpha B)]_n$ gave results which agreed with the intensities of the x-ray reflections, and this agreement was excellent. A detailed description of this work will be given elsewhere in the future. The iodine zigzag sequence is (111122). The space group is $P3m1$, $Z=4$, $a_0=4{\cdot}24$ Å and $c_0=27{\cdot}34$ Å.

The writer has also grown, from aqueous solution at room temperature, one specimen each of types 12H and 26H. The stacking structures of these have not yet been determined. Because a 12 layered unit has forty-seven possible arrangements and a 26 unit has many more, the task of finding the true arrangement becomes exceedingly difficult, though perhaps not impossible.

Many x-ray films show evidence for the existence of numerous other polytypes consisting of many layers. The difficulty of identifying these lies in the inability of getting good resolution of x-ray reflections on the films. It is hoped that the Laue method which proved so useful in the identity of many-layered silicon carbide polytypes (Mitchell 1953) will also be useful in this case.

This work has definitely upheld Forty's (1952) idea that polytypism occurs in cadmium iodide crystals. His assumption, however, that the 4H stacking sequence $[(A\gamma B)(C\alpha B)]_n$ is the ' ideal structure ' and that all polytypes are derived from dislocations of this structure does not seem true. If this were true types 8H and 12H, with ' even ' dislocation groups, would not appear as x-ray distinguishable types, since they would have the same structure as the ' ideal structure ' 4H. In addition, Forty's idea would require that 6H have the structure $[(A\gamma B)(A\gamma B)(C\alpha B)]_n$ while, according to Pinsker (1941 a, b), it is $[(A\gamma B)(C\beta A)(C\alpha B)]_n$. So far no polytypes have been discovered whose c_0 corresponds to the step heights measured by Forty, but there is no reason to believe that this condition will remain. Step heights corresponding to the c_0's of 24H and 28H, both neighbours of 26H, were observed by him.

The writer wishes to thank Professor L. S. Ramsdell, Chairman of the Mineralogical Laboratory, University of Michigan, for making available the equipment utilized in this investigation.

REFERENCES

ARNFELT, H., 1932, *Arkiv Mat., Astron., Fysik,* (B) **23,** 2.
BOZORTH, R. M., 1922, *J. Am. Chem. Soc.*, **44,** 2232.
FORTY, A. J., 1952, *Phil. Mag.*, **43,** 377.
HÄGG, G., 1949, *Bull. soc. chim. France,* D 23.
HÄGG, G., KIESSLING, R., and LINDÉN, E., 1943, *Arkiv Kemi, Mineral., Geol.*, (B) **16,** 3, 4, 5.
HASSEL, O., 1933, *Z. physik. Chem.*, B **22,** 333.
MITCHELL, R. S., 1953, *Am. Mineral.*, **38,** 60.
PINSKER, Z. G., 1941 a, *J. Phys. Chem. (U.S.S.R.)*, **15,** 559; 1941 b, *Acta Physicochim. U.R.S.S.*, **14,** 503.
RAMSDELL, L. S., 1947, *Am. Mineral.*, **32,** 64.
SMIRNOVA, L., BRAGER, A., and ZHDANOV, H., 1941, *Acta Physicochim. U.R.S.S.*, **15,** 255.

Direct Evidence for Dislocations in Aluminium–Copper Alloys

By Heinz Wilsdorf
National Physical Laboratory, South African Council for Scientific and Industrial Research, Pretoria

and

Doris Kuhlmann-Wilsdorf
Department of Physics, University of the Witwatersrand, Johannesburg

[Received July 19, 1954]

In the course of a recent investigation with the electron microscope into the nucleation of precipitates in dislocations, using aluminium with a few per cent of copper, structures have been observed which the authors believe to be precipitation on individual dislocation lines. These structures were found on rolled specimens which were annealed at 530°c for several hours, quenched in water, and, sometimes, strained up to 2% within the first 15 minutes after quenching, or not strained at all. Then the specimens were aged at temperatures between 180° and 210°c in order to produce precipitates, and polished electrolytically.

The traces consist of rows of similarly oriented precipitates which are very closely spaced, their smallest mutual distance being in the order of 200 Å. Two different cases can be distinguished : (i) straight or slightly curved traces in various crystallographic planes, apparently oriented at random, fig. 1 (figs. 1 and 2, Plate 34), and (ii) series of nearly parallel traces, or traces which apparently were parts of concentric loops, lying in (111) planes, fig. 2.

Traces of the first kind are thought to be rows of precipitates formed in dislocations which are links in a dislocation network as postulated by Mott (1952), and accidentally lie in the surface examined. The main reason why these links appear as if they were isolated and not linked to other dislocations is thought to be that they are joined to links outside the surface examined. The length of the traces varies between 0·5 and 10 microns with an average value of about $l=2{\cdot}4\,\mu$. If the yield stress of the polycrystalline material is calculated on the assumption that those links of the network which happen to lie in (111) planes are Frank–Read sources of dislocations, and that all links have the same average length, then, using the formula $\tau_y=Gb/l$, where τ_y is the resolved shear stress at which the source is activated, G is the shear modulus and b is the Burgers vector—a value of 0·7 kg/mm^2 is obtained. This value is somewhat lower than the experimentally determined yield stress of the specimens, but in view of the rather big uncertainties involved, it appears entirely reasonable.

The second kind of trace which form patterns in (111) planes are identified with sequences of dislocations emitted by sources during plastic deformation. Their average spacing is about 0·75 microns. According to the elastic theory of dislocations, this average spacing between successive dislocations lying in one glide plane corresponds to a tensile stress of 1 kg/mm^2, a value slightly larger than the calculated yield stress. This agreement is most satisfactory. The structure shown in fig. 2 shows only parts of loops instead of closed loops probably because the traces leave the surface examined. A more detailed account will be published soon.

This letter is published by permission of the South African Council for Scientific and Industrial Research.

REFERENCE

MOTT, N. F., 1952, *Phil. Mag.*, **43**, 1151.

CXXI. *Notices of New Books and Periodicals received*

Millimicrosecond Pulse Techniques. By Lewis and Wells. (Pergamon Press.) [Pp. 310.] Price £2.

With the advent of radar the techniques of handling microsecond pulses became familiar to many, and possible methods of extension to the millimicrosecond region began to emerge. For radar alone there appears to be no great demand for very considerable extensions, but in nuclear physics there are now sources of extremely fast rising pulses (namely the scintillation counter, Čerenkov counter and spark counter) which allow either very great counting rates or the measurement of very small time intervals. By the use of Kerr cells or image converters it is now also possible to take photographs with exposure times in the millimicrosecond region.

This book is an excellent and up-to-date summary of the techniques of generation, amplification and oscillography of these short pulses, with sufficient detailed practical information to make it immediately useful in the building of apparatus and sufficient basic theory to make it, one may expect, a useful reference book for some time to come.

Although it is hardly possible to criticize the allocation of space to the various topics in any very objective way, it did appear to the reviewer that the treatment of ‘ conventional ’ wide band amplifiers was rather brief (not that the space devoted to distributed amplifiers should be reduced). In the chapters on applications the main emphasis is naturally on nuclear physics, but there is little doubt that the techniques described will be found valuable in many other fields.

D. F. G.

Ferromagnetic Domains. By K. H. Stewart. (Cambridge University Press.) [Pp. 176.] Price 25*s*. net.

This is a book on the properties of Bloch walls and ferromagnetic domains. In two introductory chapters our knowledge on ferromagnetic anisotropy and magnetostriction is briefly summarized. The main part of the book deals with the general aspects of the technical magnetization curve rather than with the properties of special materials. It is closed by two (rather brief) chapters on relaxation effects and energy dissipation. As the book is written in a simple and unsophisticated style, and as it contains a full account of the recent beautiful experimental studies in domain structure, it will certainly be welcomed by everybody who wishes to make himself familiar with some of the modern developments in the field. The book is, however, probably not detailed and critical enough to be a substantial help to the research worker. A. S.

[*The Editors do not hold themselves responsible for the views expressed by their correspondents.*]

Fig. 5

$b=0{\cdot}3$ inch

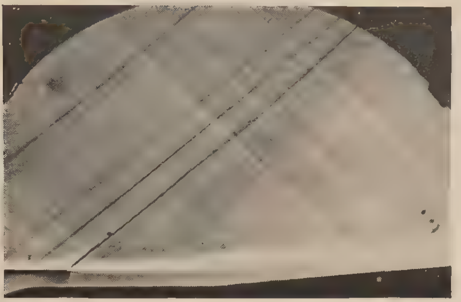

(*a*) $M_3=0{\cdot}75$

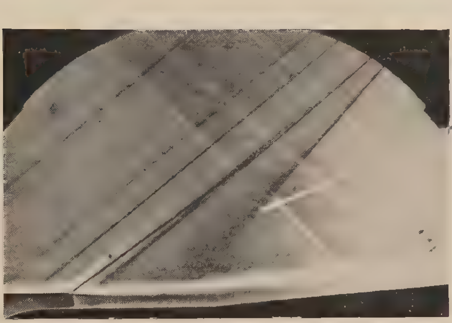

(*b*) $M_3=0{\cdot}91$

Compression due to the presence of the wedge.

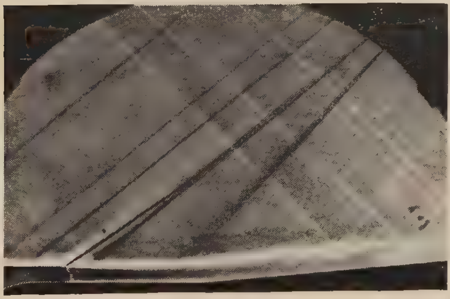

(*c*) $M_3=0{\cdot}98$

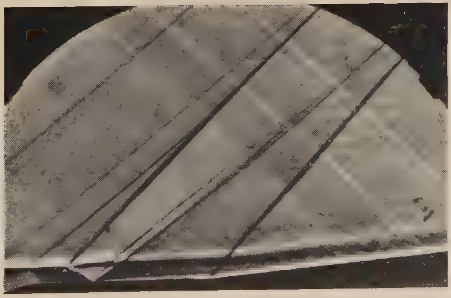

(*d*) $M_3=1{\cdot}59$

Schlieren photographs of the flow up the 5° wedge with constant secondary-stream width.

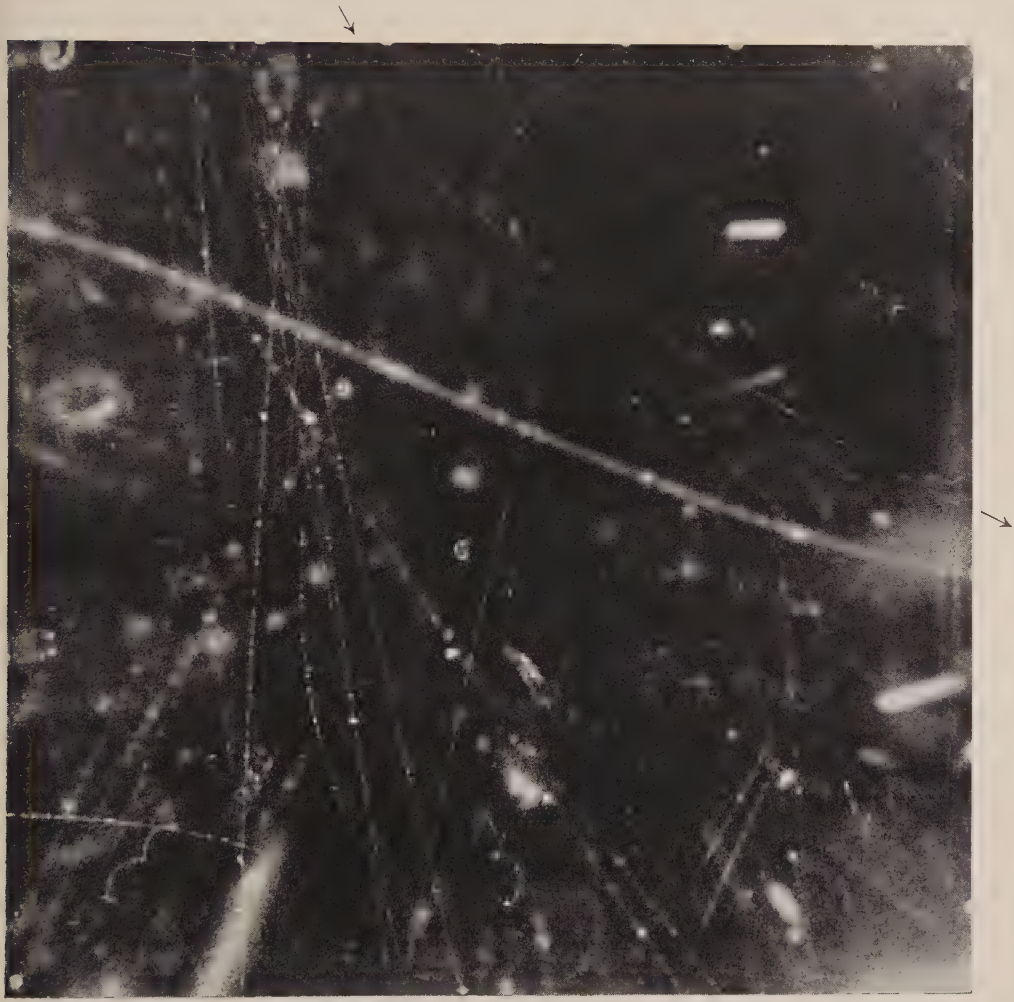

Event RM 253. A typical example of a charged *V*-event. The primary particle is one of a shower of 6 particles coming from an interaction in the lead above the cloud chamber. The measurements made on the event are given in table 1.

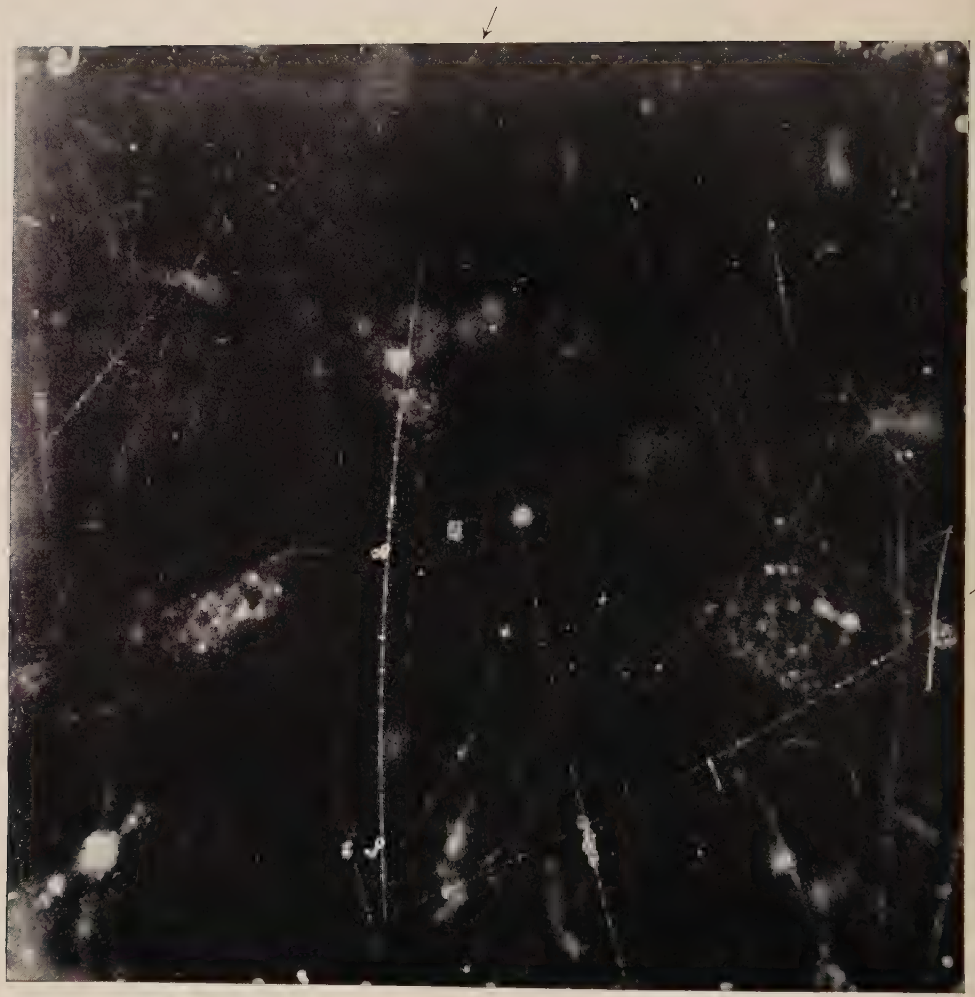

Event RP 993. Analysis of this event shows that the primary particle has a mass greater than 1000 m_e. The measurements made on the event are given in tables 1 and 2 and the event is discussed in detail in § 5.

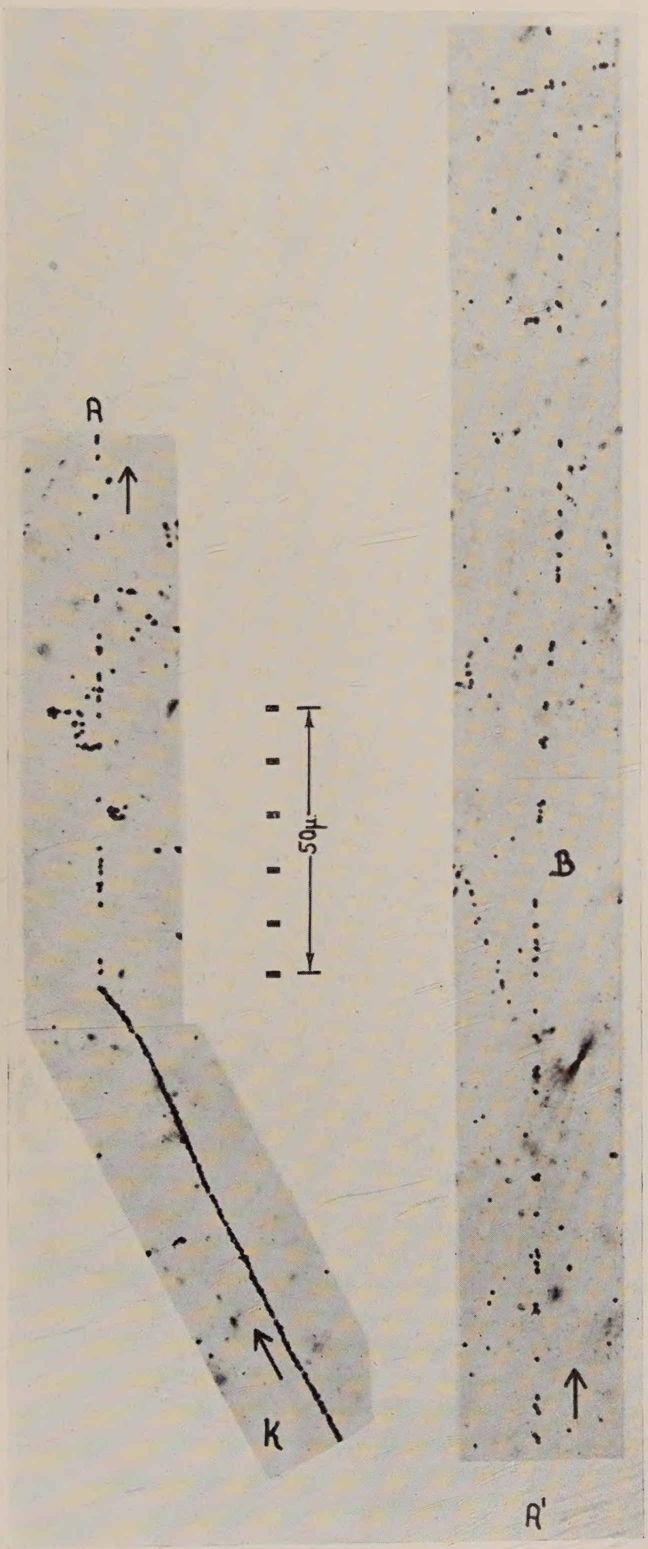
A
50μ
B
K
A'

Fig. 1

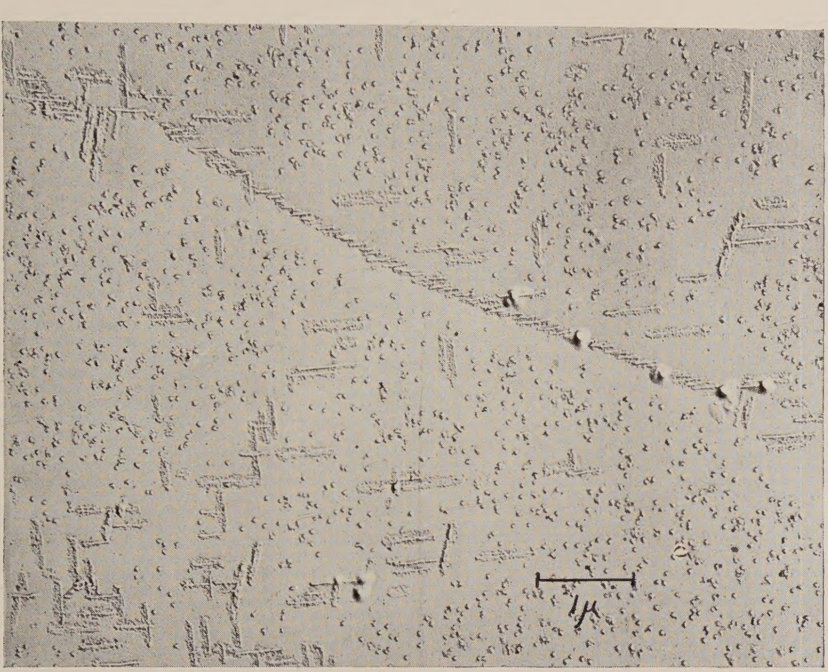

Example of a structure thought to be precipitation on an individual dislocation.

Fig. 2

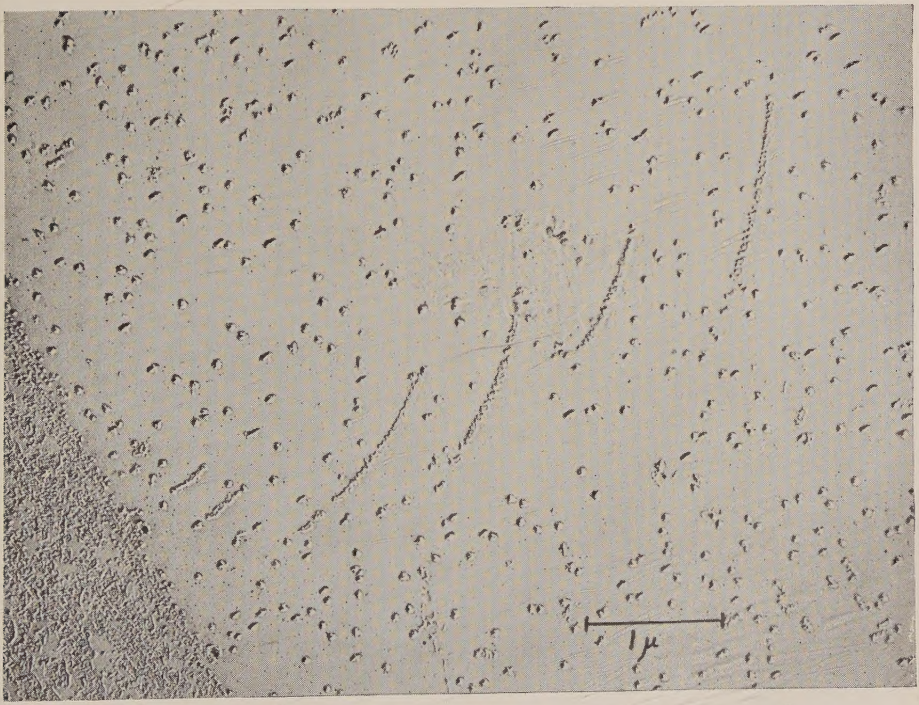

Sequence of traces presumably being parts of dislocation loops in a (111) plane. Since the precipitation is in an early stage, the precipitates have not yet grown into the shape of plates.